THE INSTITUTE OF PAPER SCIENCE AND TECHNOLOGY

Corrosion in Electrostatic Precipitators

Project 2926-9

REPORT TWO

To The Technical Division

of the

Containerboard & Kraft Paper Group

of

The American Paper Institute

June 18, 1990

Institute of Paper Science and Technology
Atlanta, Georgia

TABLE OF CONTENTS

EXECUTIVE SUMMARY

In order to find the main factors influencing the costly corrosion occurring in wet bottom precipitators and to develop cost effective corrosion control means, a comprehensive investigation was conducted, including literature review, field and laboratory corrosion experiments, and chemical analysis of deposits, condensates and flue gases.

The results show that the most important factor controlling the corrosion in precipitators is the water dew point. The effect of low pH had a prominent effect below the water dew point in increasing the corrosion rate. Under "dry" conditions none of the factors studied showed any significant effect. Increasing the incoming flue gas temperature to increase the wall temperature above the water dew point was ineffective. Heat jacketing appeared to be more promising, but it is difficult to apply at some critical locations.

Molybdenum bearing stainless steel grade 316L was evaluated to be the most cost effective construction material for the lower precipitator parts and outlet ends. Carbon steel and weathering steels, both showing similar corrosion resistivity, are satisfactory materials for the upper parts and for the ductwork. The vinyl ester coating systems tested were evaluated to be an alternative to protect carbon steel exposed to wet, aggressive precipitator conditions.

A reliable corrosion monitoring method was developed based on the changing electrical resistance of corroding metal sensors. This method allows effective monitoring of the corrosion rate at specific locations in a precipitator.

INTRODUCTION

Corrosion damage to electrostatic precipitators is a very costly problem for the kraft pulping industry. Millions of dollars are spent each year to repair and replace precipitator components damaged by corrosion. The loss of production associated with lengthy downtimes due to corrosion related failures and repairs adds to the total cost of corrosion to the industry. Corrosion damaged precipitators experience reduced efficiencies which lead to increased emissions of particulate matter. The objective of this study is to identify the causes and mechanisms of electrostatic precipitator corrosion and to develop cost-effective corrosion control methods.

BACKGROUND

One of the major problems associated with wet bottom electrostatic precipitators is the severe corrosion that occurs on steel and concrete surfaces exposed to the flue gases. Corrosion of electrostatic precipitators usually leads to expensive maintenance and/or frequent replacement of the units. Besides the costs of repair and replacement, there are also costs associated with downtime or reduced operating levels when the precipitators fail to maintain environmentally required emissions standards. In a survey conducted in 1985 almost 75 per cent of new, state-of-the-art precipitators had undergone severe corrosion at some locations soon after startup. Corrosion in electrostatic precipitators has become one of the most serious problems affecting kraft mill operations.

The causes of the corrosion are not well understood, and there are many aspects of the problem where the understanding is very primitive. When the surface temperature falls below the dew point, moisture will condense on the surface. The liquid films that form may be enriched in acids precipitated from the flue gas environment. Carbon steel and concrete are readily susceptible to corrosion under these circumstances. Areas within the precipitator which are relatively cool, i.e., outlet regions, and the side wall surfaces and collector plates near the wet bottom, are particularly at risk.

There are two hypotheses concerning the condensation that occurs in electrostatic precipitators. The favored hypothesis is that sulfuric acid condenses directly from the flue gas onto the precipitator surfaces. This should occur at a temperature of over 200 °F. The second hypothesis is that water vapor in the flue gas stream will condense on the precipitator surfaces and the water film will become acidic over time. This should occur at a temperature that is much lower than the acid dew point.

Some progress has been made in reducing precipitator corrosion by maintaining the temperature of the entire precipitator structure above the water dew point, thus preventing moisture condensation. This is accomplished by improved insulation, heat-jacketing, and by passing hotter flue gases into the precipitator. However, in many cases, these remedies

are neither effective nor suited to the protection of existing precipitators, or they may be too expensive.

Even with the remedial measures now available, corrosion of electrostatic precipitators continues to be a significant problem because of the lack of understanding of the interaction among corrosion and recovery boiler operation, precipitator design, and operating conditions. The basics of condensation of moisture from flue gases are known, but the effects of changes in design or operating practices are only crudely understood. As an example, the changes in flue gas composition that occur when recovery boiler operation is changed may have an enormous impact on the corrosivity of the flue gases that are present in the precipitator environment, but these changes have not been investigated. The effects of changes in operating practices are equally unclear. It was not clear whether frequent washing of precipitators is harmful or beneficial to the resistance of corrosion in precipitators. The effects of soot blowing in the boiler are also unknown. There are many other variables which could affect corrosion that are either unknown or poorly understood.

In order to increase the understanding of corrosion control in electrostatic precipitators, the Institute undertook a research project that has four goals:

1. The development of an on-line corrosion monitoring system for detecting corrosion in precipitators during routine operation. This system will provide feedback about the effects of changes in recovery operation on precipitator corrosion.
2. The examination of the corrosion resistance of alternate materials of construction -- metals, non-metals, and coatings -- that might be used in repairs or new construction.
3. The on-site evaluation of the effect of operating practices and system design on the corrosion occurring in precipitators, including an evaluation of conventional corrosion control strategies.
4. Field investigations of the factors contributing to precipitator corrosion, such as temperature, water content, gas composition, deposited salt composition, etc.

Each of these goals addresses a practical question likely to be encountered by mills with severe precipitator corrosion. Testing for this study was done in actual precipitators during routine operation since the complex precipitator environment is difficult to simulate in the laboratory.

The data acquisition phase of the study was divided into a number of separate tasks in order to maintain a structured program of study.

Task 1. Fact-Finding

This task will culminate with the preparation of a detailed summary of the status of corrosion in electrostatic precipitators in the pulp and paper industry.

Task 2. Development of On-Line Corrosion Monitoring

The objective of this task is to develop a simple, inexpensive, but effective method of monitoring the instantaneous corrosion rate inside electrostatic precipitators during routine operation. This development will be valuable because it will give mill operators real-time feedback concerning the corrosion consequences of seemingly harmless changes in the operation of recovery boilers.

Task 3. Evaluation of Alternate Materials

The objective of this task is to develop a materials database for use by mills seeking to replace inadequate materials of construction in precipitators. Metals, non-metals, and coatings will be analyzed in this task. Two different types of information are being sought in this task. First, a ranking of different materials under the most demanding service conditions will be obtained. The corrosion resistance of each material will be ranked by weight loss measurement, visual examination, and other indicators, e.g., pitting. Second, the limits of useful operations will be determined by varying the conditions to which the materials are exposed, and following the resulting changes in the corrosion of the selected materials.

Task 4. Evaluation of Conventional Corrosion Control Measures

In this task, the objective is to understand the reasons for the failure of conventional corrosion control measures used in precipitators. Studies of precipitators in which corrosion control measures were not completely successful will determine if the failure of the approach is inherent in the method or caused by difficulties in execution.

Task 5. Contributing Factors in Precipitator Corrosion

The objective of this task is to identify the factors that promote severe corrosion so that mills might take action to minimize their impact. Since corrosion varies in severity from mill to mill, differences in precipitator design or operation could be responsible.

RESULTS

Task 1. Fact-Finding

A comprehensive review of the literature regarding corrosion in electrostatic precipitators has long since been completed. A report was issued in January 1986.

Task 2. Development of On-Line Corrosion Monitoring

Efforts to evaluate the validity of electrical resistance and dew point monitoring methods for measuring corrosion and/or indicating corrosive conditions in operating precipitators have proven successful. Both methods were investigated on an operating precipitator at the Weyerhaeuser mill in Springfield, Oregon.

At the Springfield mill, a multichannel electrical resistance (ER) system with remote data acquisition capabilities was installed (Fig. 1). After a long period of problems relating to electronics and probe designs, the system was finally employed successfully and corrosion rates were measured on-line in the No. 3 precipitator.

Six ER probes were installed at access ports along the north wall of the precipitator. This is at the outlet end of the precipitator where extensive corrosion damage historically had occurred (Fig. 2). Both flush mount and retractable probes were used, with one retractable and two flush mount probes installed in each of the east and west chambers of the precipitator (Figs. 3 and 4). The locations of the ER probes are shown in a schematic diagram of the precipitator in Fig. 5.

The dew point monitoring technique was employed as a second on-line monitoring method. The dew point method employs the use of a cooled conductivity probe placed in the flue gas stream. The conductivity probe provides for a direct measurement of the flue gas dew point (Figs. 7 and 8). The instrument output -- a temperature value -- was recorded on a strip chart recorder. The location of the conductivity probe is shown in Fig. 5.

A number of weld pad type thermocouples were installed in the precipitator in conjunction with the installation of several panels of corrosion coupons and coated specimens (discussed in Task 3 results). The thermocouples provided for direct metal surface temperature measurements in the precipitator. The data are important, especially when related to the dew point measurements, because it gives an indication as to whether condensation, and hence corrosion is likely to occur on the internal precipitator surfaces. Sixteen of the weld pad thermocouples were installed as shown in Fig. 9. The locations of the thermocouples are also shown in Fig. 5. The thermocouples were connected to a data logger where continuous temperature readings were recorded.

Measurements were recorded for a period of time under routine boiler operating conditions with the electrical resistance corrosion rate monitoring equipment, the dew point monitoring equipment, and the internal surface temperature recording instrument all operating simultaneously. Shortly after the routine data were collected, the mill experienced a coincidental "trip-out" of the recovery boiler associated with the monitored precipitator. This presented a unique opportunity to measure and record the effects of an unplanned, but typical upset condition on temperature and dew point. After normal boiler operations were restored, arrangements were made with the recovery personnel to manipulate boiler operating conditions. The methodology and results of these tests are described below.

Test A. Routine boiler operation

Method: The dew point probe was adjusted to maintain and record the temperature required for a 100 μA conductive film on the probe surface. This is a film setting consistent with the literature, but no significant change in dew point was revealed when the conductivity setting was adjusted from 50 μA to 500 μA. The accuracy of the dew point probe and meter was verified upon installation by the probe vendor using a portable probe unit. Data were also secured regarding earlier tests (May 1986) conducted by the vendor that indicated the dew point was not significantly different when measured in the east or west chamber of the precipitator, or when measured at the inlet or outlet of the precipitator.

Temperature data from the sixteen direct metal contact thermocouples was recorded as described above. Data collection began with the electrical resistance system using newly installed ER probes, but the early data were unreliable, probably due to the probe's initial surface condition. It had previously been observed during related laboratory testing that the active element strips on the ER probes needed to "pre-corrode" slightly before corrosion (indicated by increasing metal loss values) proceeded in a relatively stable manner.

Results: Readings with the dew point probe indicated dew points that ranged from 160 - 175 °F during typical boiler operating conditions (Fig. 10). Data from the sixteen internal surface thermocouples revealed temperature values that ranged from 140 - 300 °F (thermocouple location dependent) during routine boiler operation and corresponding precipitator gas inlet temperatures of 310 - 340 °F. Temperatures were found to be greater on internal surfaces at the inlet end of the precipitator and in the upper portions of the precipitator. The inside surfaces of sidewalls (approx. 240 °F) were cooler than the chamber dividing wall (approx. 280 °F) at intermediate levels in the precipitator. The inside surfaces of the double door access ports were at a higher temperature than the single doors, regardless of the door location in the precipitator.
The lowest temperatures, and the only temperatures that measured at or below the dew point, were found at the outlet end at low levels of the precipitator near the liquor bath. Note, however, that similar locations

were not heavily instrumented at the inlet end. A dramatic reduction in the metal surface temperature was observed toward the level of the liquor bath, at elevations beginning near the bottom of the collector plates (approximately 6 feet from the floor of the precipitator). A vertical temperature profile for the lower outlet wall of the west chamber of the No. 3 precipitator is shown in Fig. 11. The lowest thermocouple (#11) was most likely immersed in the liquor bath and therefore indicates liquor temperature. The other thermocouples were located at higher elevations and all resided in the flue gas stream. It is apparent that proximity to the liquor bath results in a cooler wall surface temperature, a condition which promotes condensation and therefore corrosion.

The effect of thermal insulation on the retention of heat along wall surfaces was determined at similar elevations along the outlet end wall. The effects of full insulation (with no heat jacketing), partial insulation, and no insulation are shown in Fig. 12. For a completely uninsulated plate the average internal surface temperature was less than 150 °F, for a moderately (approximately 2" fiber fill) insulated plate the temperature was close to 200 °F, and a heavily (approximately 4" fiber fill) insulated plate resulted in an average temperature of around 230 °F.

Test B. Boiler upset condition

Method: The mill experienced a "trip-out" of the No. 3 recovery boiler. The boiler nearly blacked out, gas fuel had to be supplemented, etc., and the effects of an unplanned, but typical upset condition on temperature were recorded.

Results: The precipitator inlet temperature drop related to the trip-out of the boiler resulted in a corresponding drop of dew point. Apparently, the dew point tends to parallel the flue gas temperature (Fig. 13). A plausible explanation for this result, relative to the water dew point theory, is that the cool flue gas contained less water vapor, which resulted in the lower dew point. As the furnace bed cooled during the upset, a lesser quantity of water driven off during liquor combustion would be dismissed in the resulting flue gas. Also, the cooler flue gas would not pick up as much water from the black liquor while passing through the cascade evaporator. If other factors are equal, a decrease in liquor solids content at the cascade evaporator (indicative of reduced water removal) almost always results from a low load firing recovery boiler.

It is doubtful that the dew point drop was related to flue gas composition (other than water vapor content) for reasons determined from other tests that were conducted, with some data to be presented shortly. The effect of burning supplemental fuel (natural gas) to bring the boiler back is insignificant on the dew point. Natural gas is a relatively clean fuel with low levels of sulfur, and substantial increases in sulfur oxide compounds in the flue gas would not be expected as a result of combustion of this fuel.

An assessment of boiler upset conditions suggests that substantial drops in flue gas temperature to the precipitator caused by a decreased boiler load do

not result in an aggressive corrosive environment in the precipitator. From Fig. 13, it can be seen that the difference in temperature between the flue gas and dew point remains fairly constant during the upset period. This temperature margin can be thought of as a measure of corrosion safety, provided that some measurements or knowledgeable assumptions are made regarding the relationship between flue gas temperature and internal surface temperatures.

Test C. Recovery boiler operation manipulation

Method: Arrangements were made with recovery personnel to intentionally manipulate boiler operating conditions within the constraints of safe and effective operation. Arrangements had been made earlier for simultaneous on-line flue gas monitoring with Weyerhaeuser Technology Center (WTC) personnel who were coincidently at the mill with their gas test equipment. The WTC people monitored outlet precipitator flue gases for SO_2 and TRS, while SO_2, TRS, CO, O_2, flue gas temperature, and dew point where monitored using Institute equipment and recovery control room instrumentation.

Following discussions with the recovery operations personnel, it was determined that the boiler could be fired at three different extremes throughout the course of a day. Even though SO_2 and TRS could be measured directly, there was no way to determine SO_3 except by inference from the dew point readings. It was decided that the possibilities for SO_3 generation during any normal operation of the boiler would be spanned by firing the boiler at the extremes of possible operation.

Boiler Firing Condition 1. "Cold bed firing" was the target because there is evidence (Pulp & Paper Canada 87:1 (1986), p. 26) that suggests elevated levels of sulfur oxides are generated in this conditions.

Method: Liquor gun pressure (and flow) was increased and the liquor temperature reduced. This flooded the bed with relatively cold liquor. The effect of this upset condition is described below:

	Net effect	
	Start	Final
TRS	30 ppm	15 ppm
SO_2	18 ppm	nil
CO	50-500 ppm	nil
Excess O_2	1-2 %	5 %
PPT inlet temp.(East/West)	320-330°F/290-300°F	290-310°F/270-290°F
Dew point	155-170°F	150-160°F

The previous evening the mill had begun to fire unoxidized liquor in the boiler to elevate total sulfur levels (TRS + SO_2) in the flue gas for meter calibration early that morning. Early in the test it was likely that this was responsible for the high TRS and SO_2 start values.

Boiler Firing Condition 2. Boiler operations were adjusted to cause carryover burning, or burning the liquor at high elevations in the boiler with carryover of some unburned fuel.

Method: The liquor sprays were "fined-up" (to obtain smaller average liquor droplet sizes) by increasing liquor pressure and by increasing liquor temperature. Air flow was reduced at the primary air ports.

	Net effect	
TRS	------->	30 - 40 ppm
SO_2	------->	25 - 32 ppm
CO	------->	4400 ppm
Excess O_2	------->	nil
PPT inlet temp. (E/W)	------->	295-310°F/285-300°F
Dew point	------->	165 - 180°F

Boiler Firing Condition 3. Continued carryover with an increased level of excess O_2.

Method: Flood the boiler combustion zone with air from the primary and secondary air ports.

	Net effect	
TRS	------->	10 ppm
SO_2	------->	5 ppm
CO	------->	nil
Excess O_2	------->	7 - 8 %
PPT inlet temp. (E/W)	------->	310-325°F/270-290°F
Dew point	------->	150 - 160°F

The results of these findings suggest that under the most extreme boiler operating conditions, the flue gas composition could be changed significantly, but the dew point could be changed very little. Therefore, optimization of recovery boiler operating practices, aside from maintaining good temperature control at the precipitator inlet, is probably not an effective method for controlling electrostatic precipitator corrosion.

Another test measured the effects of bypass damper positioning at the cascade evaporator on flue gas, internal metal surface, and dew points.

Method - The dampers on both the east and west side were simultaneously positioned for approximately two hours at the following positions:

0 % open
50 % open
75 % open
100 % open

Both dampers were rodded out and air blown prior to the start of the test to remove saltcake buildup that would interfere with the results of the test.

Results

Damper position %	PPT inlet temp. °F East / West)	Dew point °F
0	295 - 305 / 300 - 310	170 - 180
50	310 - 320 / 305 - 315	155 - 175
75	315 - 325 / 310 - 320	165 - 170
100	365 - 375 / 300 - 310	160 - 175

During the last test (100 % open), the west side damper apparently plugged, resulting in flue gas temperatures which were unbalanced from one side of the precipitator to the other. Unbalanced flue gas temperatures of low magnitude (20 - 30 °F) are not uncommon and likely are the result of cyclone effects in the boiler or the configuration of the cascade evaporator. Liquor enters the cascade at one side where most of the water removal occurs; the other side contacts a black liquor that is already somewhat concentrated. As can be seen from the results above there was no significant effect on dew point due to damper repositioning.

On-Line Monitoring

So far, no mention has been made regarding the results of corrosion measurements made with the electrical resistance corrosion monitoring instrument and probes. Data relating to metal loss on the ER probes were sporadic for a few days following startup of the system. This continued through the period when the above tests were conducted, thus no reliable data were available for correlations with operating conditions and the other measurement techniques. A later trial was run under varying operating conditions; results will be discussed in the Task 4 section of this report.

Finally, after several days, valid data collection was initiated during routine boiler operation, though electrical noise in the vicinity of the precipitator still resulted in some scatter in the data on a few non-shielded/grounded probes and cable systems. All the probe systems were subsequently electrically shielded and grounded.

Incremental metal loss values in mils (1 mil = 0.001 inches) and probe temperatures are plotted versus time for each of the six electrical resistance probes installed in the precipitator (Figs. 14 - 19). All the probe elements were plain carbon steel. The slope of the curve represents the rate of corrosion.

Normally, the most appropriate presentation of the data would be to subtract successive metal loss values, divide by the time increment, and plot corrosion rate directly versus time. This was not an attractive method in this case because of the degree of scatter in the data. Examples of this are shown in Figs. 20 - 21. Electrical noise picked up by the probes and/or cables caused much of the scatter in the data. This is illustrated in Figs. 20 - 21. Figure 20 is of an unshielded flush mount probe while Fig. 21 is that of a shielded.

Referring to Figs. 14 -19, it can be seen that substantial corrosion rates were measured on many of the probes. The flush mount probes experienced the highest corrosion rates (up to 200 mpy) and, as a result of corrosion, all of the probes failed in less than 150 hours due to loss of the thin (4 mil thick) element strips . All the probe temperatures were consistently less than 200 ^{o}F during service.

Relating corrosion rate to temperature is difficult due to the scatter in the data and frequent, but short, changes in probe temperature. Some generalizations, however, can be made between average corrosion rate over the life of the probe and the average probe temperature. An example of this is shown in Fig. 22 where two flush mount probes that experienced substantial differences in temperature also experienced different rates of corrosion. Similar data for all flush mount probes are presented in Table 1. Notice that the maximum corrosion rates determined in the precipitator are at or near the measured flue gas temperature.

Both the electrical resistance and dew point methods appear to be effective on-line monitoring methods for corrosion in electrostatic precipitators. The dew point method requires some related internal precipitator surface temperature information before assumptions can be made with regard to corrosion activity. Dew point monitoring may be effective when used only as a periodic "spot-check" method since recovery boiler flue gas dew points do not change appreciably during most boiler operations.

On-line corrosion rates were measured with the electrical resistance corrosion monitoring apparatus. Before substantial corrosion rates were measured, steps had to be taken to ensure relatively low temperatures were experienced by the flush mount probes . The flush mount probes provided the clearest, most trustworthy data and closely represent an actual wall surface in a precipitator. Probe site selection and installation methods are critical with both ER probe types, but probably more so with the retractable probes. Two earlier installed retractable probes measured no discernible corrosion of the probe elements during lengthy service periods. Upon removal, it was discovered that, only a few inches from the uncorroded elements, severe attack of narrow regions of the probe shaft had occurred (Fig. 23). If the probe elements had been located in this zone, the high rate of corrosion would have been measured.

It is clear that steps must be taken to ensure that ER probes and cable systems are electronically shielded and grounded for the most effective operation of the system. Longer lived probes with thicker detection elements of 10 to 20 mils would be more suitable for the high rates of corrosion that

can be experienced in a precipitator. As will be discussed in a later section, the retractable probes are not as reliable as the flush mount type.

Task 3. Evaluation of Alternate Materials

This section of the report can be divided into four parts:
1) Corrosion coupons installed at Westvaco mill,
2) Corrosion specimens installed at Weyerhaeuser mill,
3) Coated specimens tested at Weyerhaeuser mill, and
4) Coated collector plates tested at Chesapeake mill .
The results obtained will be discussed and a ranking of alternate construction materials will be given.

Coupon Tests at Westvaco Mill

The corrosion test chamber that was installed at the Westvaco mill in Charleston is shown in Fig. 24. The chamber was insulated and heated to 400 °F to prevent condensation on the sidewalls. Ten temperature controlled probes, or "cold fingers" (Fig. 25), with ten corrosion coupons mounted on each were placed into the test chamber, and three thermocouples were located along their length to monitor temperature and to provide temperature control. The selected temperature was maintained by passing either air or water through the cold fingers, depending upon the amount of cooling required to maintain the desired temperature.

Twenty-one different alloys were examined to rank their corrosion resistance in the flue gas environment. The alloys examined are shown in Table 2. The alloys included plain carbon steel as a control, in addition to various stainless steels, high nickel alloys, weathering steels, and titanium.

During the test, relatively low corrosion rates and lower than expected dew point prompted a series of investigations that ultimately led to gas sampling and analysis of the recovery flue gases. The recovery flue gases were determined unsuitable for further testing when the gas analysis revealed that SO_2 and SO_3 levels were well below the norm. Eventually, a decision was made to move the testing to the Great Southern Paper Company mill in Cedar Springs, Georgia. The results of the tests at GSPC will be discussed under Task 5.

The weight loss tests completed at the Westvaco mill did, however, provide a ranking of alternate materials for use in electrostatic precipitator construction. Although dew points were lower than expected, some significant corrosion rates were obtained on carbon steel materials when the specimens were held at low temperatures. All the test materials were eventually exposed at those low temperatures and a material ranking was developed. Corrosion rates for the test alloys throughout the test temperature range are given in Figs. 26a-u.

Most of the alloys that experienced significant corrosion at any test temperature also experienced a dramatic increase in the rate of attack at about 150 °F, very close to the water dew point, from which point on corrosion rate continued to increase until a maximum rate was obtained at approximately 90 °F.

The plain carbon steels experienced the greatest corrosion rates, ranging from 25 to 40 mils per year (mpy). The Corten "weathering steels" were only slightly more resistant than the common C1010 and A285 Gr C carbon steels.

The stainless steels were much more resistant to corrosion than the plain carbon steels. Corrosion rates ranged from 3 mpy for AISI 304L to nearly 0 mpy for some of the more highly alloyed stainless steels. 304L experienced attack in the form of pitting corrosion, unlike the carbon steels which underwent uniform corrosion . The molybdenum bearing austenitic stainless steels (316L, 316LM, 317L, 317LM) performed better than 304L, with 317L and 317LM not revealing any significant attack. Type 310 stainless, which has no molybdenum but is significantly higher in chromium and nickel content than any of the other 300-series stainless steels tested, performed as well as the 317-grade stainless steels. The other high alloy stainless steels did not suffer any significant corrosion attack at any temperature.

The nickel base alloys all performed well with measured corrosion rates of less than 0.2 mpy, at the limits of corrosion detection using weight loss techniques. The two titanium alloys had measured maximum corrosion rates of 2 - 3 mpy.

Coupon Tests at Weyerhaeuser Mill

Six specimen racks were designed for the purpose of measuring corrosion rates and evaluating materials in "cold spots" of the No. 3 precipitator at the Weyerhaeuser mill in Springfield, Oregon. The panels were welded to various surfaces in the precipitator. The panels each contained weight loss coupons (21 different alloys), U-bend specimens (10 different alloys), and crevice corrosion specimens (3 different alloys), and underwent a total exposure of 157 days. The specific locations are shown in Fig. 5 and an example of one of the panels is shown in Fig. 27. Several of the test panels were mounted adjacent to weld pad thermocouples for a measurement of the temperature at the exposure site.

The corrosion tests were conducted in accordance with standard practices for weight loss, crevice corrosion, and stress corrosion cracking testing as described in the ASTM Standard Test Methods G-1, G-4, G-30, and G-78.

The results of corrosion rates measured by weight loss techniques are given in Table 3. The corresponding temperatures at each location are also given. With the exception of panel No. 3, most of the test materials experienced very low corrosion rates, even on the carbon steel varieties. Upon examination of the exposure temperatures, measured directly or estimated

from temperature data gathered for the precipitator, it was apparent that all of the test panels were located at sites where the temperature was above the water dew point. Panel No. 3, where some of the carbon specimens exhibited severe corrosion, was exposed at a temperature that was only slightly above the dew point. All the other test panels and specimens were exposed at higher temperatures, well out of the range of the dew point, so little or no corrosion occurred. This data, when supplemented with the low temperature weight loss data obtained from the Westvaco mill, indicates that under all conditions many of the test materials are immune to the corrosive conditions in precipitators.

Substantial corrosion was not measured on the high grade stainless steels, the nickel base alloys, or the titanium alloys in exposures that span three different precipitators and in some instances resulted in corrosion rates on carbon steel variety materials of over 100 mpy. For these reasons the high alloys were removed from the test program. The alloys that remained in the test program were the plain carbon steels, 304L, 310, and 316L.

Tests were conducted to determine whether stress corrosion cracking conditions were present in the precipitator. U-bend specimens of the following materials were exposed on each of the six test panels installed in the No. 3 precipitator:

A285-C, A285-C(w),
304, 304(w), 304L, 304L(w),
316, 316(w), 316L, 316L(w).

An "L" indicates a low carbon variety of the material, and a "(w)" indicates a U-bend specimen with a weld pass in the peak stress zone.

Both macro- and microscopic inspections (Fig. 28) revealed that none of the material types exposed at any of the test locations in the precipitator had undergone cracking. None of the test specimens were exposed below the level of liquor at the precipitator bottom, where some mills claim to experience cracking of stainless steel plate materials. Caution is advised that the absence of stress corrosion cracking was related to only one test location.

Crevice corrosion tests were conducted on 304L, 310, and 316L stainless steels. Specimens of each type were fitted with Anderson type crevice washers and installed on each of the six test panels. None of the materials exhibited localized attack in the form of crevice corrosion at any of the test locations (Fig. 29).

Coating Tests at Weyerhaeuser Mill

At the same time that the six panels discussed above were installed in the No. 3 precipitator, three panels containing coated specimens were also installed. The locations of these panels are shown in Fig. 5.

Coated specimens were solicited from the Wisconsin Protective Coating Corp., Green Bay, Wisconsin; and PrecipTech/BHA Co., St. Louis, Missouri; for installation in the electrostatic precipitator at the Weyerhaeuser mill. The candidate coatings consisted primarily of organic polymer formulations -- in particular, epoxy and vinyl ester resins. A description of the coatings is given in Table 4.

The coating vendors completed surface preparation and coating application procedures on carbon steel specimens in their shops and delivered the test samples to the Institute. Two specimens of each test coating were fastened to stainless steel panels for installation. The coated surface of one specimen of each test pair was intentionally damaged in a reproducible fashion with an "X" that penetrated the coating to the metal surface. This was done in an effort to simulate damage that can result during the installation or service period of an actual coating system. Included on each panel of coated test specimens were two carbon steel weight loss coupons, enabling a baseline corrosion rate measurement on unprotected mild steel at each test location.

Temperature measurements were conducted at each site with the use of thermocouples installed either on, or in the vicinities of the test panels. The panels of test coatings were exposed to typical precipitator operating conditions for a period of 157 days. Upon retrieval, the panels were washed with water to remove saltcake and debris prior to inspection and documentation of coating performance. The carbon steel coupons were removed immediately for weight loss determinations.

The estimated temperatures and measured corrosion rates on carbon steel at each exposure site are given in Table 5.

Visual examination of each of the retrieved test panels revealed that nearly all of the coating materials had darkened or become otherwise discolored. Upon close inspection, various types of damage were noted on several of the coated specimens. The individual specimens were removed from the panels for macro- and microscopic examination and, also for coating thickness measurements. Coating thicknesses were measured before and after exposure using a magnetic pull off gauge according to standard practices described in ASTM D1186 -- "Method for Nondestructive Measurement of Dry Film Thickness of Nonmagnetic Coatings Applied to a Ferrous Base." Summaries of coating performances and thickness determinations are given in Tables 6 - 7.

A laboratory temperature resistance test was conducted for all the candidate coatings. The test was conducted because it was felt that the performance of the coatings could be strongly related to temperature resistance for an electrostatic precipitator application. The results of the temperature test are given in Table 8.

Photographic examples of the various forms of damage experienced by some of the coatings described in Tables 6 and 8 are shown on Figs. 30 - 36. Figure 30 shows cracking experienced by a S&G 350 coated specimen

exposed on panel No. 7. Cracking was not dependent upon proximity to surface defects for the S&G 350 coating as is shown in Fig. 31. It can be seen from Fig. 32 that cracking of the S&G 350 coating resulted in the exposure of the underlying carbon steel. Continued exposure under such circumstances would likely result in disbondment and delamination of the coating over a period of time. Much better performance was exhibited by the S&G 500 coating in similar exposures (Fig. 33).

Specimens coated with Plasite 5306 suffered several different types of damage during the precipitator exposures. Examples of cracking and attack on the coating in the form of pitting and pinholing are shown in Fig. 34. Plasite 9500 performed quite well in the coating tests, but the similar Plasite 9570 coating system experienced damage that generally resulted from the simulated surface defects (Figs. 35 - 36). Both of the vinyl ester coating types, Plasite 4100 and 470, exhibited good performances in the precipitator exposures.

The temperature resistance tests were useful for determining the approximate maximum temperatures that individual coating types could withstand under optimal (ambient air) conditions. In addition, several thermal failure modes were identified.

Plasite 5306 failed at the lowest temperature (350 °F) of the test coatings as a result of cracking, blistering, and pitting of the coating material. The S&G 350 coating system failed at about its stated temperature rating of 350 °F, as was revealed by widespread cracking and flaking of the coating. At 400 °F, both Plasite 9500 and 9570 showed evidence of thermal coating failure. Plasite 9500 was observed to swell, blister, and crack (Fig. 37) resulting in perforation of the coating (Fig. 38). Plasite 9570 failed as a result of embrittlement, cracking, and subsequent flaking of the coating as shown in Fig. 39. The S&G 500 coating system did not experience thermal related damage until about 450 °F, at which time the coating experienced widespread cracking and peeling (Fig. 40). Neither of the vinyl ester coating materials exhibited any damage other than slight swelling and discoloration during the thermal resistance tests, which were concluded at 450 °F.

The thermal and environmental conditions experienced by the coatings at the different test locations were not significantly different and did not span the entire range of temperatures and corrosive conditions in the precipitator. Only the mid- and upper-temperature regimes, with correspondingly low corrosion rates, were examined during this test. However, it is believed that the lifetimes of coatings in kraft recovery precipitator applications are dominated by temperature limitations due to the lack of highly acidic conditions that would cause rapid failure of some coating systems, regardless of temperature. Acidic conditions in the environment are discussed in Task 5.

Both thick and thin film systems were among the candidate test coatings as shown in Table 7. None of the coatings revealed any substantial loss of thickness during the precipitator exposures. There appears to be little

relationship between coating thickness and performance as revealed by the relatively good performances of the S&G 500 coating (thin film) and the Plasite vinyl esters 4100 and 470 (thick film). Under long-term exposures in actual precipitator applications, thick, multi-layer coatings may prove more durable, and able to withstand possible slow diffusion of corrosive species through the coatings.

After review of the data, the relative performance of the coating systems were ranked and are reported in Table 9. Criteria for development of the ranking included the results of the precipitator exposures, the laboratory temperature tests, and the resistance of a coating to further damage resulting from a surface defect. The relative performances were developed, keeping in mind that slight swelling, discoloration, etc., have little adverse affect on a coating's ability to provide corrosion protection for a carbon steel precipitator surface.

Of the candidate coatings tested, two epoxies, Seal and Glaze 500 and Plasite No. 9500, and both vinyl esters, Plasite No. 4100 and the conductive Plasite No. 470, are recommended as valid coating systems for electrostatic precipitators and related ductwork applications. It must be remembered, however, that the recommendations are based upon data that were largely limited to one precipitator exposure, though the host precipitator is believed to be of representative design and typical of most kraft recovery furnace precipitators.

Conductive Coating Tests at Chesapeake Mill

Tests were also carried out to evaluate the effectiveness of conductive coating systems for collector plate applications. The Chesapeake Corporation mill in West Point, Virginia, offered its No. 4 electrostatic precipitator as a location for the installation of coated test plates. The Institute contracted the services of CoroTech, Inc. for the preparation and application of coatings formulated by both CoroTech and Wisconsin Protective Coating Corp. The collector plates were manufactured by Cleveland Manufacturing, Inc. and shipped to the Chesapeake mill for on-site surface preparation and coating application.

Two different coatings were recommended by the vendors for testing and both were selected for the study. The first was Plasite 4140, a conductive vinyl ester coating supplied by Wisconsin Protective Coating Corp. The second was CoroTech's conductive coating No. 1505C, also a vinyl ester resin formulation. The Plasite 4140 coating is a thick film system (30 - 40 mils) that requires a 4 mil substrate surface profile prior to application. 1505C is a thin film system (6 - 8 mils) and a 2 mil surface profile is recommended to provide a suitable anchor pattern for the coating.

CoroTech initiated the study in its shop by investigating surface preparation methods on short sections of collector plates supplied by Cleveland Manufacturing. Grit blasting methods and grit types were examined, and it was determined that only a 1 - 2 mil profile white metal blast was obtainable. The specified 4 mil surface profile for the 4140 coating

could not be reached due to warpage and distortion of the thin collector plates during heavy blasting. Although the suggested surface preparation could not be completed, the test was continued by coating plates blasted to the available 1 - 2 mil profile.

The full-size collector plates measured 19 inches in width, approximately 30 feet in length, and were constructed of 16 - 18 gauge mild steel. The plates were blasted in an outside area, but coating applications were completed in an enclosed, dust-free building. Conventional spray equipment was used for the application of both test coatings.

Six plates were coated with the Plasite 4140 coating. Coverage was estimated at 27 - 32 sq. ft./gal. Wet film thickness was 16 - 20 mils per coat and two coats were applied. Three plates were prepared and coated with the CoroTech conductive coating No. 1505C. One coat was applied to a 6 - 8 mil thickness. The color of all nine plates was a nearly identical charcoal gray. The plates were tagged and allowed to cure for 12 days.

The plates were then installed in the No. 4 electrostatic precipitator which has a wet bottom design. Eight coated collector plates were installed because one was damaged during installation and had to be discarded. The locations of the plates are described in Table 10. Plates were installed in both chambers of the precipitator, near the center of the flue gas stream, near vertical sidewalls, and at both inlet and outlet locations in an effort to expose the coatings to the different temperatures and corrosive conditions present in an operating precipitator.

The coating tests were conducted with regard only to the integrity of the exposed coating materials and the protection afforded the carbon steel substrate. No attention was given to the flue gas particulate collection efficiency of a coated plate, as this would have involved the electronic isolation and instrumentation of one or more coated plates. It was assumed that the coatings are highly conductive, i.e., there would be no difference in the collection efficiencies of coated versus non-coated collector plates.

After a seven month exposure, the coated collector plates were examined during a shutdown of the boiler. The coated plates were readily identifiable from the hundreds of uncoated plates by their charcoal gray appearance. All of the exposed test plates had retained this original color.

No evidence of corrosion or thermal degradation of either coating type was observed. No delamination or adhesion failures between the coatings and the carbon steel was evident, but some limited areas of delamination between the two layers of the Plasite 4140 coating were observed.

Numerous holidays and pinholes were evident on plates coated with both coating types. Localized corrosion of the underlying carbon steel occurred at the sites of holidays and pinholes, particularly on the lower portions of plates in the vicinity of the liquor bath where flue gas temperatures are generally lower (Fig. 41). The extent of localized attack on the plates could not be determined, but in some areas large amounts of rust-colored corrosion products were deposited on the surface surrounding voids in the

coating (Fig. 42). Above the lower 6 to 7 feet of the coated plates there was, in general, no evidence of corrosion attack.

The holidays and pinholes were often observed to form vertical arrays, especially near an edge, corner, or other discontinuity in the plate geometry (Fig. 43). However, at some locations the voids were randomly distributed along the surface of a coated collector plate (Fig. 44).

Another area where corrosion damage was noted was inside the channel areas along both the leading and trailing edges of the plate. The damage was related to an inability to obtain an adequate surface preparation during blasting and/or a sufficient layer of coating in the physically difficult-to-reach channel areas. This form of attack was significantly worse on plates coated with the 1505C system, either because the coating is a thin film system or because it is a one-layer system, indicating an increased chance to miss or inadequately coat a difficult-to-reach area.

Measurements were made at various locations on several plates to determine the uniformity of coating thickness. Nondestructive, dry film thickness measurements were conducted using a magnetic pull off gauge according to standard practices described in ASTM D1186. Dry film thicknesses for plates coated with the Plasite 4140 system ranged from 20 - 45 mils on the flat, middle sections of the plates, with 17 - 25 mils along flat edges (excluding the inside channel areas, which could not be measured). Collector plates coated with the 1505C conductive coating measured 2 - 5 mils in the middle sections and 2 - 2.5 mils along edges.

Conductive vinyl ester coatings appear to be a valid method for the protection of carbon steel electrostatic precipitator collector plates. Neither coating system suffered direct attack of the coating during the exposure in an operating precipitator. Coating delamination, a problem experienced in an earlier test by a coating vendor, was not evident in this study although plates coated with both systems underwent localized corrosion at the sites of holidays and pinholes and inside channel areas at the leading and trailing edges of plates where the coating appeared thin.

In general, the Plasite 4140 system performed better than the 1505C coating as revealed by a fewer holidays in the coating and a lower degree of attack in the channel areas. This is attributed either to fewer voids in the coating as sprayed, a retardation of holiday formation and subsequent corrosion at existing voids, or better overall protection with a thick film coating system. However, surface preparation and coating application procedures should be reviewed for both systems in an effort to eliminate or minimize this form of attack.

Task 4. Evaluation of Conventional Corrosion Control Measures

The most common methods currently used for precipitator corrosion control involve attempts to increase precipitator component and structural surface temperatures by raising the inlet flue gas temperature. Temperature maintenance is typically accomplished through increased

boiler loading, removal of economizer tubes, or installation of a bypass ductwork and damper system at the cascade evaporator. Temperature data compiled for the thermocoupled Springfield precipitator indicated that changes in precipitator inlet gas temperature had a profound effect on metal surface temperatures in the middle and upper zones of the precipitator, but had very little effect on temperatures in the lower zone near the liquor bath where most of the corrosion damage occurs.

A 25 °F increase in inlet flue gas temperature resulted in a 15 - 20 °F increase in sidewall, chamber dividing wall, and access door temperatures for moderate to high elevations in the precipitator. The same 25 °F temperature increase resulted in only a 3 - 10 °F increase in temperature on lower sidewalls and the lower outlet wall of the precipitator, where temperatures are inherently cooler. Proximity to the relatively cold liquor bath as well as the insulating effects of heavy saltcake buildup in the lower zone contribute to the low metal surface temperature. Additionally, most precipitators have baffles and distribution plates arranged to minimize flue gas flow in the lower few feet of the precipitator, which prevents flue gas dust particles from bypassing the collector plates. This results in an area of gas stagnation and minimizes the effect of increased inlet gas temperatures on metal surfaces in the lower zone.

Thermal insulation is also used to raise the temperature of the internal components of electrostatic precipitators. An uninsulated metal plate installed on the lower outlet wall of the precipitator had an internal metal surface temperature of about 150 °F. The same plate, with two inches of fiber type insulation, measured nearly 200 °F, an increase of almost 50 °F. With four inches of insulation, the temperature increased to 230 °F. It is clear that adequate, properly installed and maintained thermal insulation is a valuable asset in temperature maintenance.

Heat jacketing is another method that has been used as a corrosion control method for electrostatic precipitators. The precipitator is constructed with a double wall, or heat jacket, and air is circulated through steam/air heat exchangers to effectively raise the temperature of the inner wall. Heat jacket systems are often backed up with electrical resistance heaters for temperature maintenance during periods when steam is not available, or for supplementary heating when precipitator temperatures are very low. Heat jacket systems have been shown to be effective at raising precipitator temperatures by as much as 40 °F, though the effect is less pronounced in the lower zones of the precipitator. One important drawback of heat jacketing is that it is very difficult to heat jacket an entire precipitator. The two sidewalls are easily and most frequently heat jacketed; however, rapper mechanisms and transformers on the roof, and the wet bottom agitator dry drag scraper systems on wet and dry bottom pans often prevent the installation of heat jacketing in those areas. The inlet and outlet walls, along with the associated large ductwork systems, are extremely difficult to heat jacket.

Bypass ductwork and damper systems at the cascade evaporator have been shown to be an effective method for raising precipitator inlet flue gas

temperatures. In this technique, a portion of the flue gases is withdrawn from the main ductwork system near the economizer section, directed around the cascade evaporator, and reintroduced into the main ductwork system just upstream from the precipitator inlet. The hot bypassed flue gas is mixed with the relatively cool flue gas that has passed through the cascade evaporator for liquor evaporation purposes. The amount of bypass gas is controlled by using an automated damper system to obtain some target precipitator inlet gas temperature. A major drawback of this method is similar to all corrosion control methods that are directed towards precipitator temperature maintenance by increasing inlet gas temperatures: The effect is most pronounced in the upper portions of the precipitator, where temperatures are already high and corrosion low, rather than in the lower portions where the temperatures are low and the corrosion severe.

In order to determine the effects of varying operating conditions on precipitator corrosion, four flush mount and two retractable electric resistance (ER) probes were installed in the No. 3 precipitator at the Weyerhaeuser mill. The sensor elements of the flush mount probes were thicker than those used in the previous test. Two of the sensors were 10 mils thick and two others were 20 mils thick, so that corrosion data could be obtained over a longer period of time. One probe of each size was mounted on both the east and west side of the precipitator at the outlet end close to the bottom area. Arrangements were made with mill personnel to vary operating conditions and the position of the bypass damper over a period of several days.

The results are shown in Figs. 45 - 48. Unfortunately, the temperature at the location of the probes was not below the water dew point for any extended period of time. The corrosion rates measured for all of the flush mount ER probes were fairly constant throughout the test, and as shown in Fig. 49, this rate was maintained for over 1000 hours, at which time the monitoring was terminated due to the relocation of the Institute. The test may not have helped to reveal any new information regarding the effect of varying recovery boiler operations on precipitator corrosion, but it did show that with thicker ER probes the corrosion rate can be monitored for long periods of time. The retractable ER probes did not work at any time during the monitoring period despite several attempts by mill personnel to correct the problem.

Task 5. Contributing Factors in Precipitator Corrosion

Efforts were undertaken to investigate the corrosion characteristics of chemical saltcake, which was believed to play a significant role in relation to a water dew point controlled corrosion environment. Saltcake samples collected from a number of different precipitators were evaluated compositionally and with regard to corrosive species. The effects of pH and saltcake composition on the corrosion of carbon steel were investigated in the laboratory by exposing the steel to various saltcake/water combinations. Samples of corrosion products from active corrosion sites in electrostatic precipitators were analyzed in a further effort to obtain mechanistic

information and identify corrosive species. The uniformity of composition of single saltcake particles was examined in an effort to prove or disprove the theory of acid adsorption on the surfaces of saltcake particles in the upper regions of the recovery furnace.

Chemical saltcakes were collected from several precipitators and analyzed with regard to composition (Table 11). Saltcakes were comprised largely of sodium sulfate (Na_2SO_4), with smaller quantities of sodium carbonate (Na_2CO_3), sodium chloride (NaCl), and sodium sulfite (Na_2SO_3). Sodium thiosulfate ($Na_2S_2O_3$) was not detected in appreciable quantities in any of the samples. Most samples also contained some potassium compounds similar to those listed, where sodium was replaced by the similar alkali metal group element potassium.

Saltcakes were dissolved in distilled water at varying concentrations and pH values were determined (Table 12). pH values ranged from near neutral (pH about 7) to moderately basic (pH around 10). Pure sodium sulfate exhibits a neutral pH in water, while sodium carbonate is basic, pH of 11, apparently causing the moderate basicity of some saltcakes.

Tests were conducted to determine the corrosivity of the various saltcakes toward plain carbon steel using weight loss methods. Corrosivity of saltcake/water combinations was evaluated at several concentrations, pH values, and with additions of potentially corrosive species. The tests were conducted to determine if the magnitude of corrosion rates determined through weight loss and electronic measurements in the field can be duplicated in the laboratory, and if so, to identify chemical constituents or conditions responsible for the high rates of corrosion found in precipitators. Tests were also conducted to see if the corrosivities of real saltcakes could be duplicated by simulated saltcakes composed of reagent grade chemicals. The weight loss exposure tests were conducted at 180 °F, which is in the range of water dew points measured for precipitator flue gases at several mills.

The tests were conducted on carbon steel weight loss specimens in closed test cells in the laboratory. The duration of the exposures was from six to eight weeks. Real saltcakes collected from various kraft recovery furnace precipitators were examined first, using concentration and pH as variables. Saltcake concentration was found to have little effect on the rate of corrosion when examined over a four decade range of concentrations. The pH had a significant affect on the corrosion rate when examined over a range from the natural pH of the saltcake to pH 3. The corrosion rate increased fivefold from the natural pH to pH 3 in the saltcake solutions.

Additions of various concentrations of species such as chloride, thiosulfate, carbonate, and sulfite to the saltcakes produced no predictable effect on the corrosion rate. Again, the pH of the saltcake solution remained the primary factor for corrosion.

Synthetic saltcakes, made up of reagent grade chemicals, behaved similarly to the real saltcakes with respect to corrosion, indicating that no particularly aggressive species had been missed during saltcake analysis.

The highest rates of corrosion determined with the laboratory saltcake studies were lower than those found with the flue gas test chambers by a factor of 2 or 3, implying that the value of the laboratory test is limited. The laboratory tests provided only the crudest representation of corrosive conditions on an actual precipitator surface at the temperature, and factors such as heat transfer, surface deposits, and gaseous environmental effects on corrosion could not be determined. It is also important to remember that the high corrosion rates measured on specimens in the flue gas test chambers occurred in the absence of flue gas particulate.

Corrosion Products

Samples of corrosion products from active corrosion sites on carbon steel in an electrostatic precipitator were secured. Multilayered corrosion products that formed beneath wet, sticky saltcake deposits (Fig. 50) were analyzed in cross-section with X-ray diffraction and energy dispersive spectroscopy (EDS) techniques. At least five distinct layers were identified, including two layers of corrosion products adjacent to the corroding metal surface, and three layers of saltcake deposits above the corrosion products. Layer 1, the layer of corrosion products next to the surface of the metal was composed of 60% goethite (FeO(OH)) and 40% hematite (Fe_2O_3). The second layer of corrosion products contained 70% hematite, 15% goethite, 10% sodium sulfate-form 5 (Na_2SO_4-V), and 5% sodium chloride (NaCl). The third layer was a dark brown layer of mostly saltcake consisting of 70% sodium sulfate-form 5, 15% sodium sulfate-form 3 (Na_2SO_4-III), and 15% hematite. Layer 4 was a light tan saltcake layer composed of 65% sodium sulfate-form 5, 25% sodium sulfate-form 3, 5% aphthitalite ($K_3Na(SO_4)_2$), and 5% hematite. The outer layer was a layer of pure white saltcake and its primary constituents were 80% sodium sulfate-form 3, 10% sodium sulfate-form 5, and 10% aphthitalite. The results are summarized in Table 13.

The corrosion products in layers 1 and 2 are attributed to compounds formed during corrosion reactions occurring at or below the dew point. The compounds are representative of reaction products of iron formed under oxidizing conditions. Condensed moisture combined with the soluble ionic saltcake species provides the corrosive environment. The rate of corrosion is then enhanced by high temperatures at neutral or slightly acidic conditions in the presence of oxygen. Tests conducted earlier with litmus paper on condensed moisture and moist saltcake deposits for actual precipitator surfaces indicated a pH range of 5 - 6.

Layers 3 and 4 are intermediate layers containing both corrosion products and saltcake species. The fifth layer is representative of the overall composition of the recovery flue gas saltcake dust. Sodium sulfate, the primary constituent of the saltcake, was discovered to exist in two polymorphic forms. The ratios of the two forms are observed to vary

through the thickness of the saltcake deposit. This is indicative of a temperature gradient through the deposit because the two forms of sodium sulfate are known to form at different temperatures. The thermal insulating effects of a significant saltcake buildup on the temperature of a precipitator surface may be profound.

Flue Gas Condensate

Condensate was collected at the Great Southern Paper Company, Cedar Springs mill at four different locations in the flue gas stream by cooling the gas 20 °F below the ambient gas temperature. Table 14 gives the analysis data obtained for the condensates.

The sodium and potassium content (cations) were low compared with anions, in all samples, indicating that the constituents in the condensate are mainly acids. An exception is the sample taken in the bypass duct before the precipitator, where a substantial amount of sodium was present. Saltcake contamination is the likely explanation for this high level of sodium. The reason for the nearly total absence of metal anions in the three other samples is the result of a lower level of solids in the flue gas after the cascade evaporator and the precipitator. The amount of metal ions in sample 3 does not balance the sulfate content, leaving part of the sulfate free in acidic form.

The pH values found were all surprisingly low. Such low values for the pH can not be explained by the presence of weak acids like H_2CO_3, or the presence of organic acids. The amounts of sulfate found, if totally in an acidic form, would result in a lower pH value than measured, less than 2, with the exception of the sample taken at location "After CE", where the sulfate content seems to match the pH measured. It is likely that the strongest acid, sulfuric, is partially neutralized by some compound not analyzed.

Additionally, the analysis results indicate that the acidic oxides, CO_2 and SO_2, react in the cascade evaporator with the black liquor giving rise to an increase in the gas of sulfur species (thiosulfate). The gas emitted must be hydrogen sulfide (H_2S) which would result in a higher apparent thiosulfate concentration. Thiosulfate is not stable at the low pH measured, but the thiosulfate could be related to more stable polythionates. Thiosulfate and polythionates are difficult to separate analytically from each other. Polythionates are known to be formed in reactions between SO_2 and H_2S.

In any case, if the acidic condensates come in contact with the precipitator components, heavy corrosive attack on carbon steel would occur. Saltcake, being neutral or moderately alkaline, will help buffer the acidic condensate in a real situation, and therefore cause the condensates to be less aggressive.

Environmental Factors

As was mentioned under Task 3, the test chamber was removed from the Westvaco mill. Two modified chambers were installed at the Great Southern Paper Company mill; one in the flue gas stream directly downstream of the economizer section (Fig. 51), and the other in the flue gas stream downstream from a cascade evaporator (Fig. 52). Flue gas is withdrawn from the main recovery boiler ductwork system, through the test chambers, and returned to a downstream location just before the precipitator. Corrosion coupons are mounted on controlled temperature surfaces ("cold fingers", see Fig. 25) that use air and water cooling to sustain preselected temperatures and simulate cold, corroding internal precipitator surfaces. Corrosion rates were determined by measuring the weight loss of the corrosion coupons. Each system was capable of simultaneously determining corrosion rates for 40 specimens in a range of temperatures from 100 to 350 °F.

The test chambers were used to supplement and confirm material rankings developed in flue gas systems at other mills. The locations of the test chambers also determined the effect of direct contact evaporators on flue gas corrosivity. Finally, the test chambers were used to determine the effects of saltcake on corrosion.

Four test runs were carried out using the test chambers. Runs 1 and 3 did not have saltcake additions while runs 2 and 4 did. Two runs were required at each condition in order to provide information over a wider range of temperatures than was possible with only one run. In the runs with saltcake additions, an approximately 1/2 inch layer of saltcake powder was placed on top of each corrosion coupon. The powder was held in place by attaching a Teflon mold to each of the temperature probes.

The results of each run are summarized in Figs. 53 - 56 for the carbon steel coupons, and in Tables 15 - 18 for the stainless steel coupons. The results obtained help to confirm the material ranking that was developed from previous test data. Below the water dew point, there was heavy corrosion on the carbon steel coupons and pitting was present on the 304L and 310 stainless steel coupons. Above the water dew point there was very little corrosion present on any of the coupons.

The corrosion data obtained at the Cedar Springs mill demonstrate that the presence of saltcake on the coupons did not change the corrosion condition in a significant way at either test location, i.e., before or after the cascade evaporator. This result is consistent for all metal grades tested. The reason is believed to be that the inlet filter at the test chambers served as good contact surface for reactions between the incoming flue gas and the saltcake collected on the filter. The acidic gaseous species became supposedly neutralized by the carbonate in the saltcake. Thus, the saltcake did not show any additional effect inside the chamber. In any case, the results show that the saltcake does not have any harmful effect. On the contrary, the carbonate, moving with the flue gas to the precipitator area, is beneficial from the corrosion point of view.

Duplicate corrosion tests were conducted with corrosion coupons without a saltcake cover at Cedar Spings mill and it was expected to obtain similar results from the seemingly similar conditions. Indeed, the results from the two runs show that relatively heavy corrosion takes place below the so called critical temperature which is believed to coincide with the water dew point and only slight corrosion was seen above it. This holds true for both test locations, i.e. in the flue gas before and after the cascade evaporator. However, some dissimilarities in results from the duplicate runs were also observed. The run conducted in December - January resulted in almost an equal critical temperature value (150 °F) for both test locations (Fig 53), but the run performed in May - June gave nearly the same value only for the test conditions after the cascade (160 °F) and a substantially lower value for the conditions before the cascade (120 °F, Fig. 55). One explanation might be that the flue gas entering the cascade was dry in summer time and after it had picked up water from the cascade the dew point and the critical temperature were higher.

A similar seasonal trend was observed in the two runs conducted with saltcake cover over the coupons. In the run conducted in June-August , the critical temperature became 110 °F for the flue gas before the cascade and 160 °F after it (Fig. 56) whereas in the run performed earlier in the spring such a difference in the critical temperature between the two test locations was not observable (Fig. 54, ca 125 °F for both).

The most severe corrosion impact should take place just below the dew point, when the surface becomes just wetted and the water film is relatively concentrated by corrosive species absorbed from the gaseous phase. At a still lower temperature, more water is condensed and the liquid film on the metal will then be diluted and less aggressive. Thus, a relatively narrow temperature range for high corrosion rate should be seen below the dew point. Unfortunately, it was not possible in each run to cover the temperature range of the most interest with evenly distributed data points in order to trace point for point the effect of the temperature below the dew point. Some of the plots obtained in this work indicate of the existence of such a maximum, e.g., Fig. 56.

CONCLUSIONS AND RECOMMENDATIONS

1. Corrosion in electrostatic precipitators is associated with the flue gas water dew point, not the acid dew point as generally is believed. This is the outstanding finding of the entire project. Chemical recovery boiler flue gases contain unusual high levels of moisture, unlike other industrial boiler systems.

2. An effective on-line monitoring system has been developed. Flush mount electrical resistance (ER) probes are useful to determine corrosion rates at sites of suspected problems; however, in order to be most effective, these probes must be properly located. There were many problems with the retractable ER probes so they are not considered reliable.

Electrical conductivity probes are helpful for spot checks of the dew point. If thermocouples are placed in locations where low temperatures are likely to occur, these temperatures can be compared with the dew point to see if a potential corrosion environment exists.

At a minimum, every precipitator should be instrumented with weld pad type thermocouples and the dew point should be checked periodically.

3. The testing of conventional corrosion control techniques revealed that changing recovery boiler operation and flue gas temperature are not effective ways to reduce corrosion problems. When flue gas temperature is raised, the water dew point also rises. Also, raising flue gas temperature has only a small effect on temperatures in those parts of the precipitator where severe corrosion is experienced (bottom near liquor bath, outlet end of precipitator, etc.).

Heat jacketing and thermal insulation are more effective at raising internal precipitator wall temperature, but it is not feasible to heat jacket the entire precipitator, and there are locations where thermal insulation is extremely difficult, if not impossible, to install. All the precipitators studied were of wet bottom design; dry bottom precipitators are not as susceptible to the severe corrosion damage sustained by wet bottom precipitators as experienced in Scandinavian mills.

4. A ranking of material resistance to corrosion has been completed for both metals and protective coatings. Austenitic stainless steel type 316L was shown to be the most cost-effective metal for use in precipitators in those areas difficult to maintain above the water dew point. Where the precipitator temperature can be maintained above the water dew point, carbon steel is a cost-effective construction material.

Two categories of protective coatings were evaluated: those for protection of precipitator structures and ductwork systems, and conductive coatings used to protect precipitator collector plates. The vinyl ester systems, Plasite No. 4100 and Plasite No. 470, had the best performance for protecting general components, while Plasite No. 4140 performed best when protecting collector plates. The protective coating systems may be useful for protecting

components that cannot be effectively protected against corrosion by other methods.

5. Environmental factors which could have an influence on corrosion were also studied. Chemical analyses of corrosion products, and saltcake, condensate, and flue gas composition were performed. Corrosion product analysis indicated that the corrosion occurs in an oxidizing environment. The composition of saltcake was predominantly sodium sulfate (Na_2SO_4) and sodium carbonate (Na_2CO_3) with a small amount of potassium compounds present. The pH measured at actual corrosion sites was around 5 - 6, while that of the condensate was much lower (pH = 2.5 - 3). The reasons for this difference are not understood. The flue gas contained an insignificant amount of SO_3.

Tests using corrosion coupons indicated that the water dew point and water condensation are the main factors affecting corrosion in electrostatic precipitators. Above the water dew point there was very little corrosion on any of the metal coupons, while below this temperature, corrosion was very severe for carbon steel. Stainless steels 304L and 310 underwent pitting corrosion below the water dew point. This behavior was repeated when there was a layer of saltcake present on the corrosion coupons. The discovery that corrosion is associated with the water dew point, not with the acid dew point, is the outstanding finding of this entire project.

The water dew point is dependent on the water content of the flue gas. This is affected by different factors such as the water content of the heavy black liquor, passage of the flue gas through the cascade evaporator, and in a minor way by air humidity and liquor composition. A higher water content means a higher water dew point and, for the coldest parts of the precipitator, a greater risk for corrosion.

ACKNOWLEDGEMENTS

A special thanks is extended to the members of the CKPG technical committee who assisted in the successful completion of this project. An expression of gratitude is directed toward those staff members at the mills who directly assisted in all activities during the project program. Very special thanks are extended to Mr. Craig Thomson who initiated the project work and successfully conducted a majority of it until the relocation of the Institute and to Mr. Greg Fonder who continued and completed the work. Finally, many thanks to the analytical staff of the Institute of Paper Science and Technology and the secretaries who assisted in the successful completion of the project.

Table 1. Average corrosion rates and temperatures experienced during the lifetime of four flush mount ER probes in the No. 3 precipitator.

Probe No.	Average probe Temperature (°F)*	Average Corrosion Rate (mpy)
3	145	180
5	155	230
6	175	200
4	180	100

*Measured flue gas dewpoint temperature was 160 - 175 °F

Table 2. Alloys for corrosion resistance evaluation.

Carbon steel	Stainless steel	Nickel base alloys	Titanium
C1010	304L 310	Hastelloy G3	Ti Gr 1
A285 GrC	316L 316LM	Hastelloy C276	Ti Gr 7
Corten A	317L 317LM	Hastelloy C22	
Corten B	254 SMO	Inconel 825	
	AL-6X-N	Inconel 625	
	SAF 2205		
	29-4-2		

Table 3. A summary of corrosion rates measured on weight loss coupons exposed at six different locations in the No. 3 preccipitator

	Test Panel I. D. Number					
	1	2	3	4	5	6
Exposure Temp.(°F)	255 - 310	230	200	240 -295	290	235 - 290
Test Material	Corrosion Rate (mils per year)					
C1010	0.5	1.8	30.4	1.2	0.5	4.8
A285-C	0.5	2.8	28.2	1.3	0.6	2.8
Corten A	0.4	1.5	46.2	0.9	0.4	0.6
Corten B	0.5	4.4	40.9	0.7	0.5	1.9
304L	nil*	0.1	0.1	nil	nil	nil
310	nil	nil	nil	nil	nil	nil
316L	nil	nil	nil	nil	nil	nil
316LM	nil	nil	nil	nil	nil	nil
317L	nil	nil	nil	nil	nil	nil
317LM	nil	nil	nil	nil	nil	nil
AL-6X-N	nil	nil	nil	nil	nil	nil
SAF-2205	nil	nil	nil	nil	nil	nil
254 SMO	nil	nil	nil	nil	nil	nil
29-4-2	nil	nil	nil	nil	nil	nil
Hastelloy C-22	nil	nil	nil	nil	nil	nil
Hastelloy C-276	nil	nil	nil	nil	nil	nil
Hastelloy G-3	nil	nil	nil	nil	nil	nil
Inconel 625	nil	nil	nil	nil	nil	nil
Inconel 825	nil	nil	0.6	nil	nil	nil
Titanium GR. 1	nil	nil	nil	nil	nil	nil
Titanium GR. 7	nil	nil	nil	nil	nil	nil

*nil corrosion is defined as < 0.1 mpy

Table 4. A description of the coatings included in the study.

Coating Name	Description	Typical Application Method
Plasite No. 9500	High bake, high solids modified epoxy, amine cured	Sprayed
Plasite No. 9570	Low bake, high solids modified epoxy, amine cured	Sprayed
Plasite No. 5306	Ambient cured, monolithic epoxy liner	Troweled
Plasite No. 4100	Vinyl ester	Sprayed
Plasite No. 470	Conductive vinyl ester	Sprayed
Seal & Glaze 350	Two-part Novoloc epoxy	Sprayed/ Brushed/ Rolled
Seal & Glaze 500	High temperature, two-part Novoloc epoxy	Sprayed/ Brushed/ Rolled

Table 5. A description of the test panel locations, exposure temperature, and corrosion rates on unprotected carbon steel.

Location in Precipitator	Temperature Range	Corrosion Rate
Welded to an I-beam support, in the inlet gas stream, approximately 10 feet from precipitator bottom in east chamber	275 - 320 °F	< 1 mpy
Welded to an I-beam support, in the outlet gas stream, approximately 10 feet from precipitator bottom in west chamber	240 - 290 °F	8 mpy
Welded to the chamber dividing wall, near the outlet, approximately 12 feet from precipitator bottom in west chamber	265 - 310 °F	1 mpy

Table 6. A summary of coating performances at each of the three exposure sites in the No. 3 precipitator.

	Performance at Each Exposure Location		
Coating Type	A*	B*	C*
Seal & Glaze 350	3,5	5 slight 3,6	5
Seal & Glaze 500	5	5 slight 3	5
Plasite No. 5306	3,5,9,10,11,12	5,9,10,11,12 slight 3	3,5,9,10,11,12 some 8
Plasite No. 9500	5	5	5 slight 6
Plasite No. 9570	3,5 slight 13	5,13	5
Plasite No. 470	slight 4	0	0
Plasite No. 4100	slight 4,5	slight 4,5,9,13	slight 4,5

0 = no change
1 = softened
2 = blistered
3 = cracked
4 = swelled
5 = discolored
6 = etched
7 = permeated
8 = dissolved
9 = embrittled
10 = pitted
11 = pinholes/holidays present
12 = air or solvent entrapment evident
13 = coating disbondment or excessive attack at surface damage site

*Locations are in same order as described in Table 5

Table 7. The results of thickness measurements for each of the test before and after exposure.

Coating Type	Average Coating Thickness Before Exposure (mils)*	Average Coating Thickness After Exposure (mils)*
Seal & Glaze 350	4	3
Seal & Glaze 500	3	2
Plasite No. 5306	> 40 (~100)	> 40 (~100)
Plasite No. 9500	17	16
Plasite No. 9570	14	15
Plasite No. 470	38	43
Plasite No. 4100	> 40 (~50)	> 40 (~50)

*average value for four thickness determinations

Table 8. The results of an elevated air temperature test for each of the candidate coatings.

Coating Type	Test Temperature (°F)*						Failure Type
	200	250	300	350	400	450	
Seal & Glaze 350	0	5	5	X			3,9
Seal & Glaze 500	0	5	5	5	5	X	3,9
Plasite No. 5306	5	5	X				2,3,10,11
Plasite No. 9500	0	0	5	5	X		2,4
Plasite No. 9570	0	0	5	5	X		3
Plasite No. 470	0	0	0	0	0	5	Did not fail
Plasite No. 4100	0	0	0	5	5	5	Did not fail

X = coating failure
0 = no change
1 = softened
2 = blistered
3 = cracked
4 = swelled
5 = discolored
6 = etched
7 = permeated
8 = dissolved
9 = embrittled
10 = pitted
11 = pinholes/holidays evident
12 = air or solvent entrapment evident

*Tests conducted in oven, ambient air, 100 hours duration per listed temperature.

Table 9. Relative overall performances of the candidate coatings for electrostatic precipitators applications.

Coating Type	Relative Performance
Seal & Glaze 350	Fair
Seal & Glaze 500	Good
Plasite No. 5306	Poor
Plasite No. 9500	Good
Plasite No. 9570	Fair
Plasite No. 470	Excellent
Plasite No. 4100	Good

Table 10. Locations of coated collector plates exposed in the Chesapeake mill No. 4 electrostatic precipitator.

Plate No.	Coating Type	Exposure Location
1	Plasite 4140	Leading edge of the inlet field, adjacent to the outside wall in the north chamber of the precipitator
2	Plasite 4140	Leading edge of the center field, adjacent to the outside wall in the north chamber of the precipitator
3	Plasite 4140	Leading edge of the center field, fourth plate from sidewall in the north chamber of the precipitator
4	Plasite 4140	Leading edge of the outlet field, adjacent to the outside wall in the north chamber of the precipitator
5	Plasite 4140	Leading edge of the outlet field, fourth plate from sidewall in the north chamber of the precipitator
6	Plasite 4140	Trailing edge of the outlet field, adjacent to the outside wall in the north chamber of the precipitator
7	CoroTech 1505C	Leading edge of the outlet field, adjacent to the outside wall in the south chamber of the precipitator
8	CoroTech 1505C	Trailing edge of the outlet field, adjacent to the outside wall in the south chamber of the precipitator

Table 11. Chemical Composition of saltcakes from four different kraft recovery furnace precipitators.

		SALTCAKE COMPOSITION (Weight Percent)					
Mill	PPT.	Na2SO4	Na2CO3	NaCl	Na2SO3	Na2S2O3	Other
A	No. 3	83.7	<0.5	3.1	0.5	<0.2	Potassium Compounds (12 %)
A	No. 4	96.2	<1.5	3.6	<1.0	<1.0	None
B	No.678	95.3	<0.5	0.2	--	<1.0	Unidentified (3 %)
C	No. 4	84.2	<0.5	1.3	<0.2	<0.2	Potassium Compounds (7 %) Unidentified (7 %)

Table 12. pH values determined for saltcakes at varying concentrations.

		SALTCAKE CONCENTRATION/pH VALUE				
MILL	Precipitator	10 ppm	100 ppm	1 g/L	10 g/L	100 g/L
A	No. 3	6.87	6.80	7.01	7.63	8.04
A	No. 4	6.80	6.86	7.49	8.14	8.44
B	No. 678	6.99	6.95	6.83	6.89	7.84
C	No. 4	7.68	7.03	9.22	10.04	10.07

Table 13. A summary of compositional data for the saltcake and corrosion product layers shown in Figure 45.

	SAMPLE COMPONENT (Weight Percent)					
Layer	$FeO(OH)$	Fe_2O_3	NaCl	Na_2SO_4-V	Na_2SO_4-III	$K_3Na(SO_4)_2$
1	60	40				
2	15	70	5	10		
3		15		70	15	
4		5		65	25	5
5				10	80	10

Table 14. Analysis for condensates collected before and after the cascade evaporator (CE), and before and after the precipitator (PPT).

	Condensate Analysis			
Location:	Before CE	After CE	Before PPT	After PPT
pH	2.7	2.5	3.3	3.0
Concentration (g/L)				
Chloride, Cl	0.2	0.1	0.8	1.6
Sulfite, SO_3	0.2	0.1	0.2	0.2
Sulfate, SO_4	9.8	0.1	5.3	8.0
Thiosulfate, S_2O_3	0.3	3.1	0.2	0.2
Carbonate, CO_3	2.0	0.7	1.8	3.1
Concentration (mg/L)				
Sodium, Na	3.7	2.8	1780	35
Potassium, K	16	0.5	158	4.2
Formic acid	5	5	2.5	2.5
Acetic acid	20	33	10	20

Table 15. Temperature and corrosion rate data of stainless steels without a saltcake layer on the coupons, 12/7/88 - 1/17/89.

Steel Grade	Before Cascade Evap.		After Cascade Evap.	
	°F	mpy	°F	mpy
304L	225	3.47	201	0.27
	175	1.12	161	0.27
	146	14.1	121	0.71
	139	1.51	201	0.42
310	233	0.29	209	0.34
	186	0.31	169	0.28
	145	5.88	122	0.29
	143	0.53	116	0.39
316L	241	0.45	217	0.35
	197	0.42	177	0.29
	151	0.38	124	0.34
	141	0.63	117	0.39

Table 16. Temperature and corrosion rate data of stainless steels with a saltcake layer on coupons, 4/6/89 - 5/23/89.

Steel Grade	Before Cascade Evap.		After Cascade Evap.	
	°F	mpy	°F	mpy
304L	206	1.26	258	0.79
	177	0.79	236	1.51
310	200	1.13	256	1.39
	165	0.67	225	1.19
	116	0.83	114	6.16
	113	1.11	102	12.2
	99	1.16	99	4.46
316L	196	1.07	254	0.77
	159	0.41	218	1.32
	125	0.61	118	1.12
	122	0.81	108	0.95
	110	0.78	97	0.74

Table 17. Temperature and corrosion rate data of stainless steels without a saltcake layer on the coupons, 5/25/89 - 6/27/89.

Steel Grade	Before Cascade Evap.		After Cascade Evap.	
	°F	mpy	°F	mpy
304L	229	2.47	231	5.87
	216	2.10	195	2.07
	102	5.78	152	24.5
	101	5.65	249	40.4
310	228	1.09	224	1.26
	223	1.70	184	1.31
	106	4.20	153	19.3
	97	4.30	150	13.5
316L	240	1.35	218	1.31
	217	1.15	173	1.07
	110	1.51	154	3.35
	93	4.84	150	2.04

Table 18. Temperature and corrosion rate data of stainless steels with a saltcake layer on the coupons, 6/29/89 - 8/22/89.

Steel Grade	Before Cascade Evap.		After Cascade Evap.	
	°F	mpy	°F	mpy
304L	250	0.03	216	0.03
	241	0.02	182	0.07
	105	1.88	133	5.02
	100	1.45	121	7.07
310	251	0.02	221	0.02
	244	0.03	198	0.04
	107	0.76	137	2.70
	101	1.31	125	8.19
316L	253	0.03	225	0.041
	246	0.02	208	0.19
	108	0.16	140	0.56
	102	0.33	127	13.3

THE INSTITUTE OF PAPER SCIENCE
AND TECHNOLOGY

Per-Erik Ahlers

Per-Erik Ahlers
Group Leader
Corrosion and Material Engineering Group
Chemical and Biological Sciences Division

E W Malcolm

Earl W. Malcolm
Director
Chemical and Biological Sciences Division

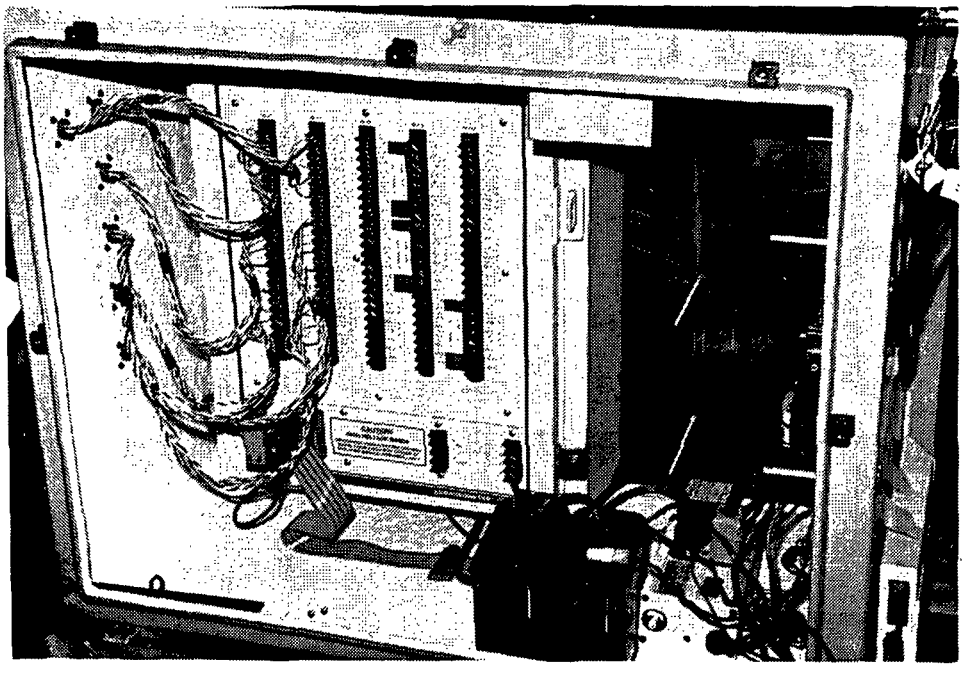

Figure 1. The ER system, microcomputer, and modem mounted in a weatherproof enclosure and installed in a control room on the roof of the No. 3 electrostatic precipitator at the Weyerhaeuser mill.

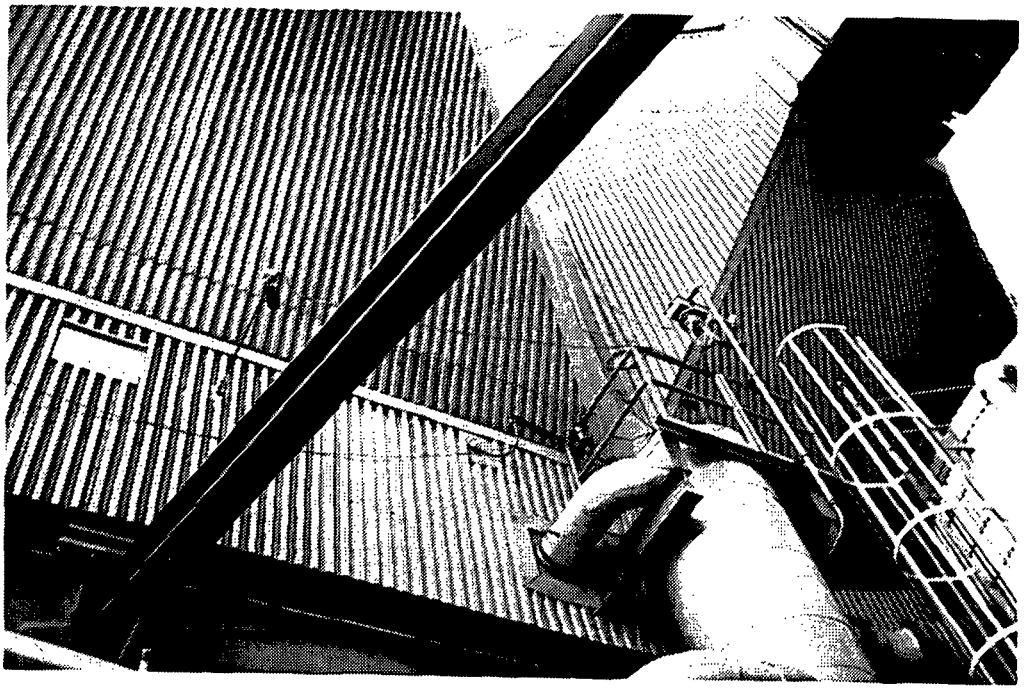

Figure 2. A view looking upward at the north wall of the No. 3 precipitator. Probes can be seen installed along the lower area of the wall, below the outlet ductwork.

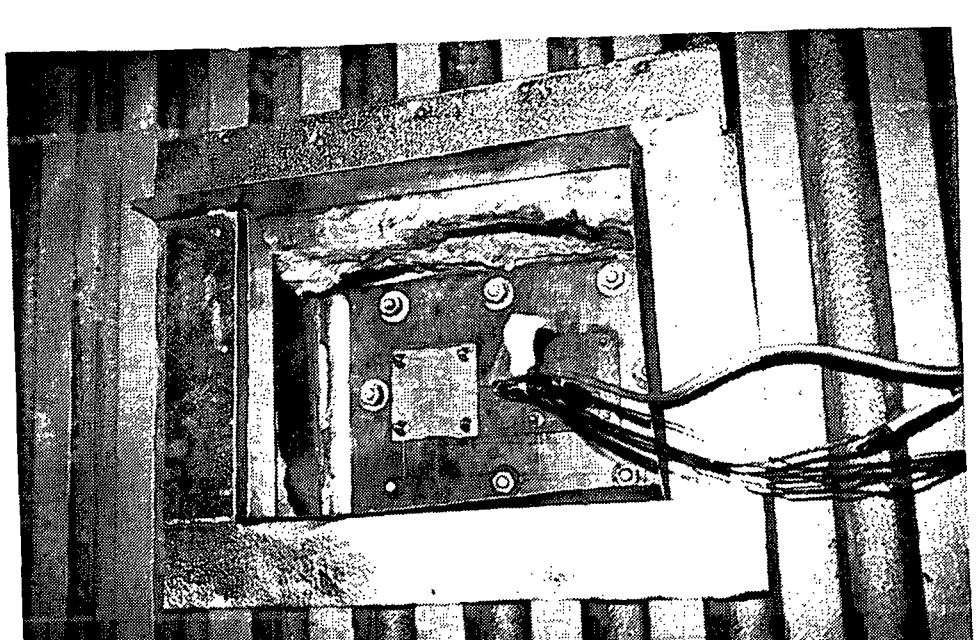

Figure 3. Flush mount ER probes were installed on access plates in both the east and west chambers of the precipitator.

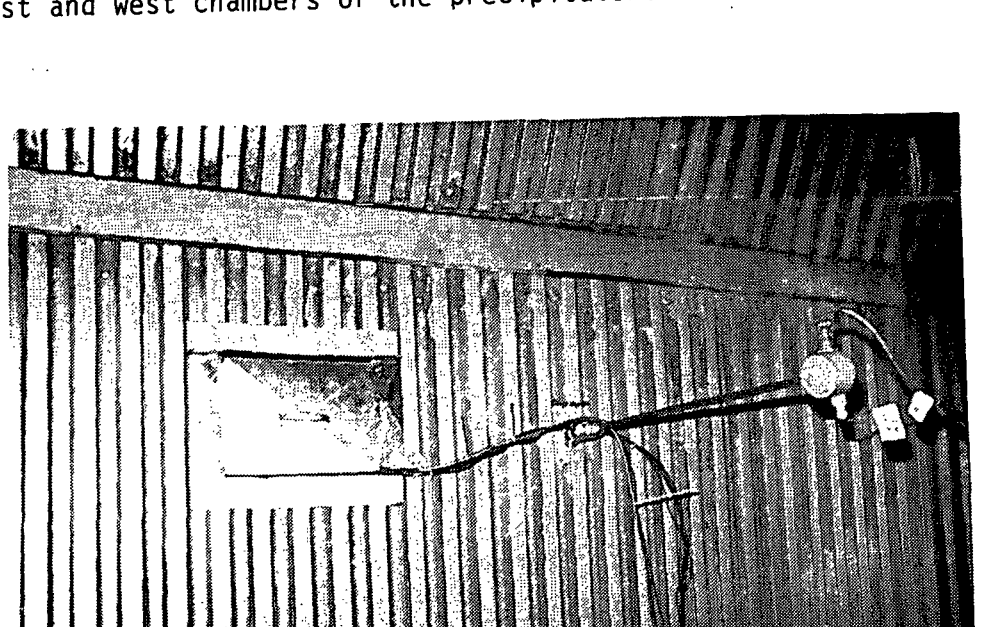

Figure 4. Retractable ER probes were installed adjacent to the flush mount probes along the north wall in both chambers of the precipitator.

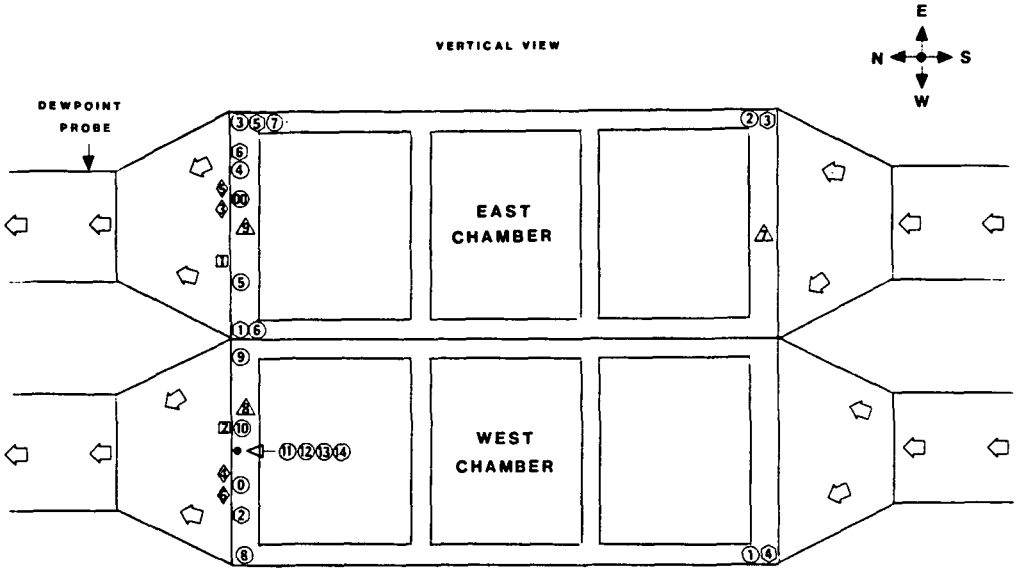

Figure 5. Springfield No. 3 precipitator showing test locations. (Key in Figure 6)

◇ LOCATION OF A FLUSH MOUNT ELECTRICAL RESISTANCE PROBE

□ LOCATION OF A RETRACTABLE ELECTRICAL RESISTANCE PROBE

○ LOCATION OF A WELD-PAD THERMOCOUPLE

⬡ LOCATION OF A WEIGHT LOSS/CREVICE/SCC SPECIMEN PANEL [a]

△ LOCATION OF A COATED SPECIMEN PANEL [b]

a Each panel contains 24 flat washer-type weight loss coupons, 3 crevice specimens, and 10 U-bend specimens.

b Each panel contains 24 coated specimens and 2 plain carbon steel weight loss specimens(for baseline corrosion data).

Figure 6. Symbol identification key for Figure 5.

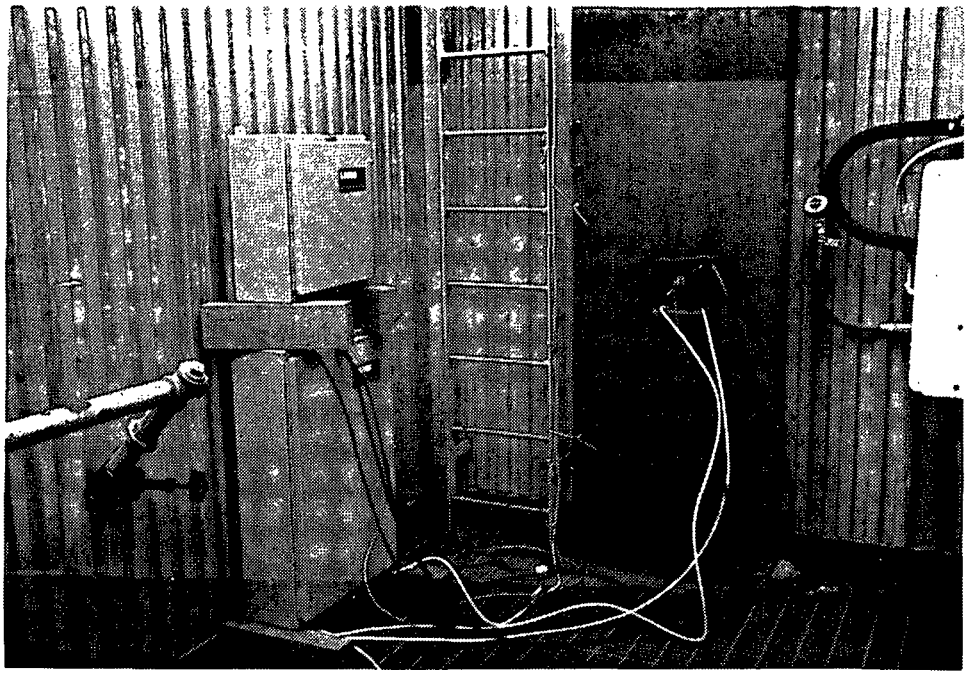

Figure 7. The dewpoint probe and related electronics were installed in the outlet ductwork at the east side of the No. 3 precipitator.

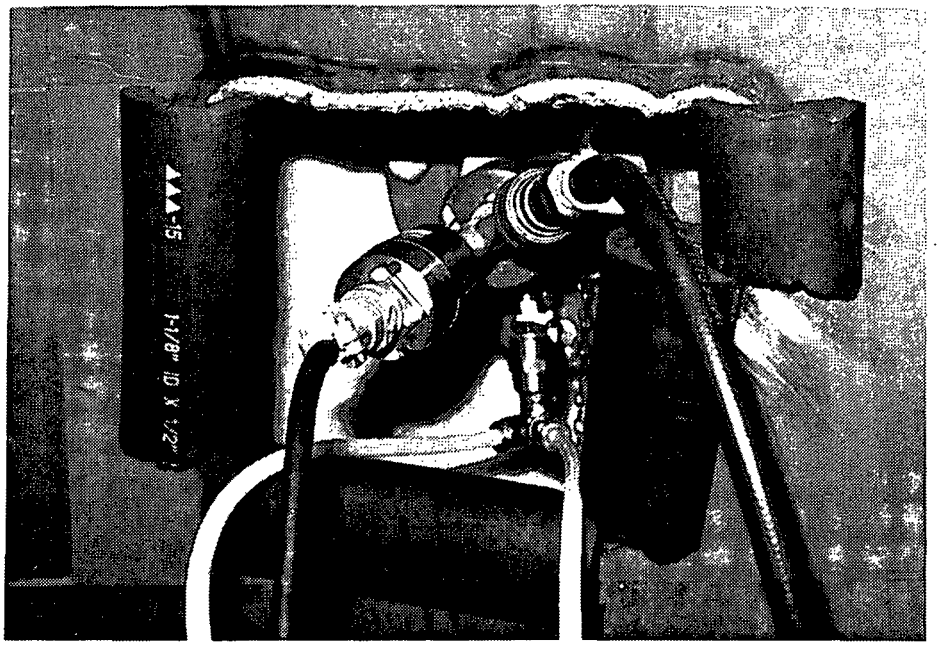

Figure 8. A close-up view of the conductivity probe shown in Figure 7. The hoses are required for periodic air cooling and water cleaning of the probe element surface.

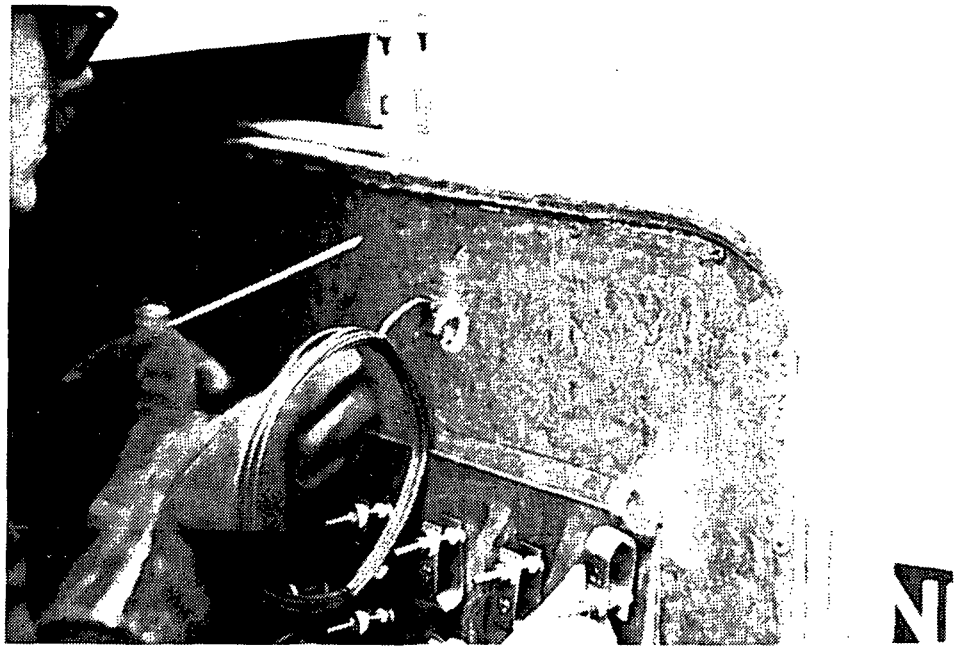

Figure 9. A weld pad thermocouple is shown being welded to the internal side of an access door of the precipitator for a metal surface temperature measurement at that location.

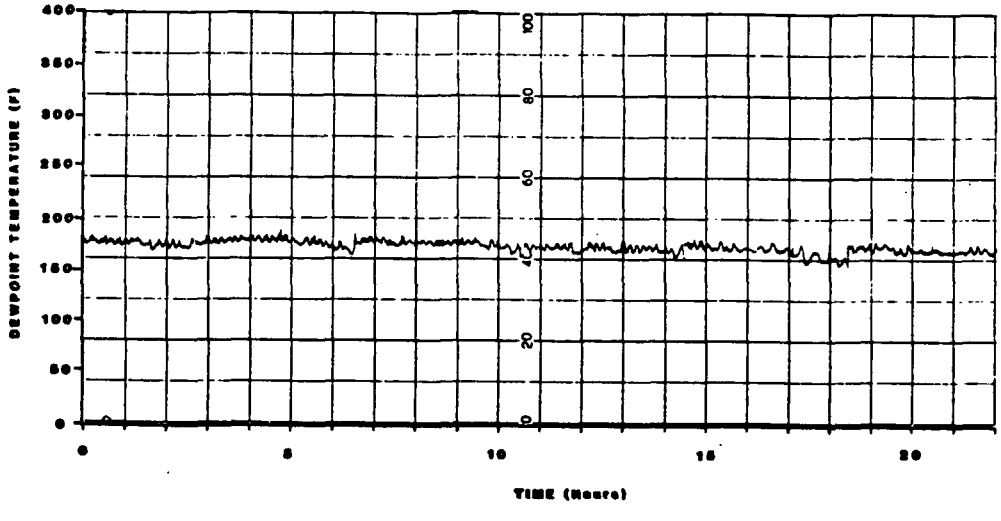

Figure 10. The flue gas dewpoint temperature typically ranged from 160-170°F during routine operation of the No. 3 recovery boiler.

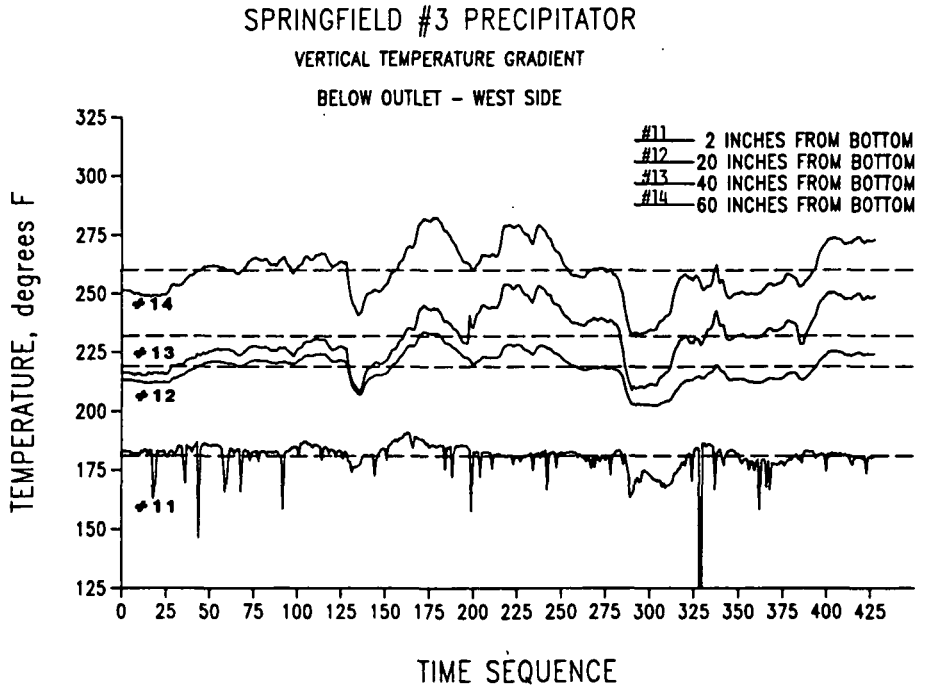

Figure 11. A vertical temperature profile for internal metal surfaces along the outlet wall of the No. 3 precipitator. Note: Dotted lines indicate average values.

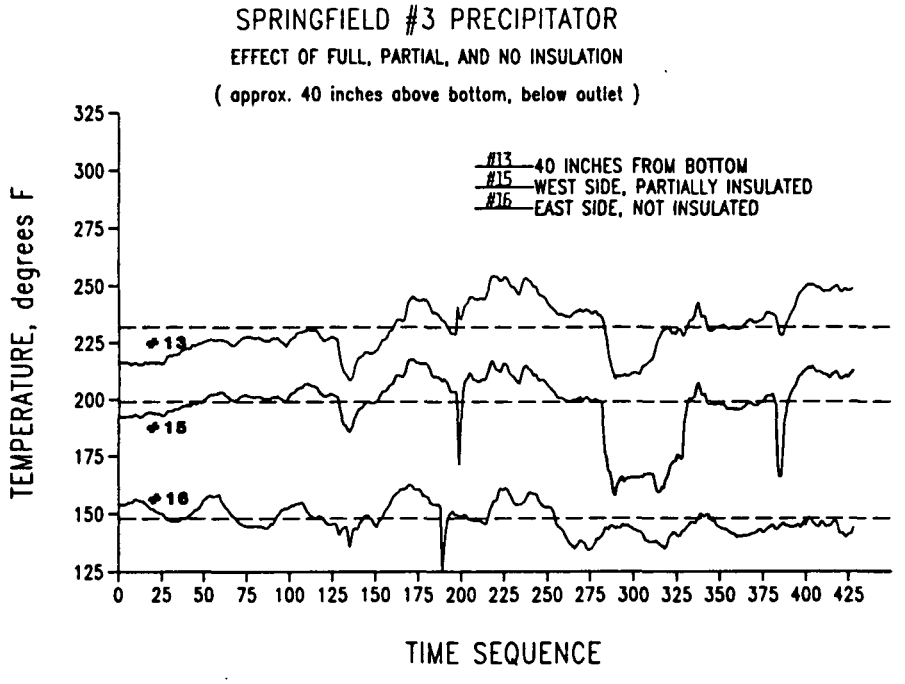

Figure 12. The effects of insulation on temperature retention of internal wall surfaces. Note: Dotted lines indicate average values.

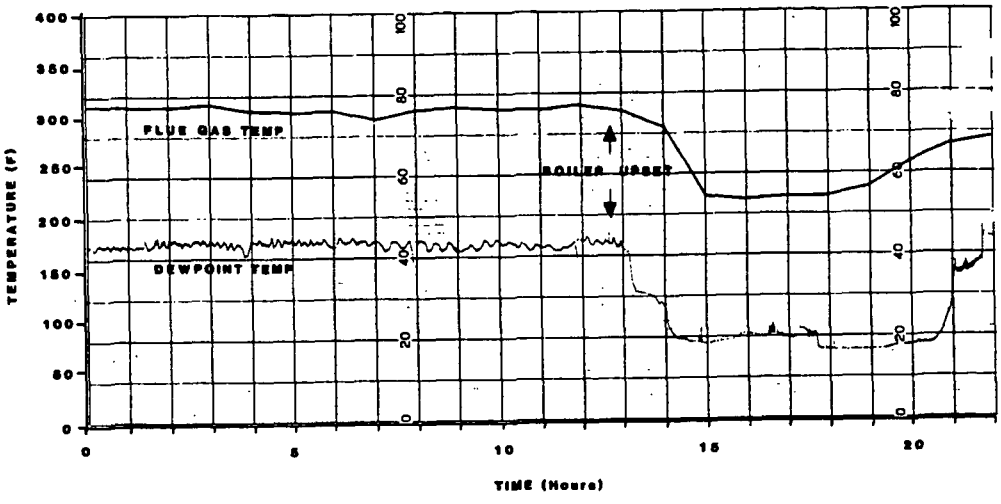

Figure 13. A recording of the precipitator inlet flue gas temperature and the dewpoint temperature. Both measurements were made in the east side ductwork system. Note the tendency for the dewpoint temperature to swing with the flue gas temperature.

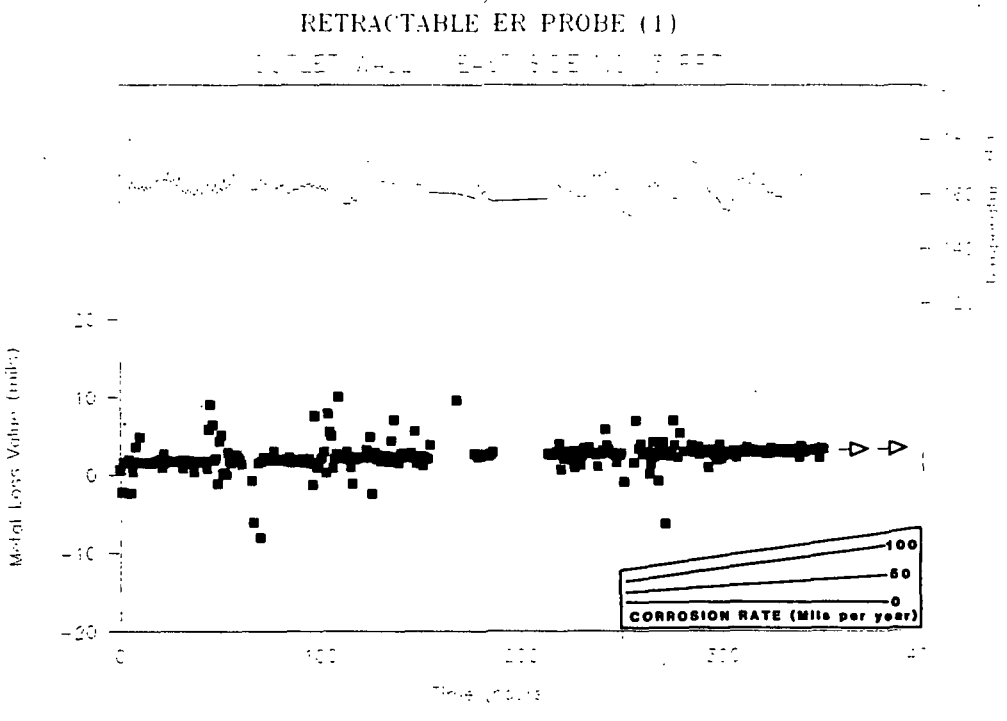

Figure 14. ER probe results from the Springfield mill.

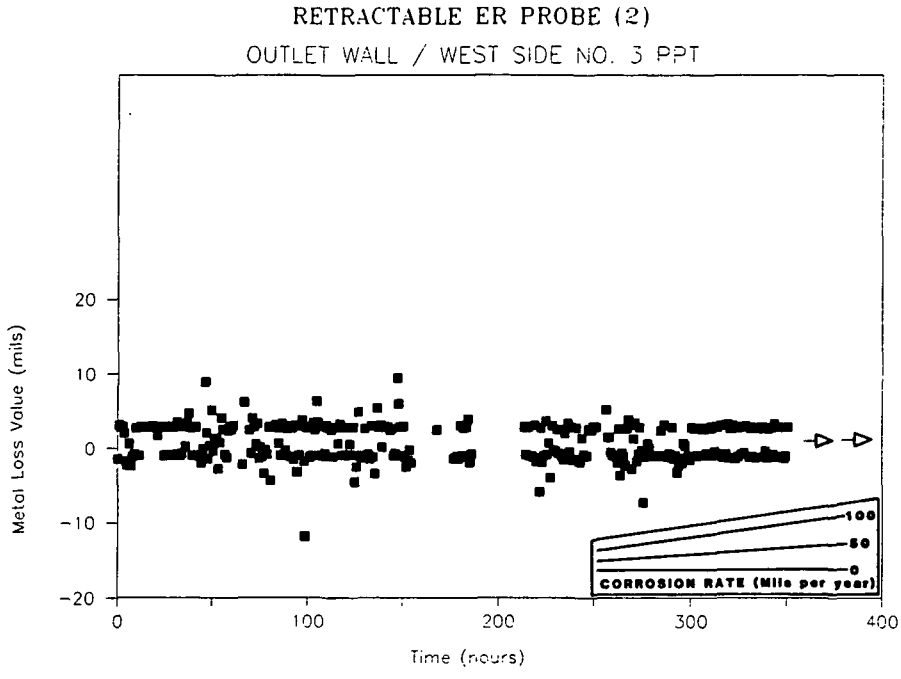

Figure 15. ER probe results from the Springfield mill.

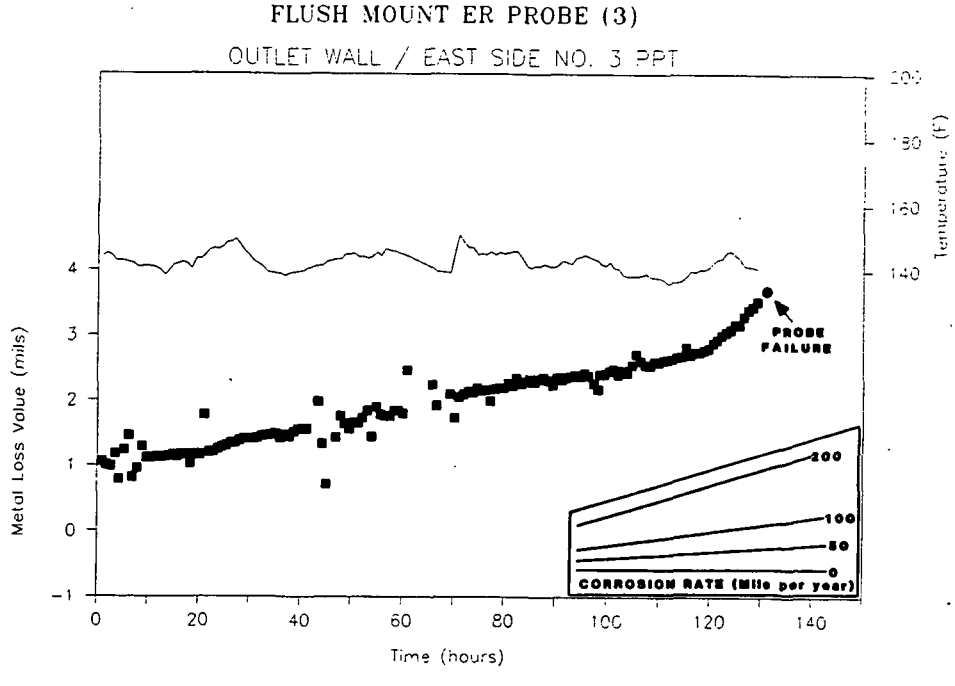

Figure 16. ER probe results from the Springfield mill.

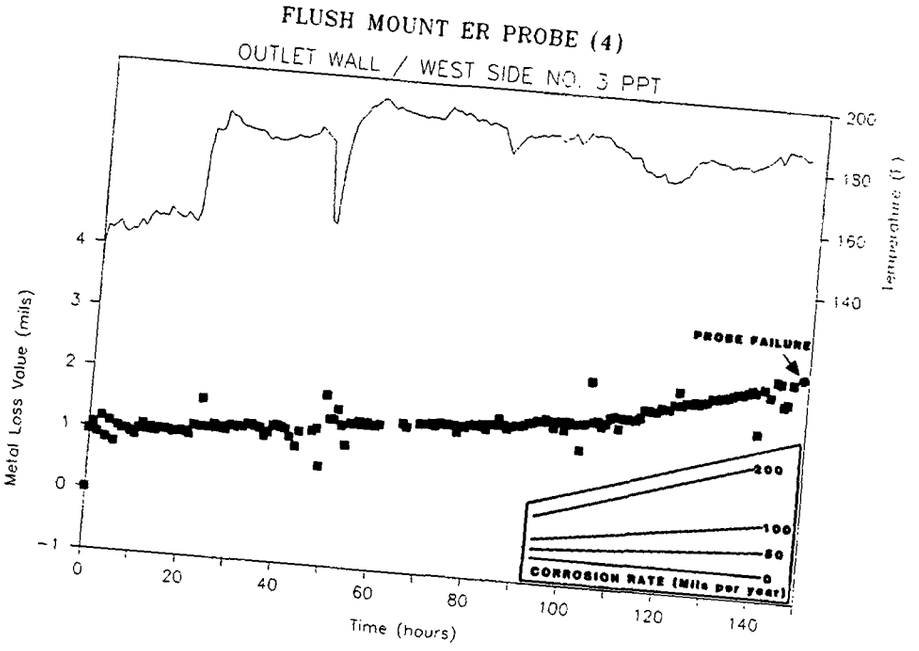

Figure 17. ER probe results from the Springfield mill.

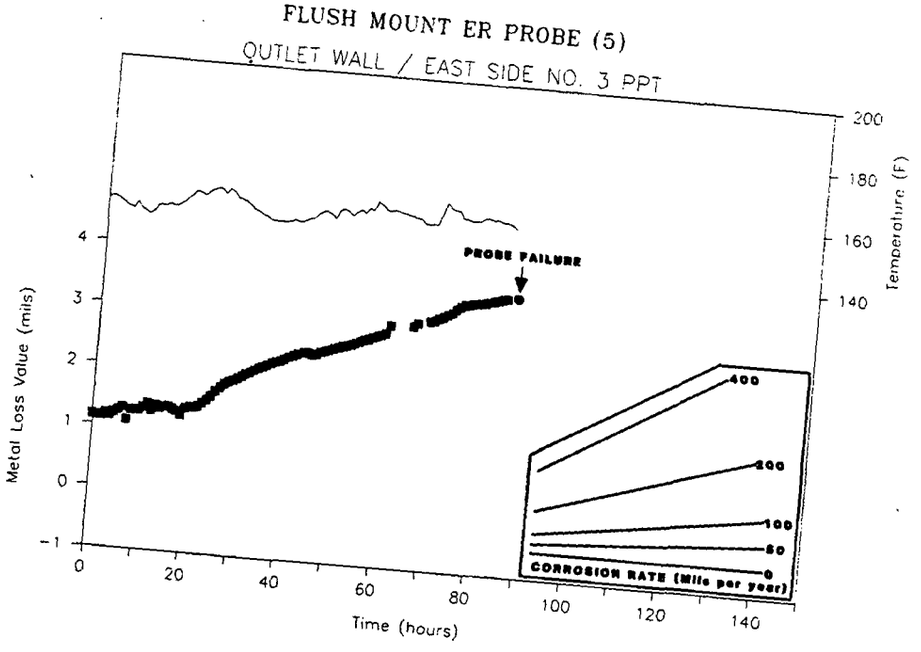

Figure 18. ER probe results from the Springfield mill.

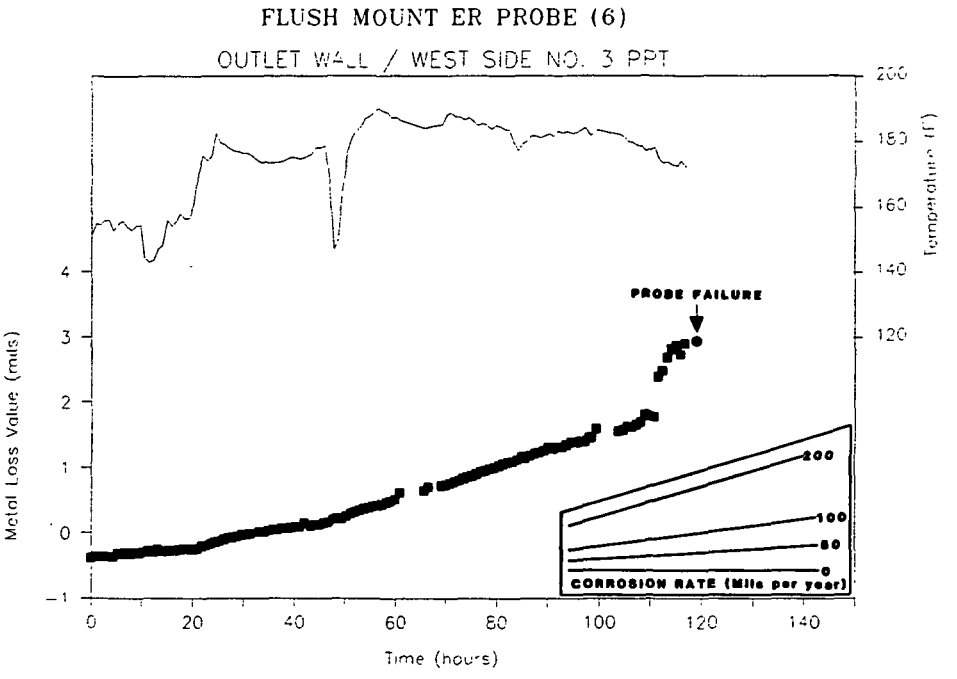

Figure 19. ER probe results from the Springfield mill.

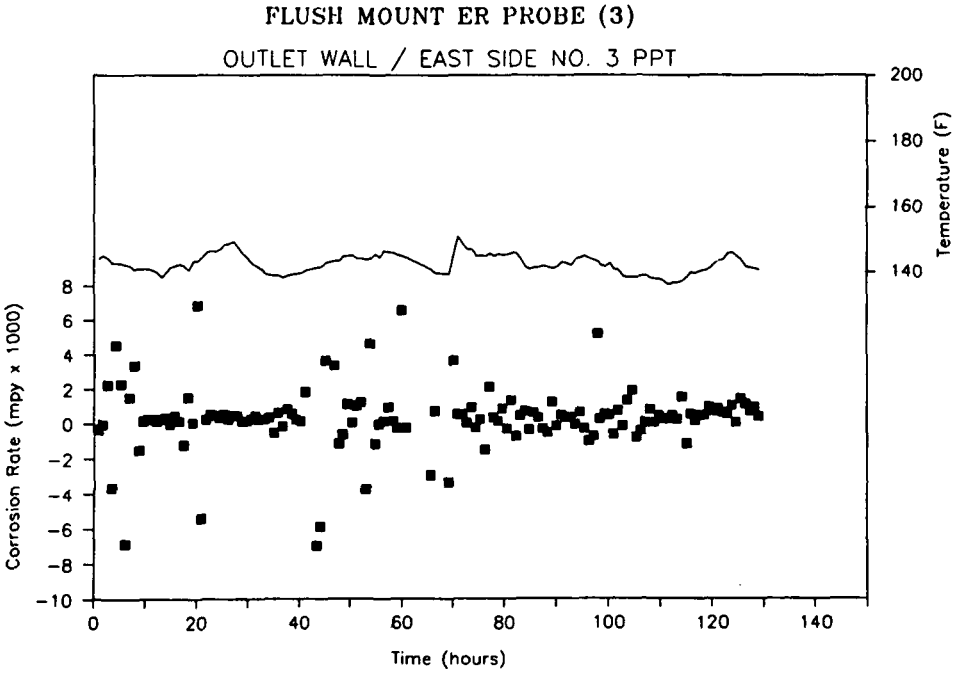

Figure 20. ER probe results from the Springfield mill.

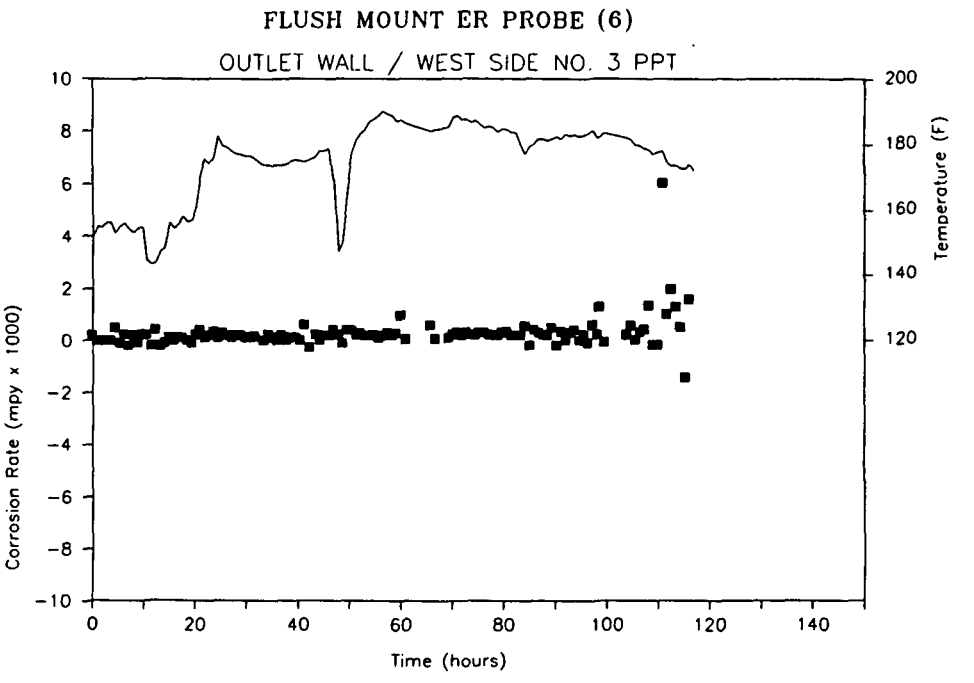

Figure 21. ER probe results from the Springfield mill.

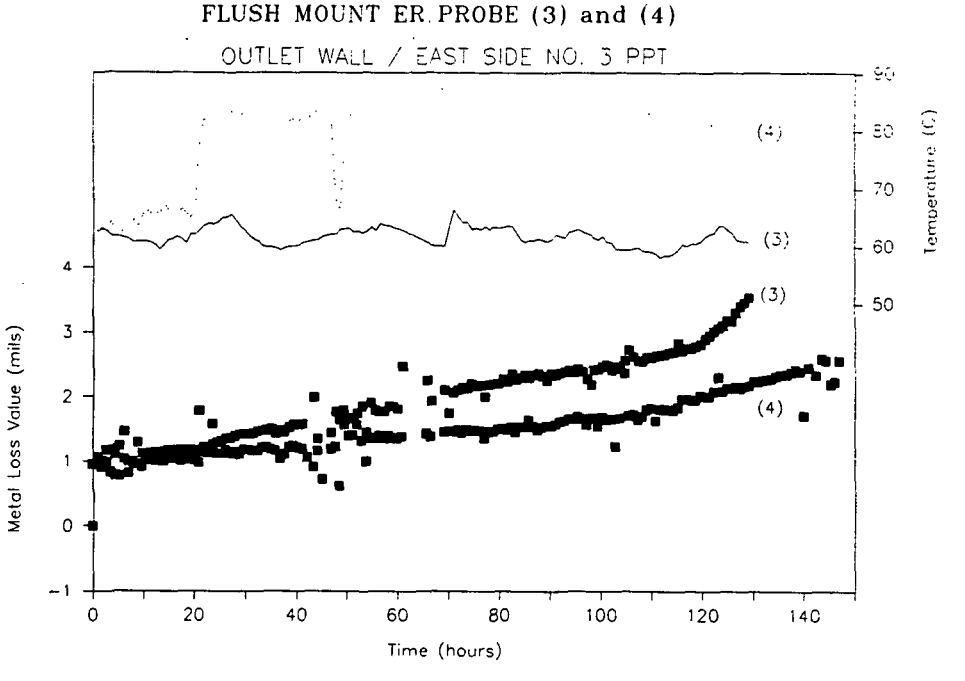

Figure 22. ER probe results from the Springfield mill.

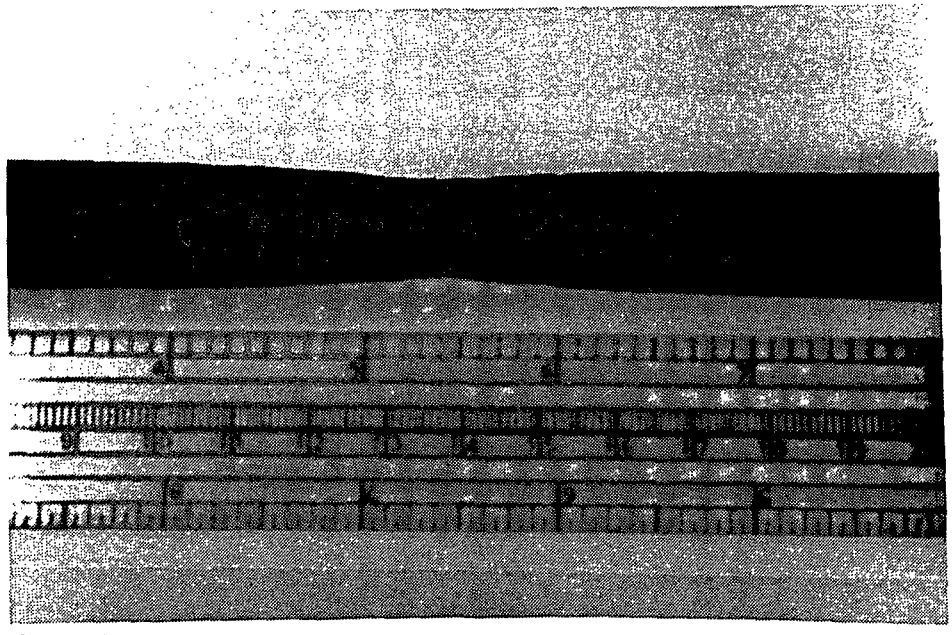

Figure 23. A view of the shaft of the west side retractable ER probe that suffered extensive corrosion.

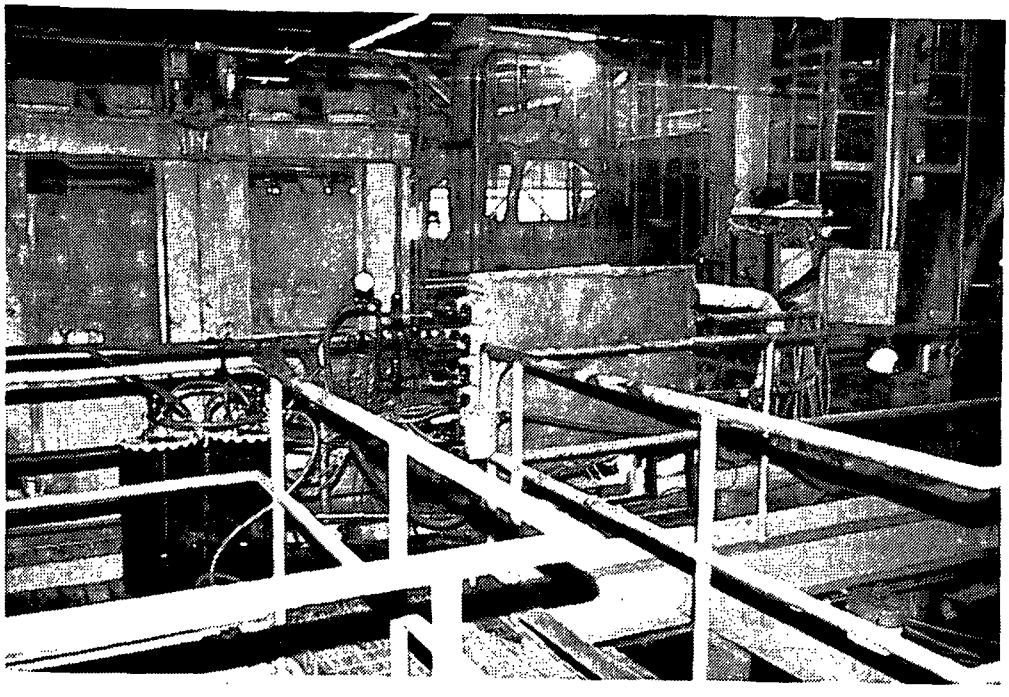

Figure 24. Corrosion chamber as installed at the Charleston mill.

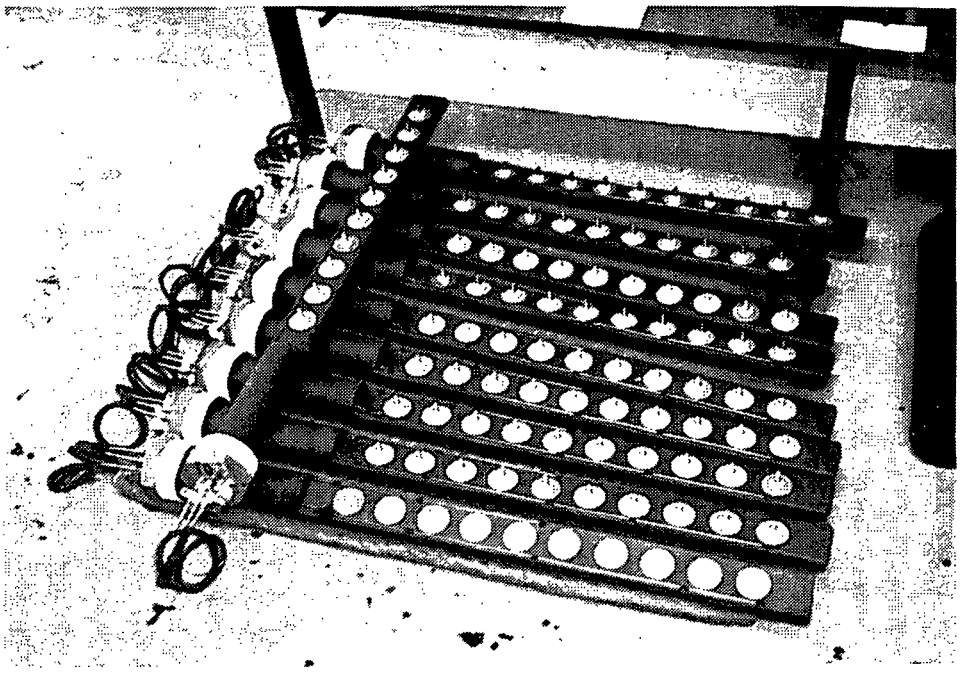

Figure 25. Ten cold finger assemblies before installation in the corrosion chamber at the Charleston mill.

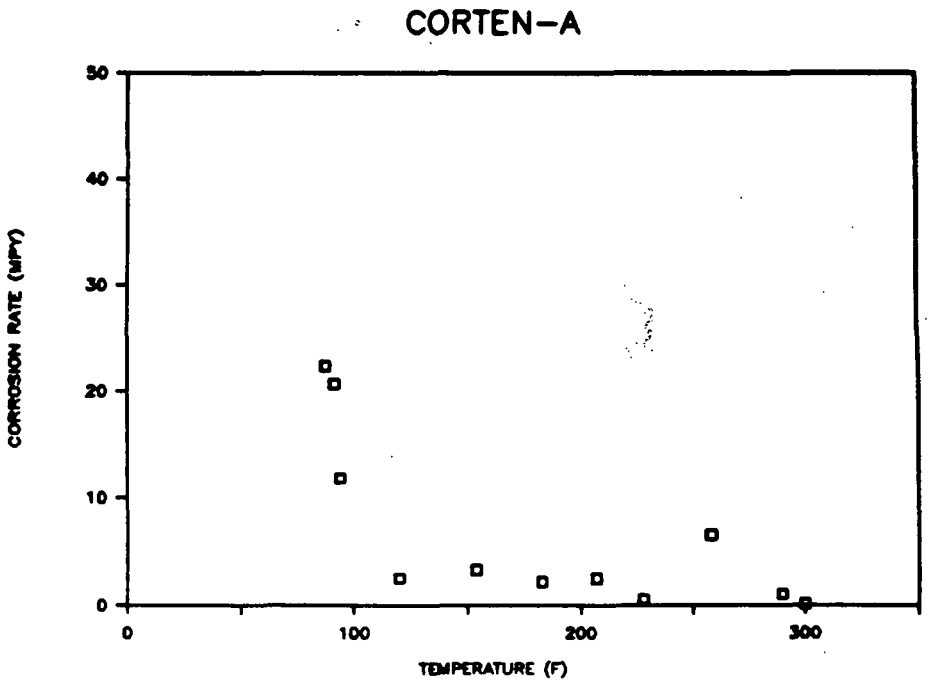

Figure 26-a. Corrosion data from the Charleston mill.

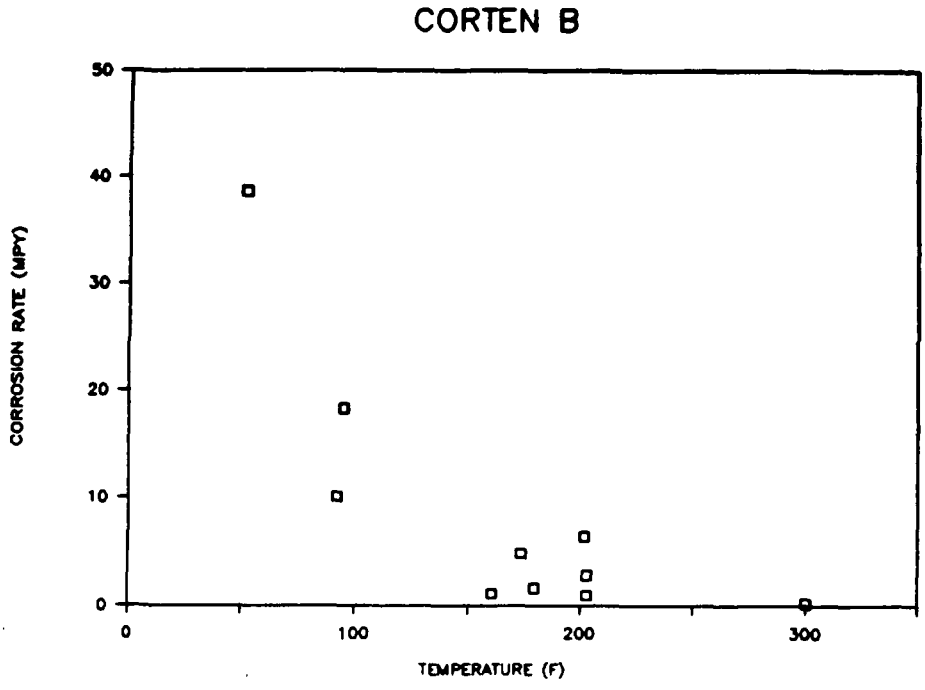

Figure 26-b. Corrosion data from the Charleston mill.

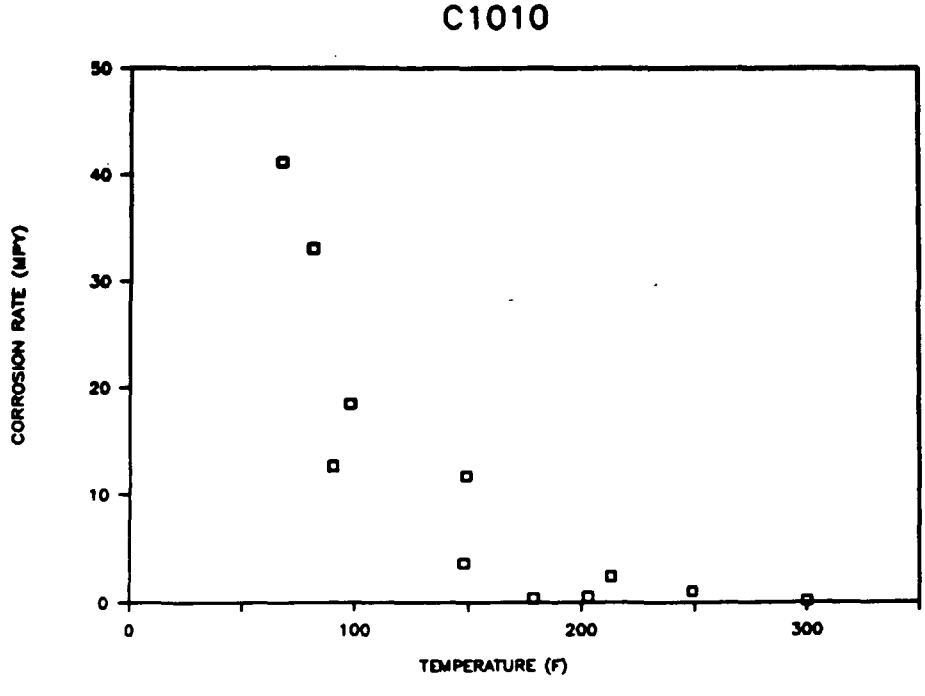

Figure 26-c. Corrosion data from the Charleston mill.

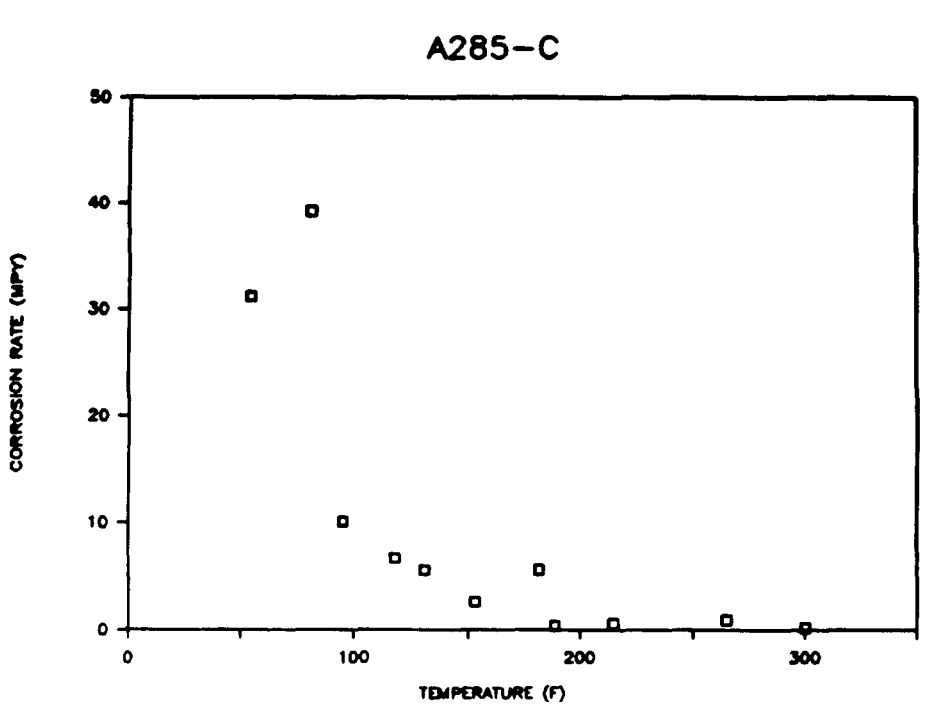

Figure 26-d. Corrosion data from the Charleston mill.

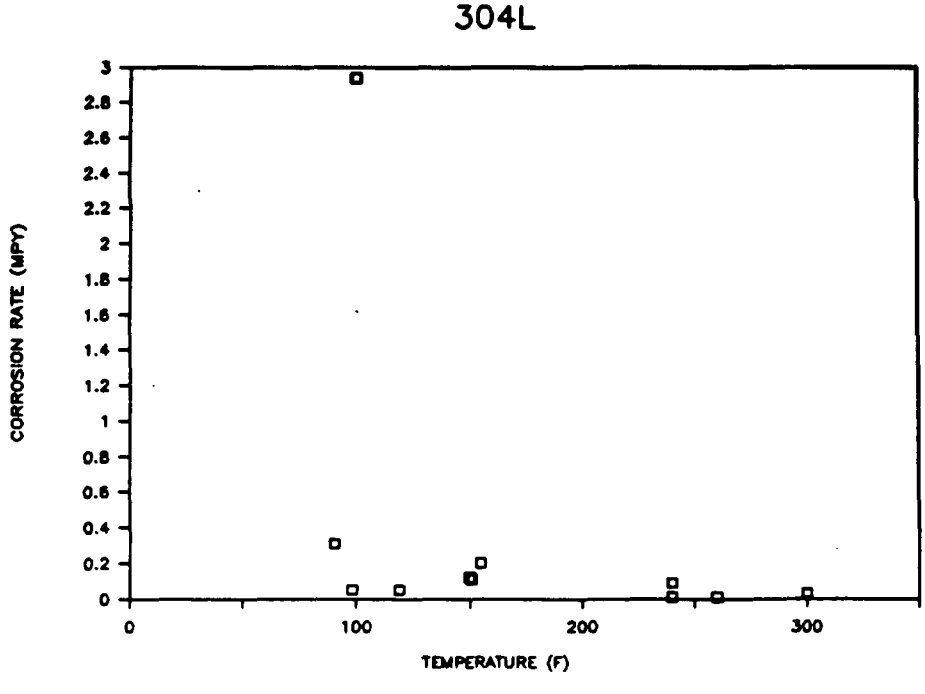

Figure 26-e. Corrosion data from the Charleston mill.

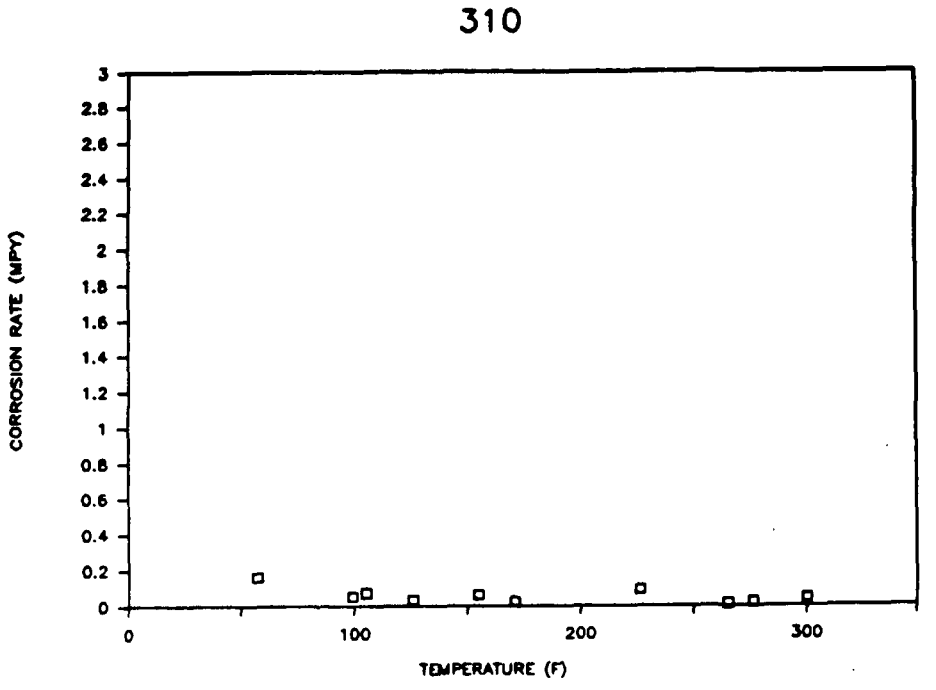

Figure 26-f. Corrosion data from the Charleston mill.

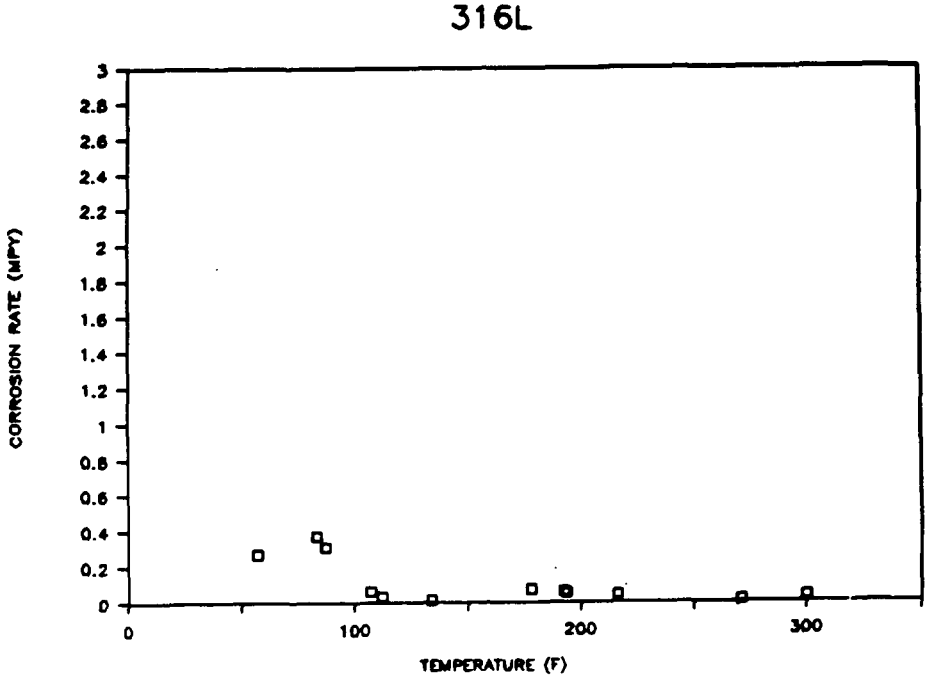

Figure 26-g. Corrosion data from the Charleston mill.

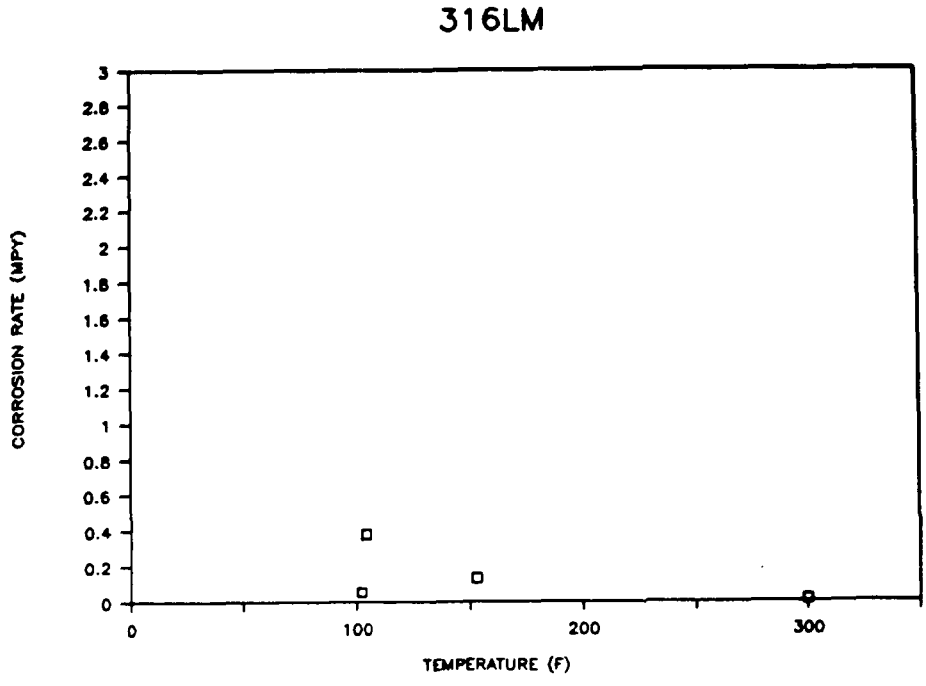

Figure 26-h. Corrosion data from the Charleston mill.

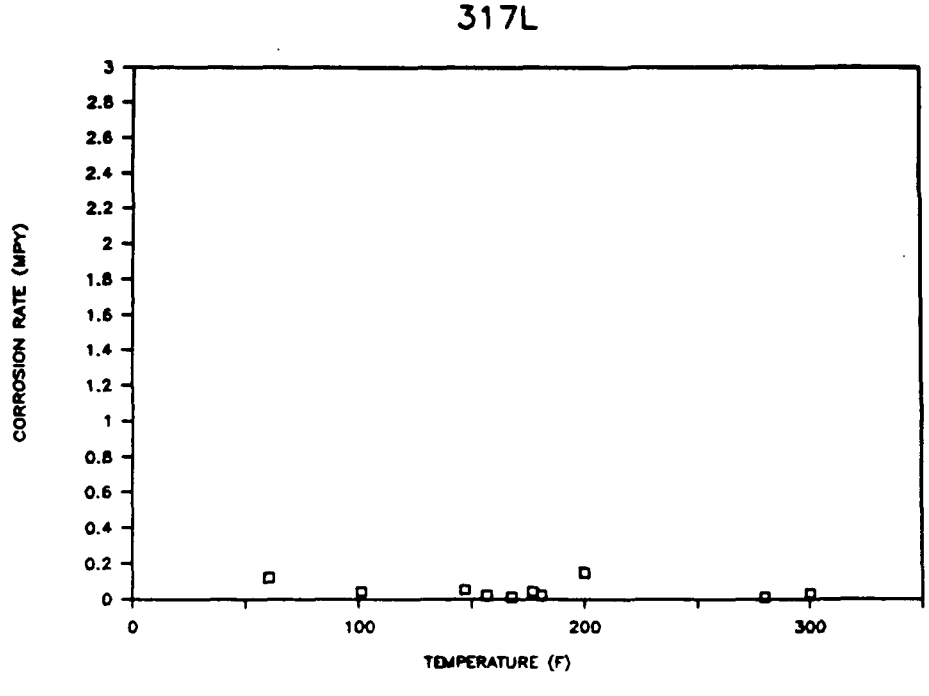

Figure 26-i. Corrosion data from the Charleston mill.

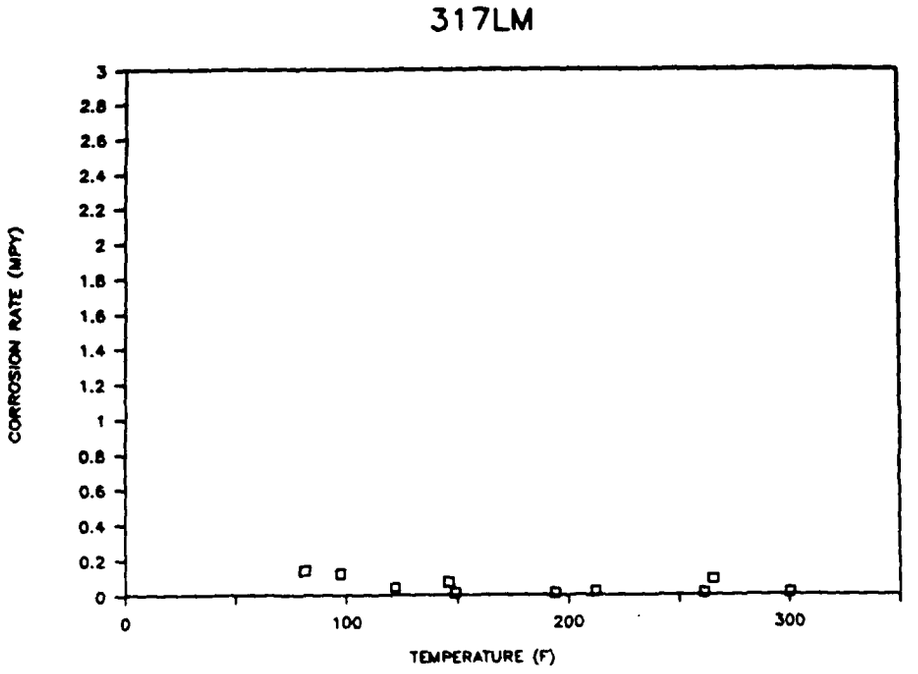

Figure 26-j. Corrosion data from the Charleston mill.

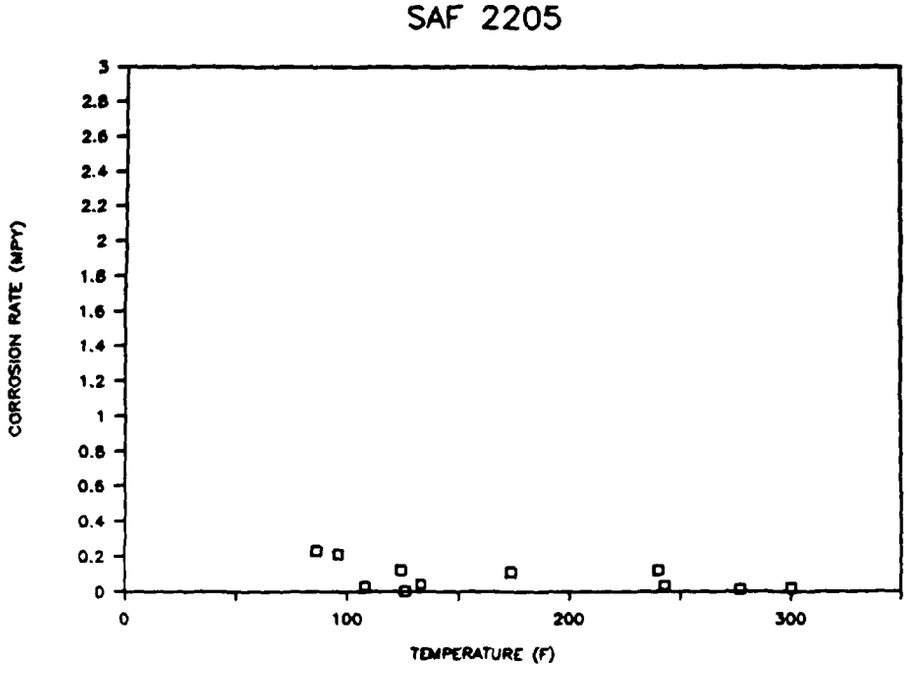

Figure 26-k. Corrosion data from the Charleston mill.

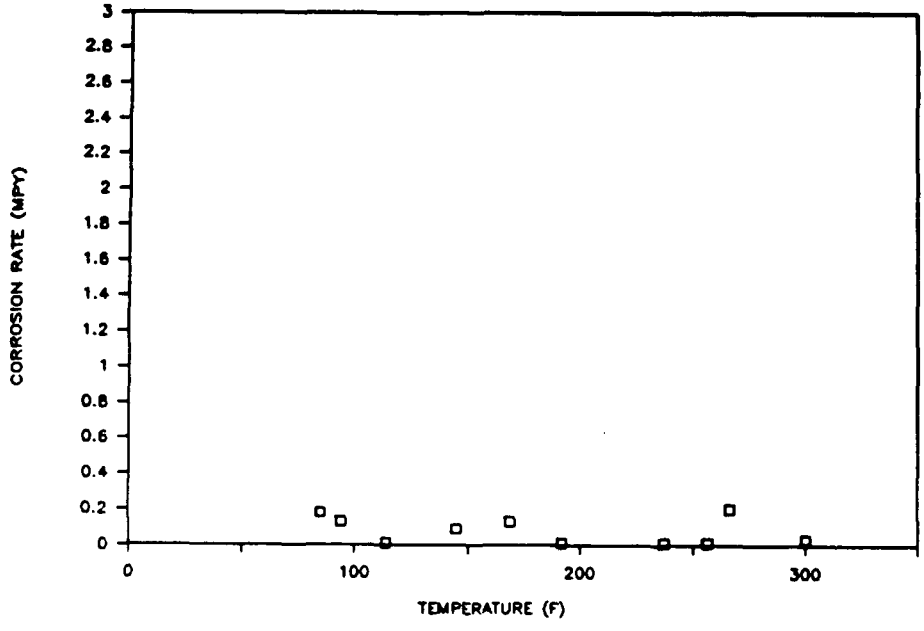

Figure 26-1. Corrosion data from the Charleston mill.

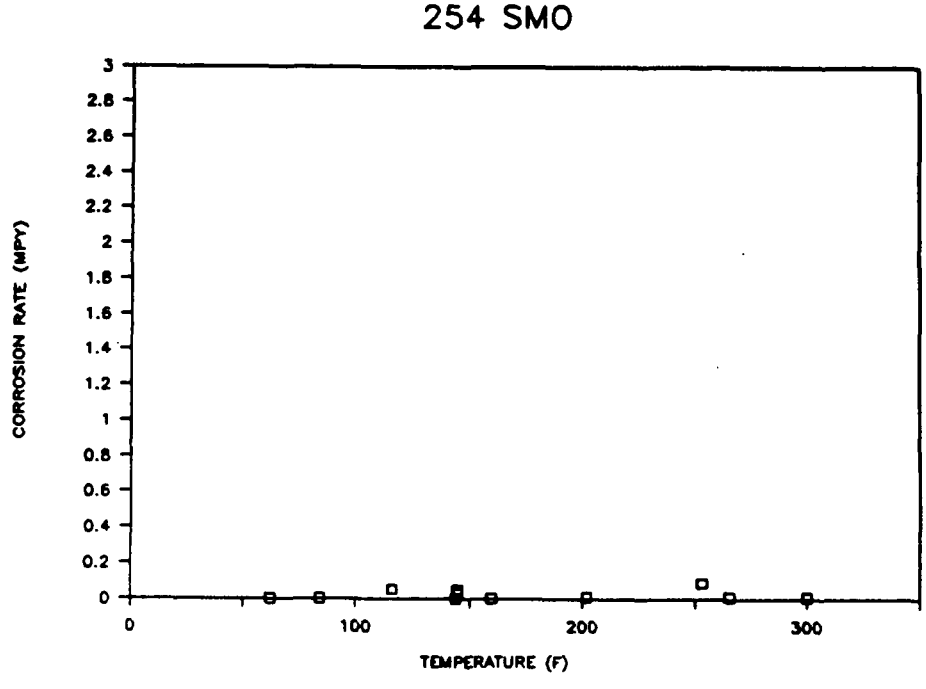

Figure 26-m. Corrosion data from the Charleston mill.

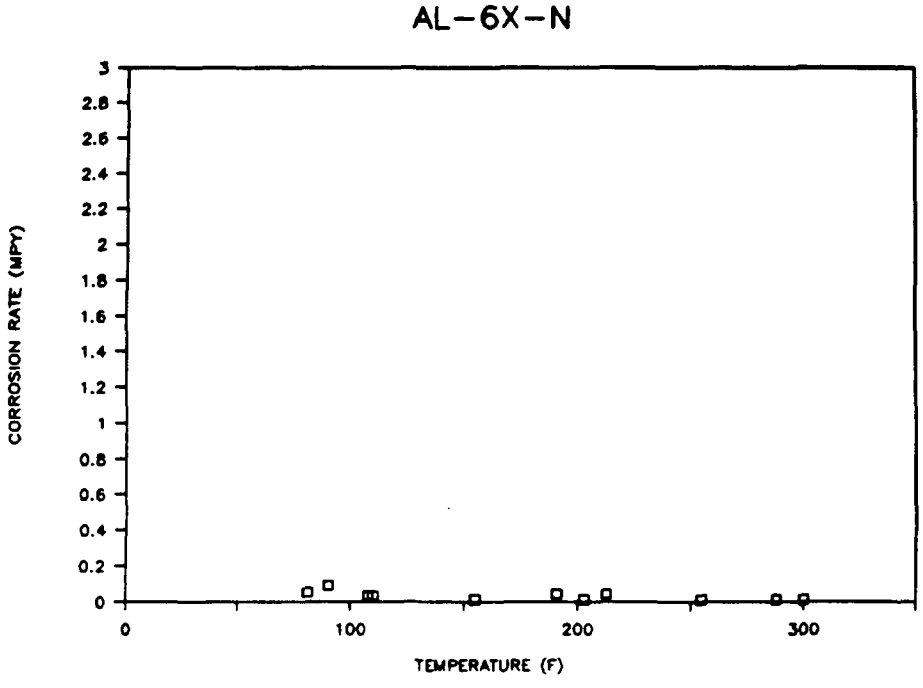

Figure 26-n. Corrosion data from the Charleston mill.

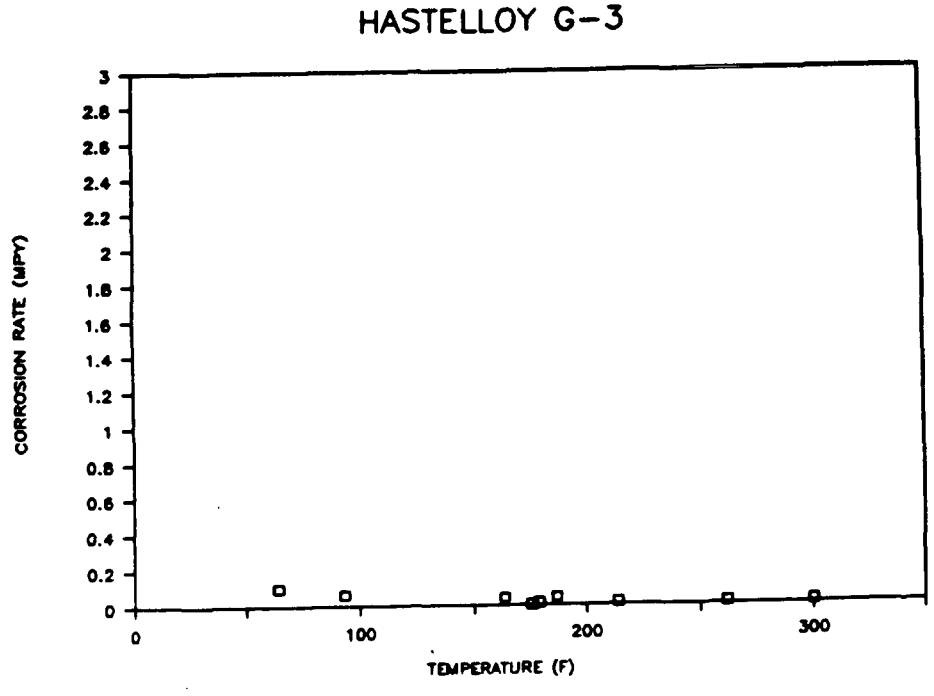

Figure 26-o. Corrosion data from the Charleston mill.

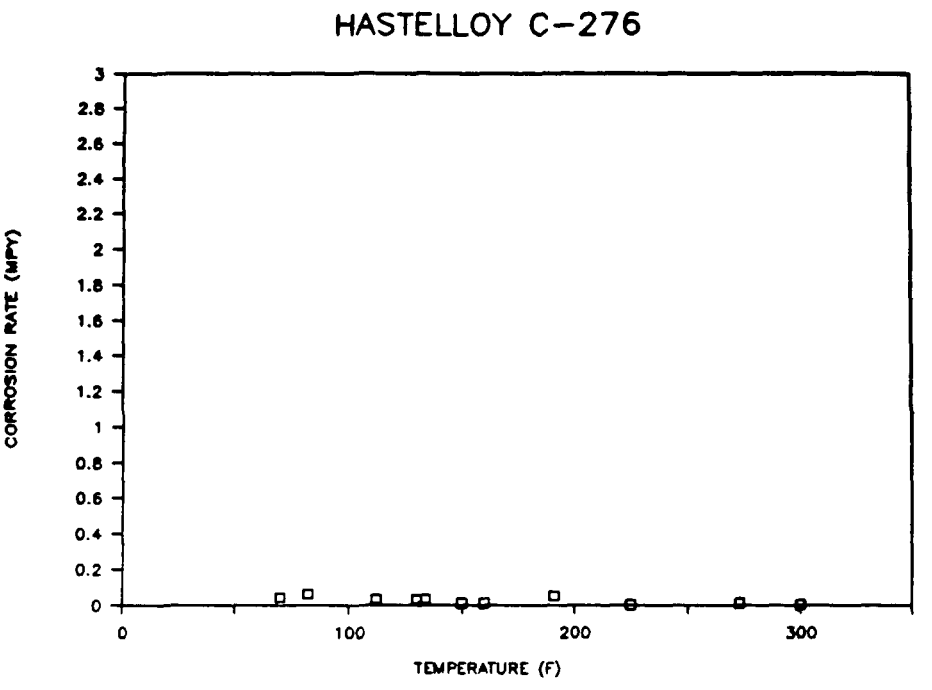

Figure 26-p. Corrosion data from the Charleston mill.

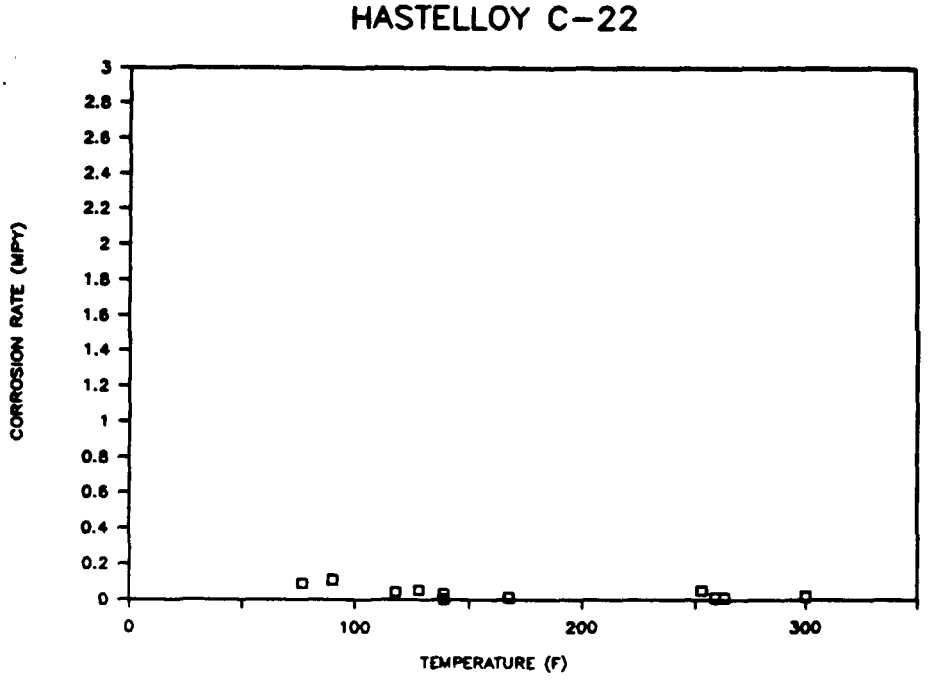

Figure 26-q. Corrosion data from the Charleston mill.

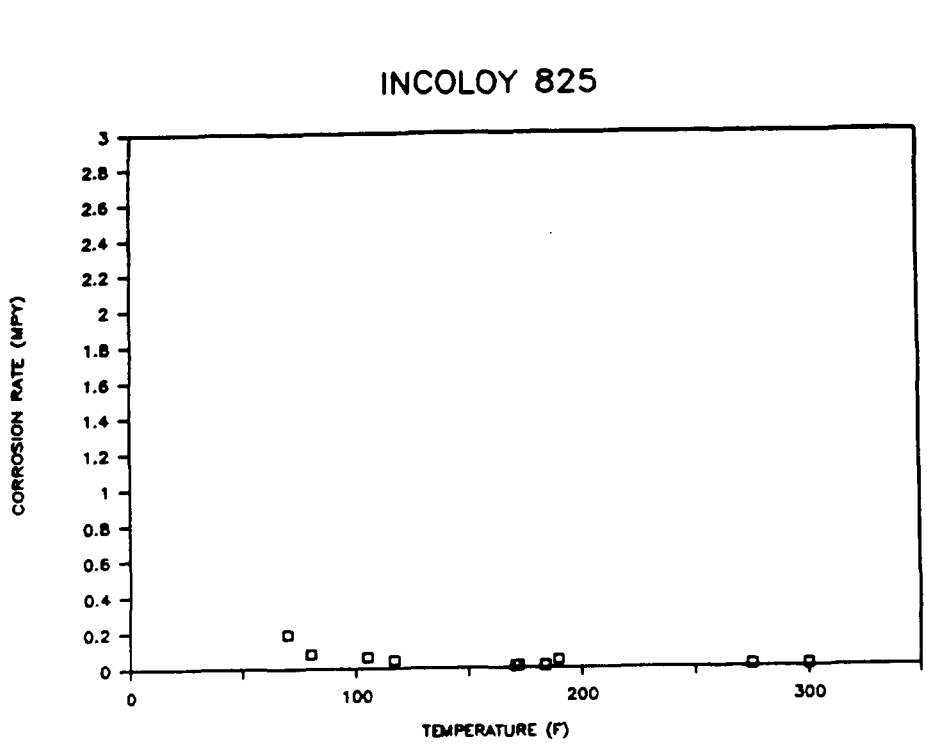

Figure 26-r. Corrosion data from the Charleston mill.

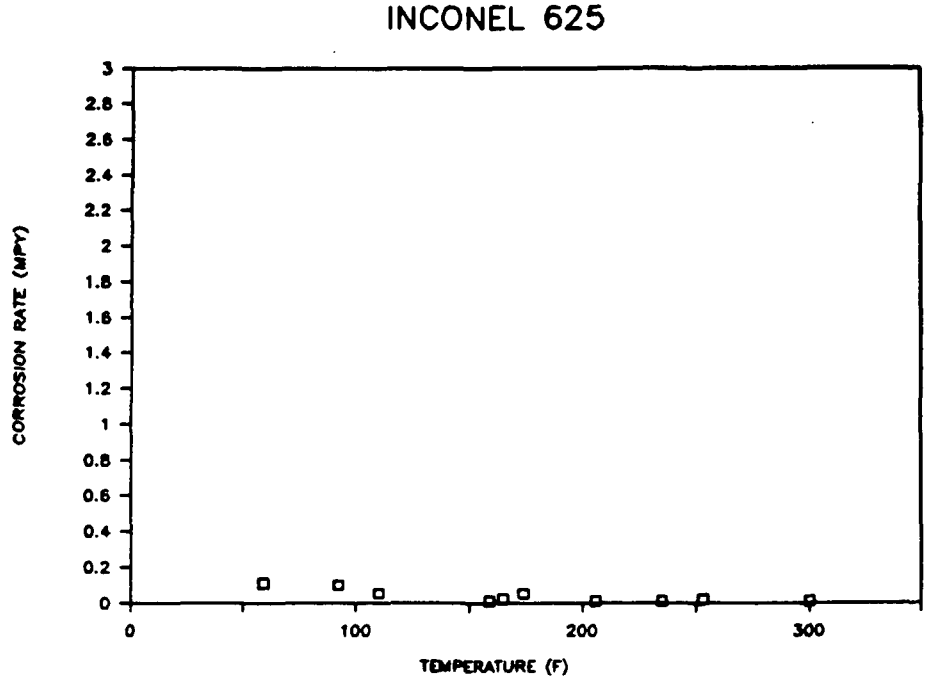

Figure 26-s. Corrosion data from the Charleston mill.

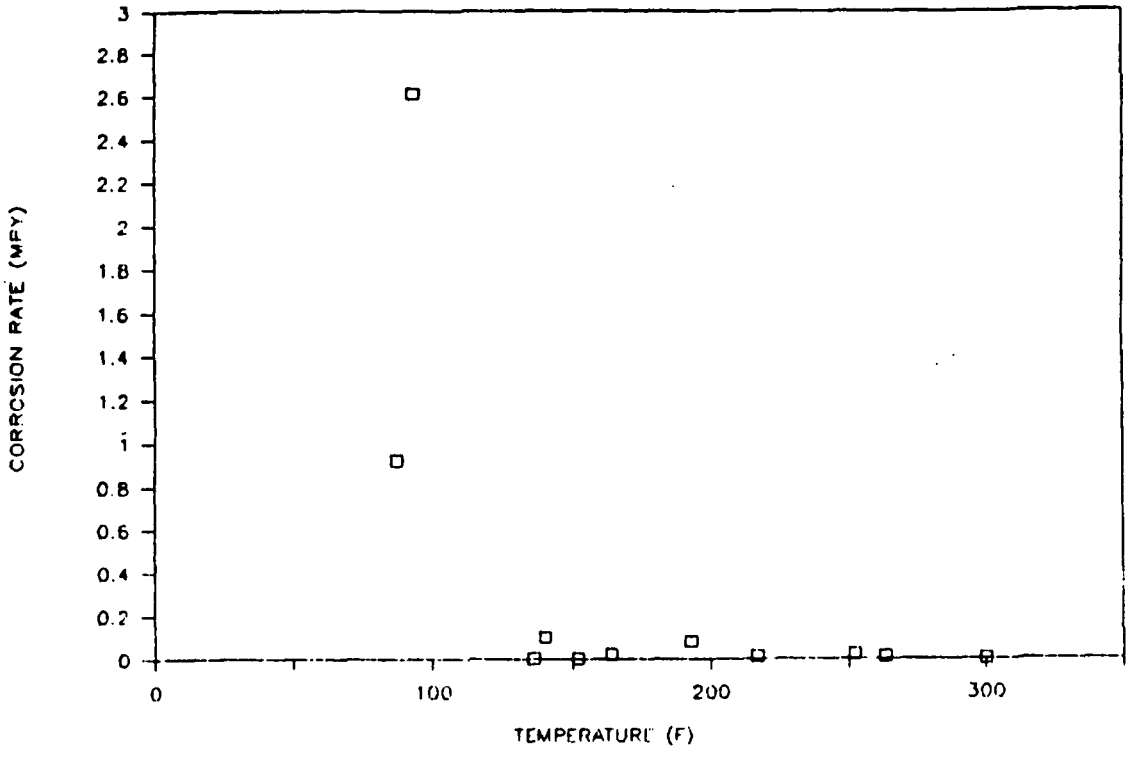

Figure 26-t. Corrosion data from the Charleston mill.

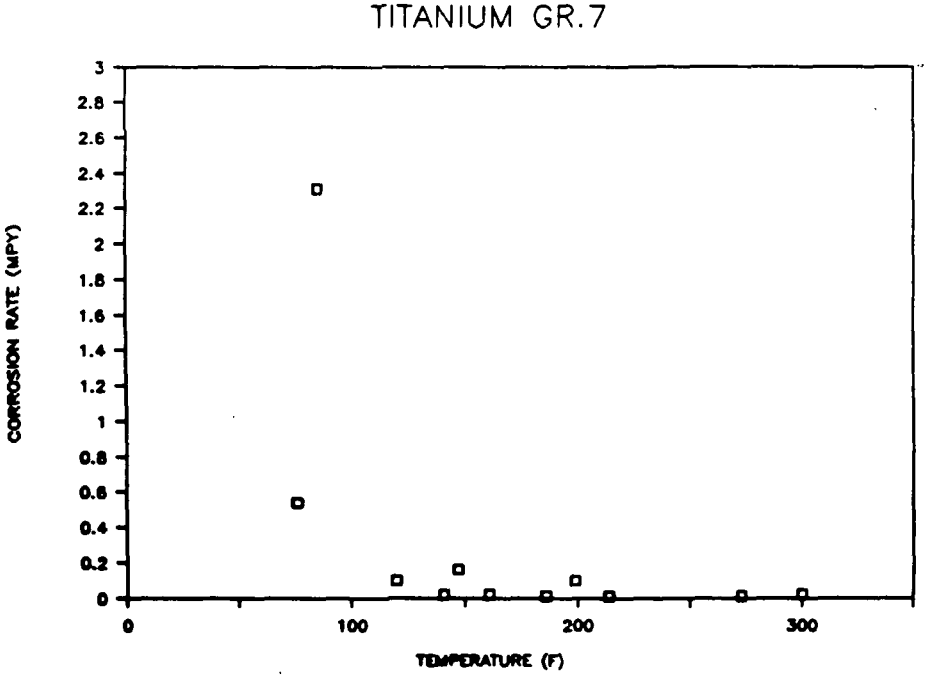

Figure 26-u. Corrosion data from the Charleston mill.

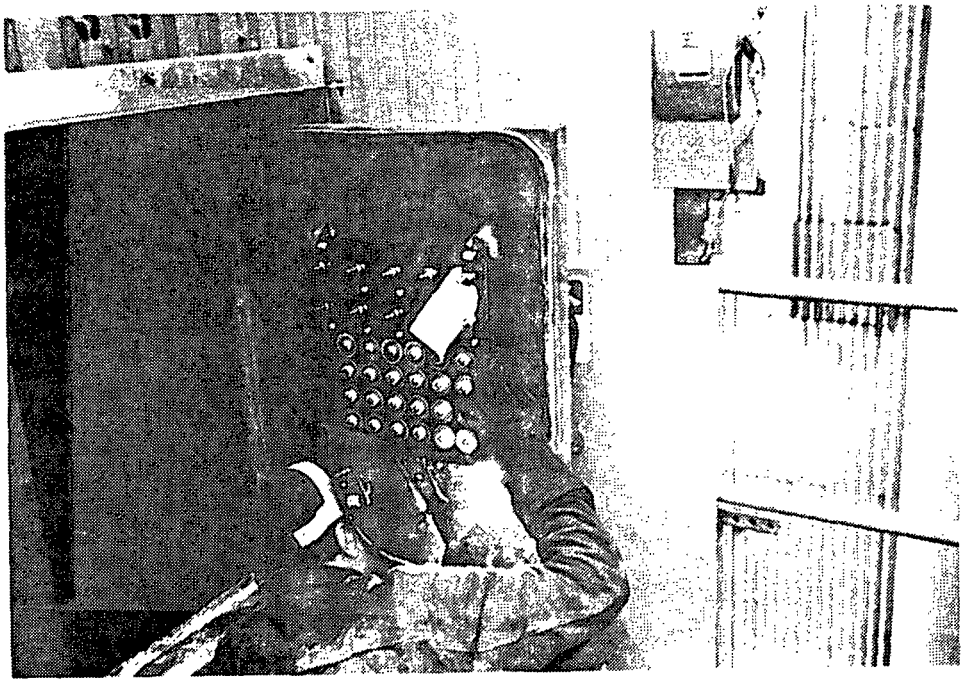

Figure 27. Test panels were mounted in the precipitator by welding to various surface locations. Shown here is a panel being installed on the internal side of an access door.

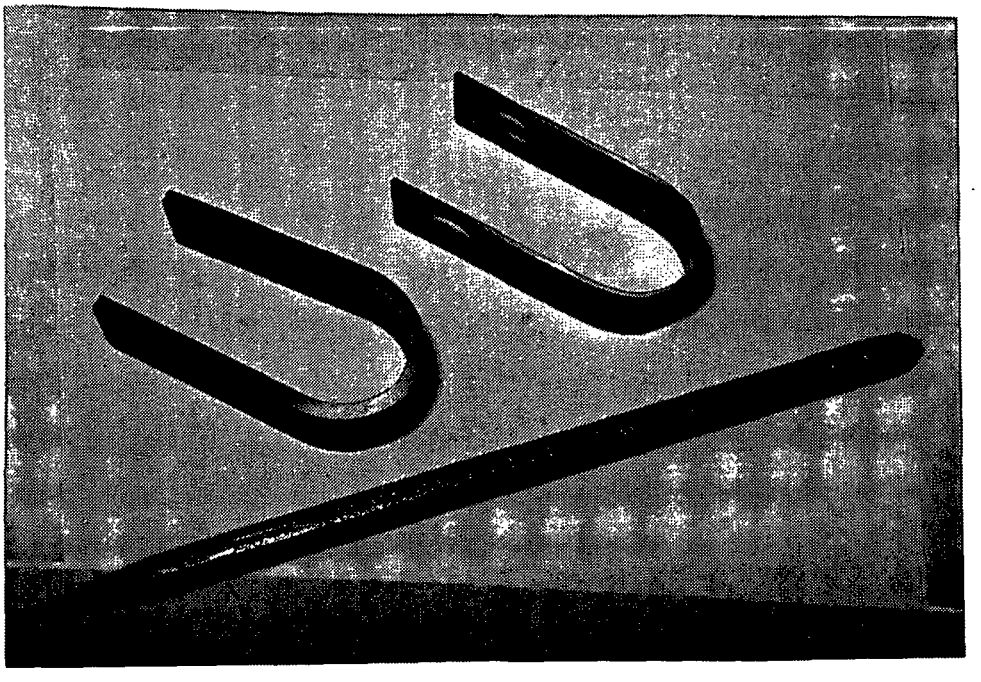

Figure 28. U-bend specimens were exposed in the precipitator, cleaned, and carefully examined at the stressed area for evidence of cracking.

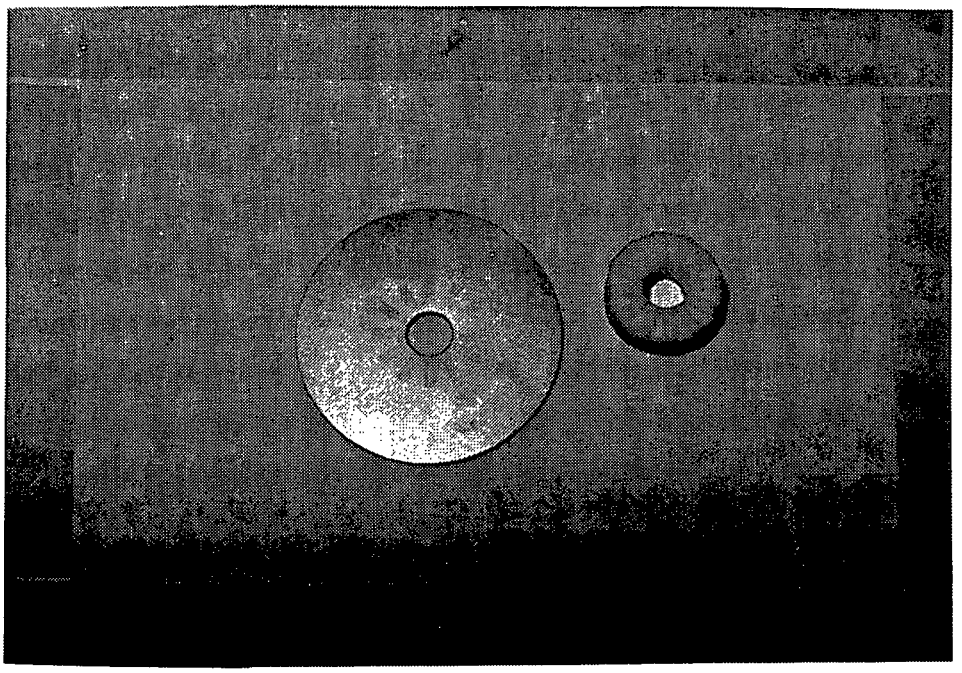

Figure 29. A 310 stainless steel specimen is shown with a standard crevice washer. Note the imprint that the washer left on the specimen surface, but no crevice corrosion was observed following an exposure in the No. 3 precipitator.

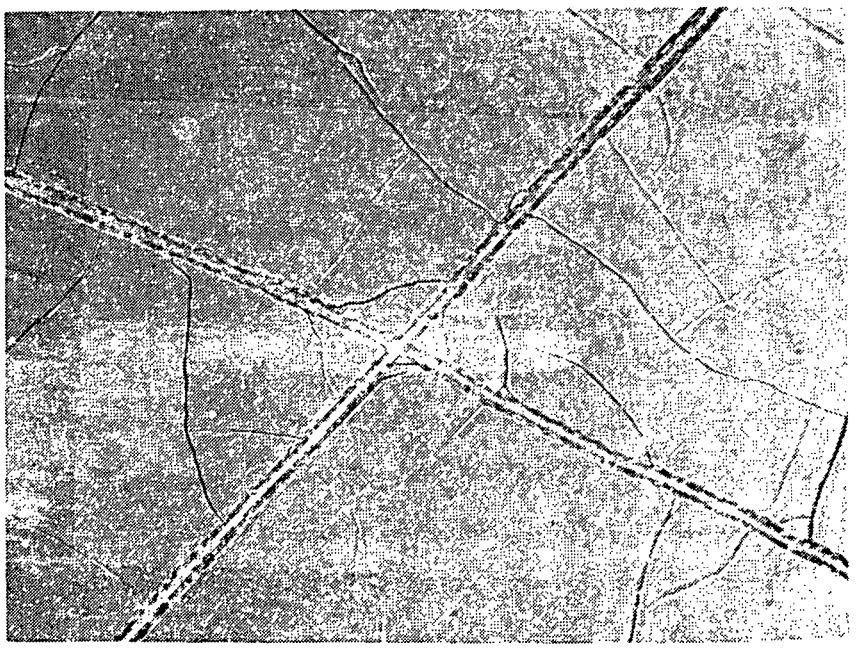

Figure 30. The S&G 350 coating was subject to cracking when exposed in the electrostatic precipitator. The large "X" is the intentional damage to the coating performed on a specimen of each coating type. (6X)

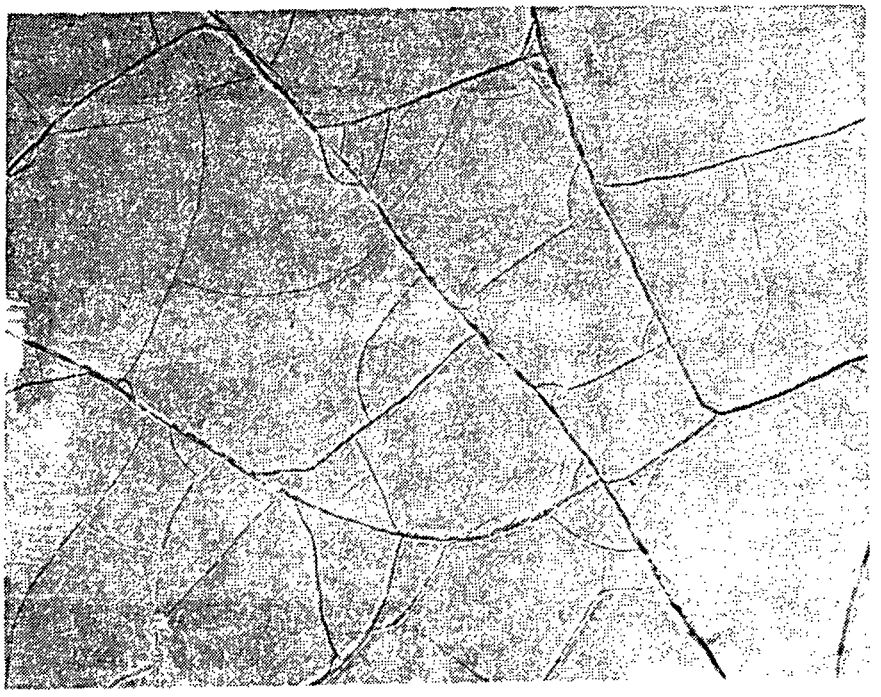

Figure 31. Cracking of the S&G 350 coating material also occurred in areas not in the vicinity of the simulated surface damage. (6X)

Figure 32. In this unwashed S&G coated specimen from the precipitator, salt-cake can be seen to penetrate the cracks, likely resulting in attack of the underlying metal substrate. (6X)

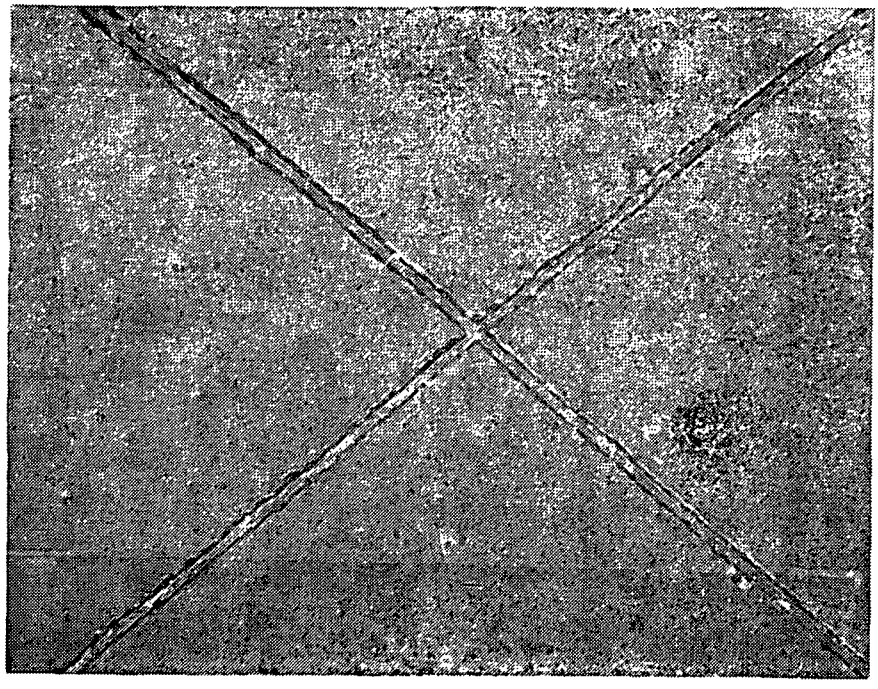

Figure 33. A specimen coated with S&G 500 did not crack when exposed to the same conditions as S&G 350. (6X)

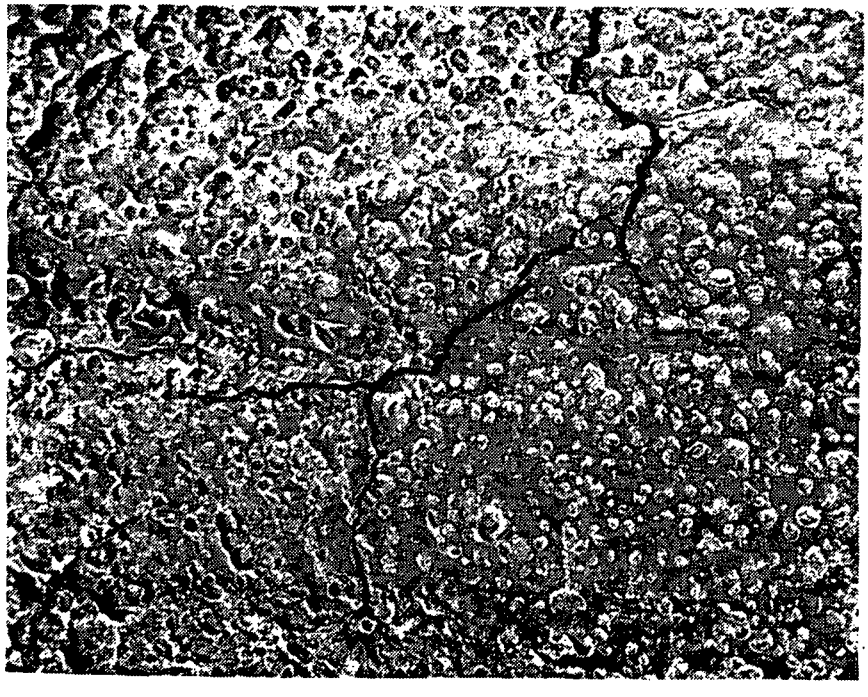

Figure 34. The Plasite 5306 coating suffered attack at the coating surface and experienced extensive, deep cracking in an exposure in the precipitator on panel No. 9. (6X)

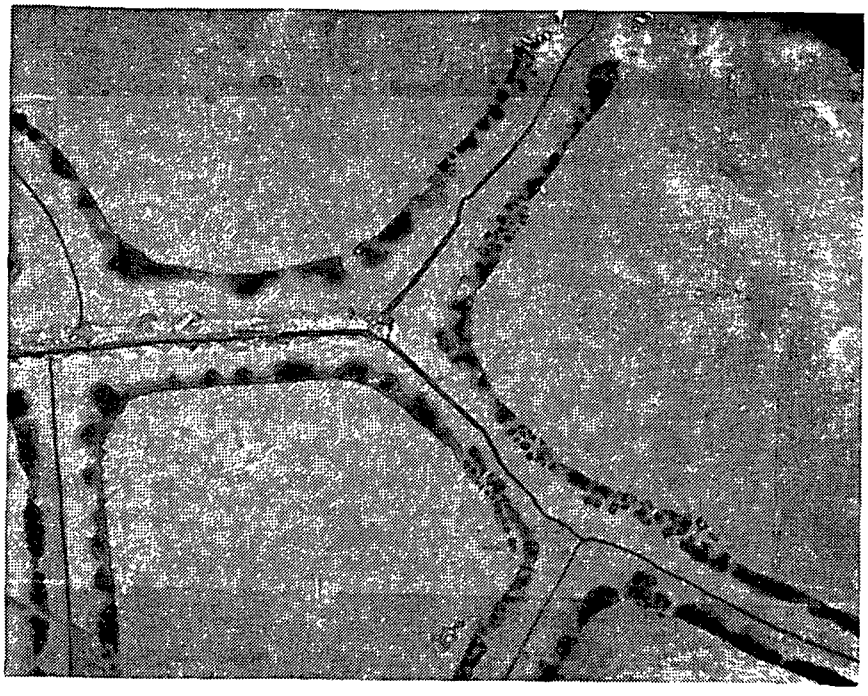

Figure 35. Cracks were observed to initiate from the area of intentional surface damage on a specimen coated with Plasite 9570. (10X)

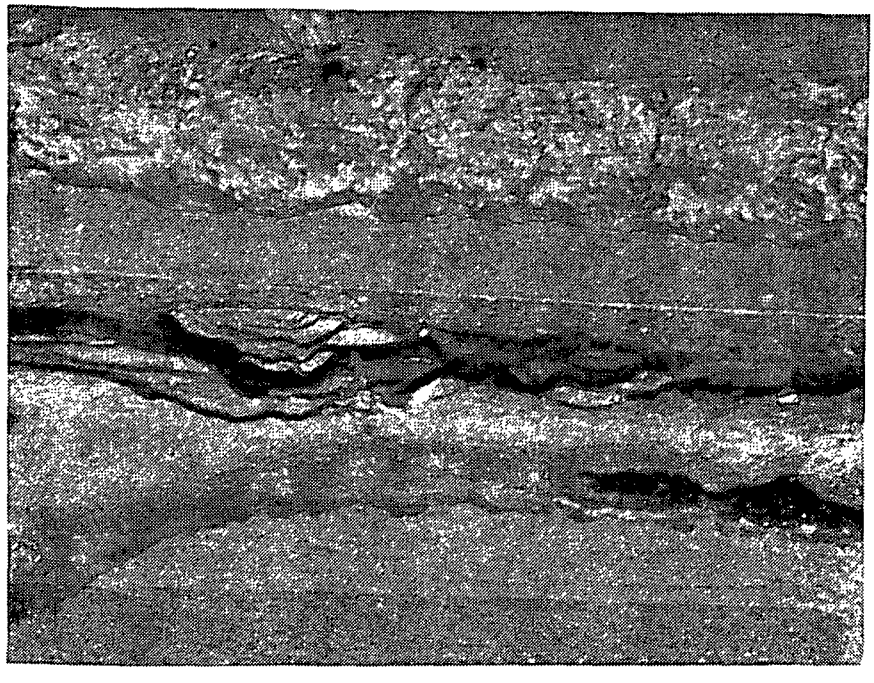

Figure 36. Cracking and disbondment of the coating was found laterally along the simulated damage zone of a Plasite 9570 coated specimen. (50X)

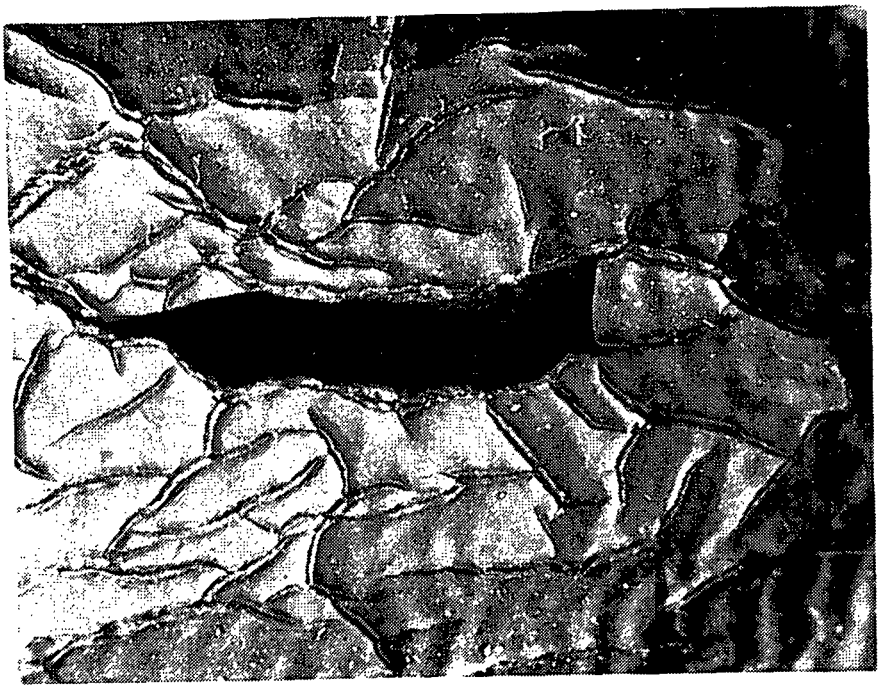

Figure 37. As the temperature limits of the Plasite 9500 coating were approached, the coating swelled, blistered, and cracked. (6X)

Figure 38. Failure of the coating was the result of coating perforation at the blistered areas shown in Figure 13. (6X)

Figure 39. A specimen coated with Plasite 9570 failed due to cracking and flaking of the coating during a temperature resistance test. (6X)

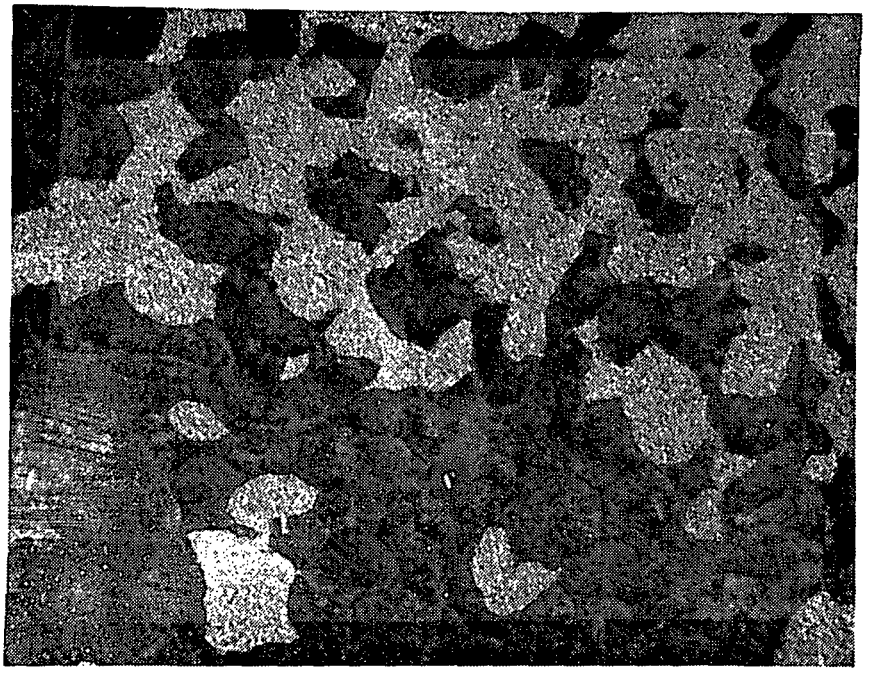

Figure 40. The Seal and Glaze 500 coating system cracked and peeled, but not until about 450°F. (6X)

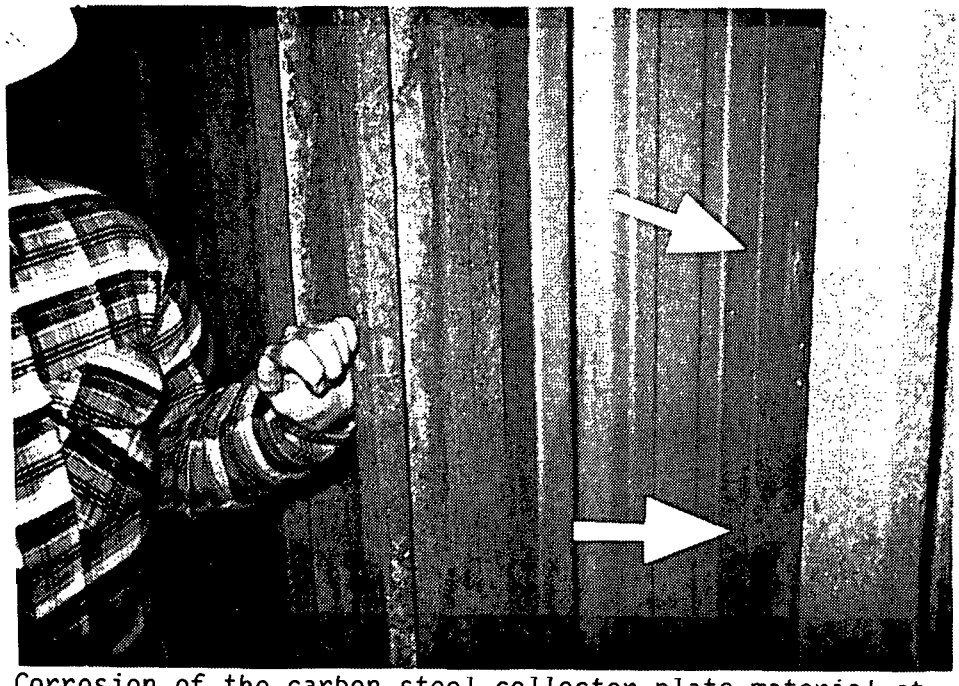

Figure 41. Corrosion of the carbon steel collector plate material at localized sites where holidays and pinholes existed in the Plasite 4140 coating system.

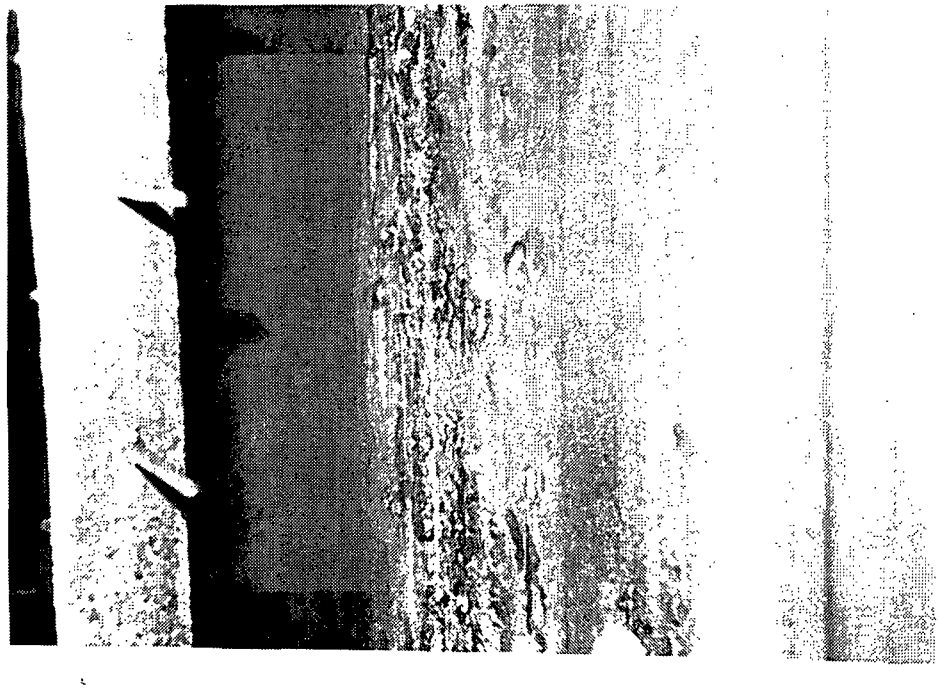

Figure 42. Deposition of corrosion products on the surface of a plate coated with the 1505C system.

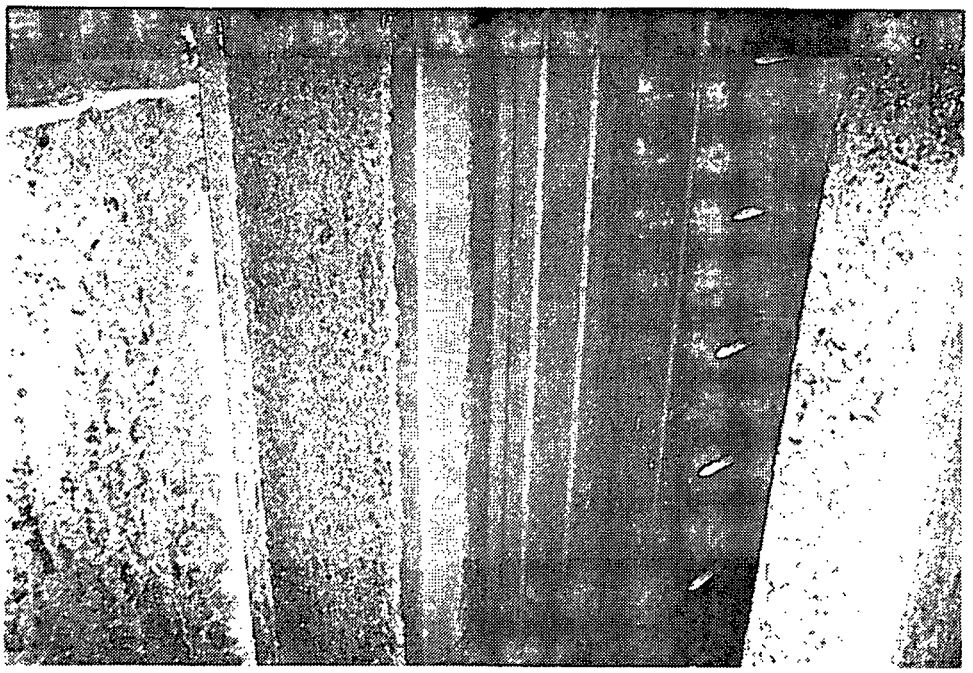

Figure 43. A vertical band of holidays and pinholes in a 4140 coated plate along an edge surface.

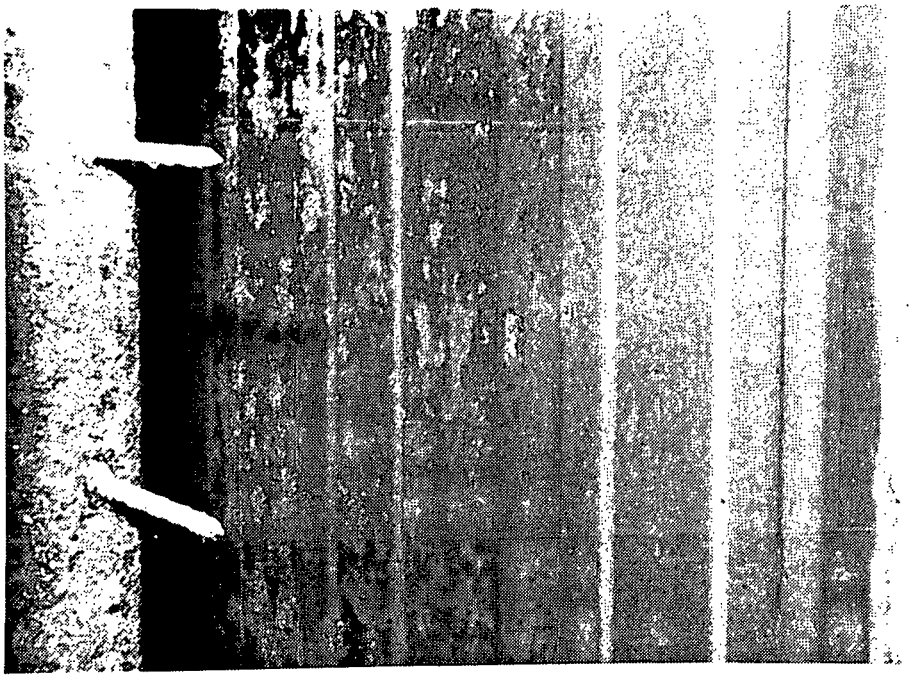

Figure 44. Randomly distributed holidays were often observed near the center of plates (1505C) coated plate shown).

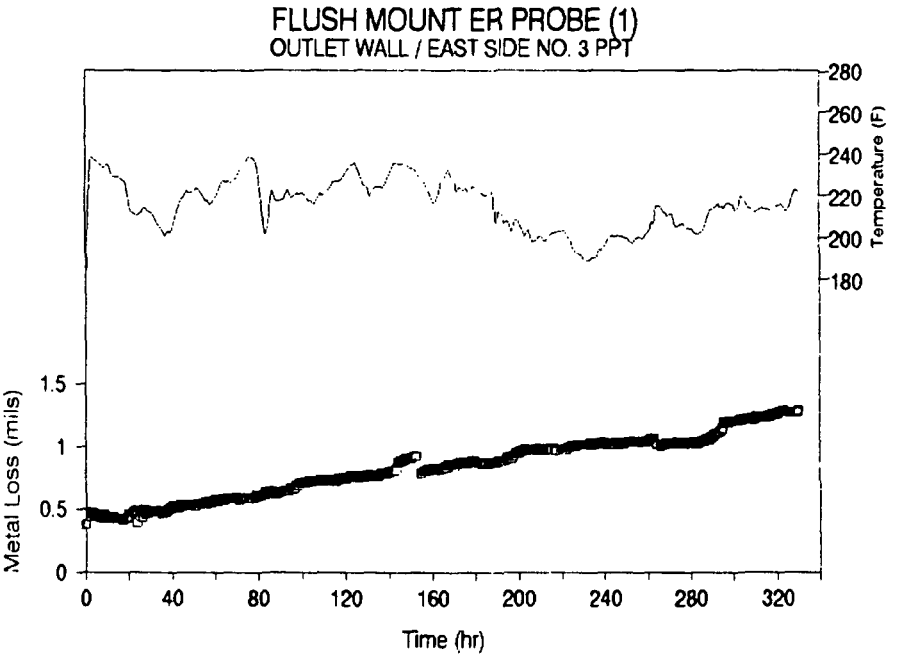

Figure 45. ER probe results from the Springfield mill.

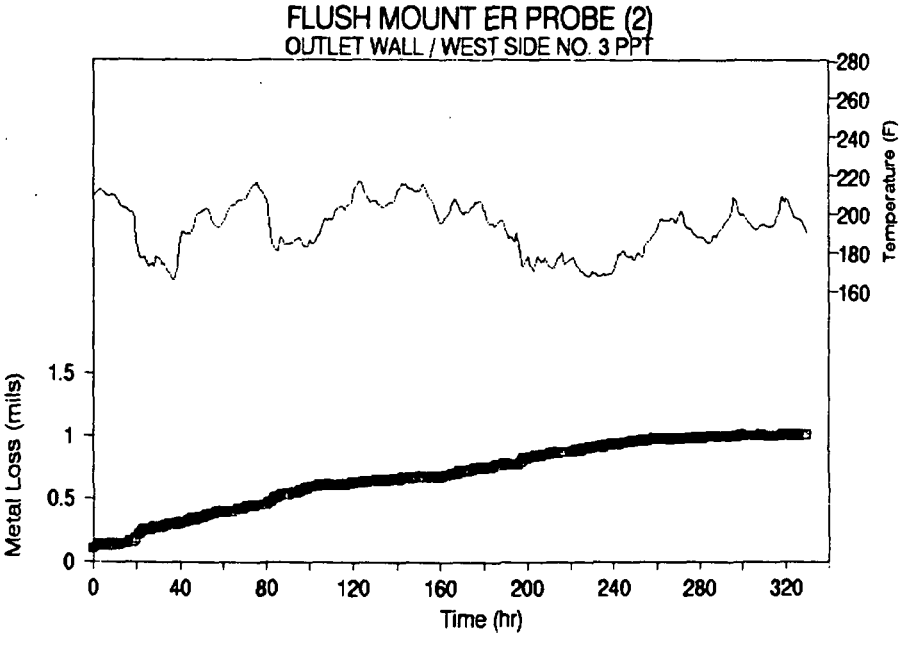

Figure 46. ER probe results from the Springfield mill.

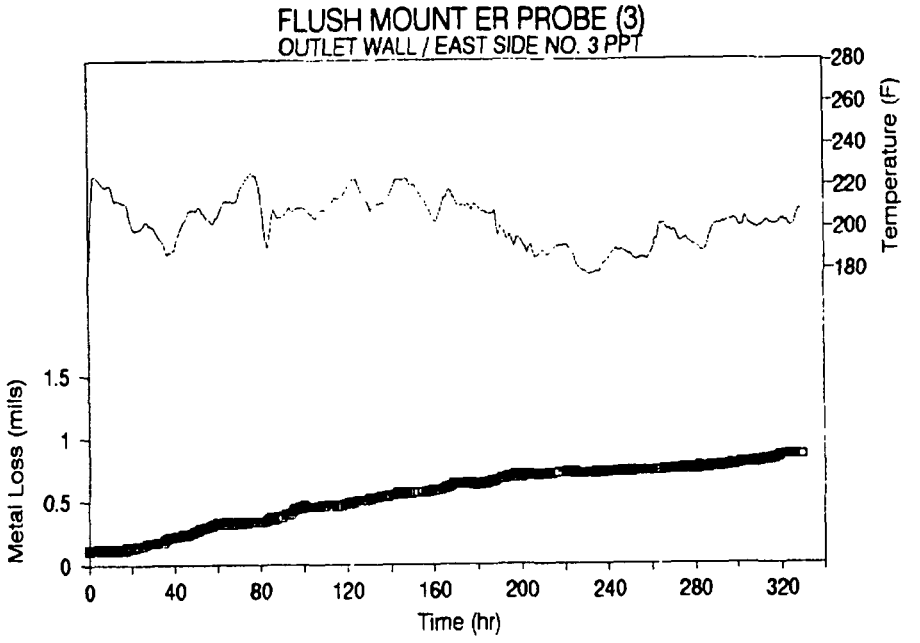

Figure 47. ER probe results from the Springfield mill.

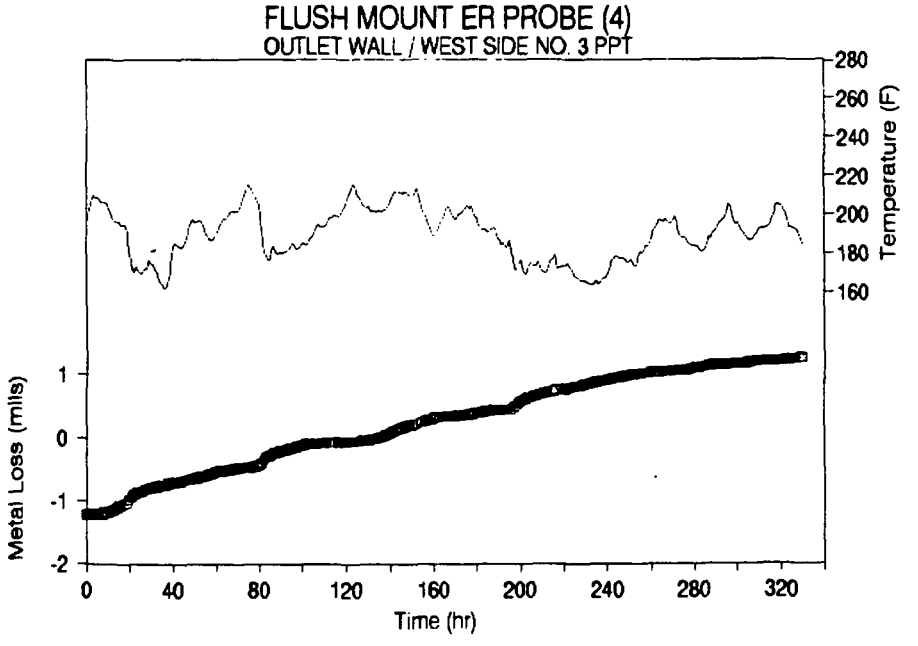

Figure 48. ER probe results from the Springfield mill.

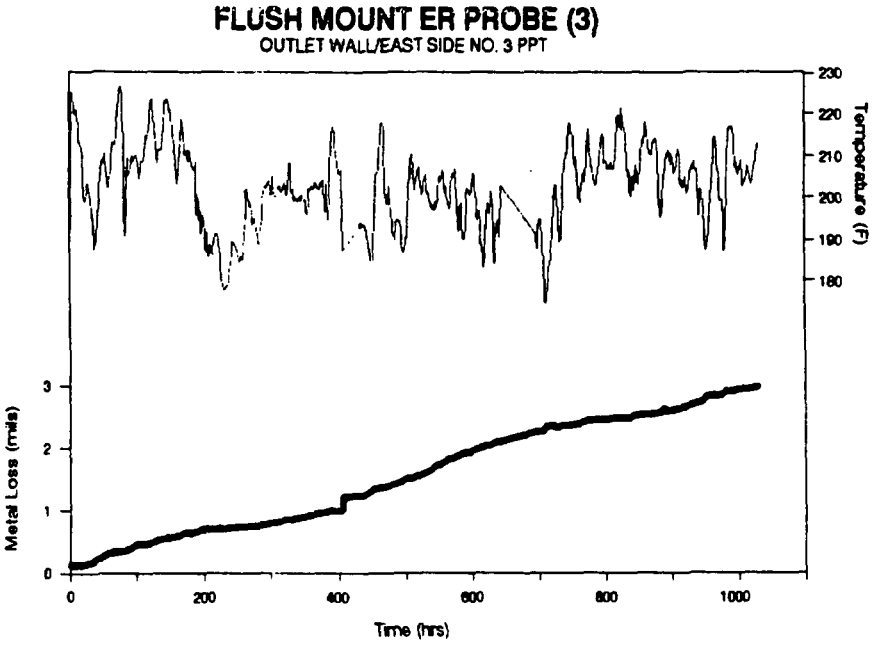

Figure 49. ER probe results from the Springfield mill.

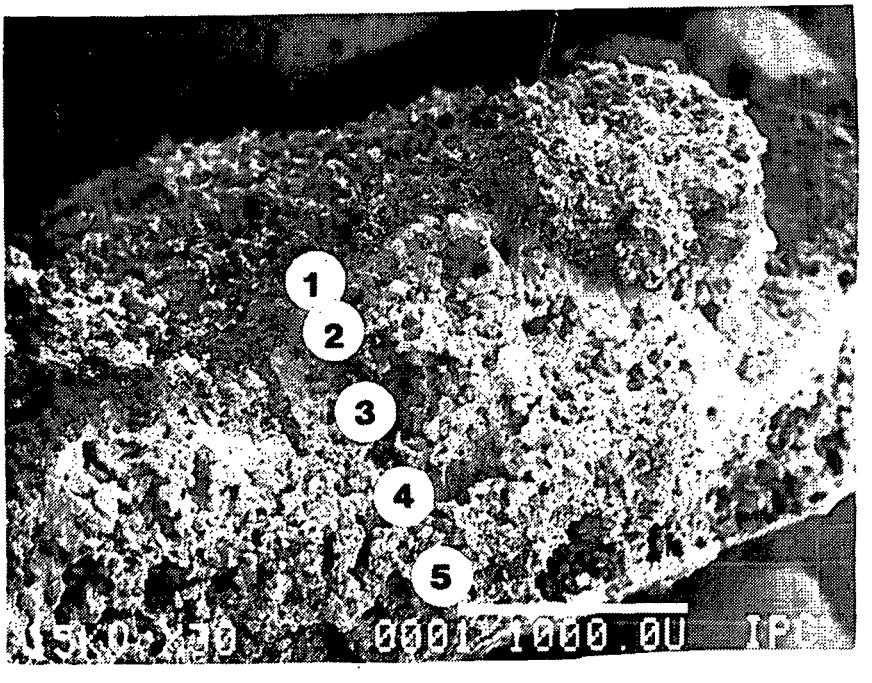

Figure 50. An SEM photomicrograph showing a layer of saltcake and corrosion products removed from an active corrosion site in an electrostatic precipitator. Multi-layered corrosion products (layers 1 and 2) formed beneath saltcake deposits (layers 3-5). (30X)

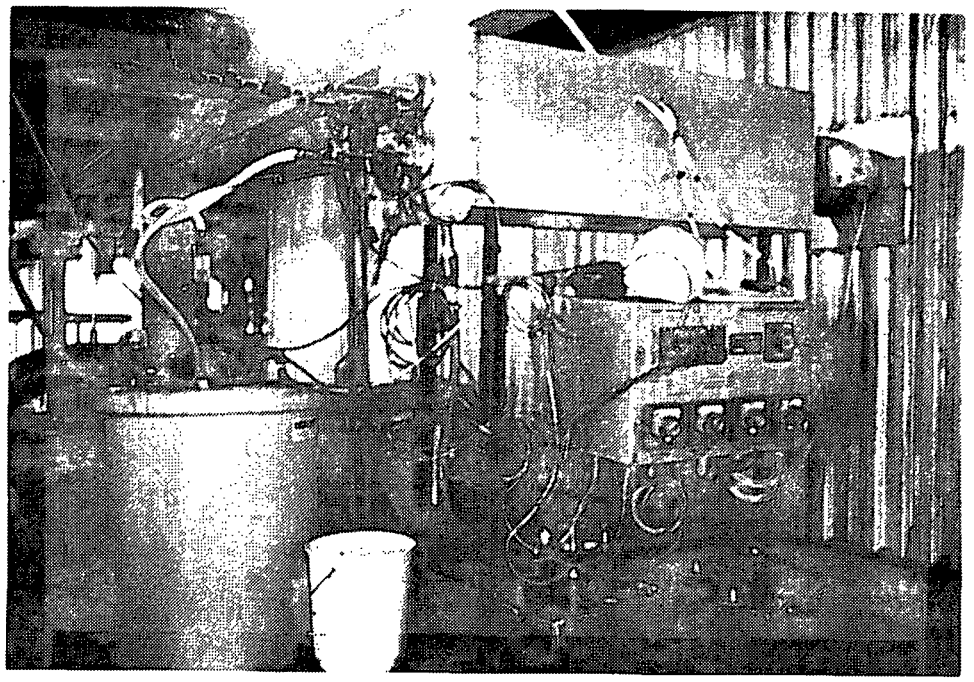

Figure 51. A flue gas corrosion test chamber was installed near the economizer section of the No. 2 recovery boiler at Great Southern. Gases are drawn into the chamber through a heated pipe system, where corrosion specimens are mounted on controlled temperature probes.

Figure 52. A second test chamber was installed in the flue gas stream downstream a direct contact evaporator.

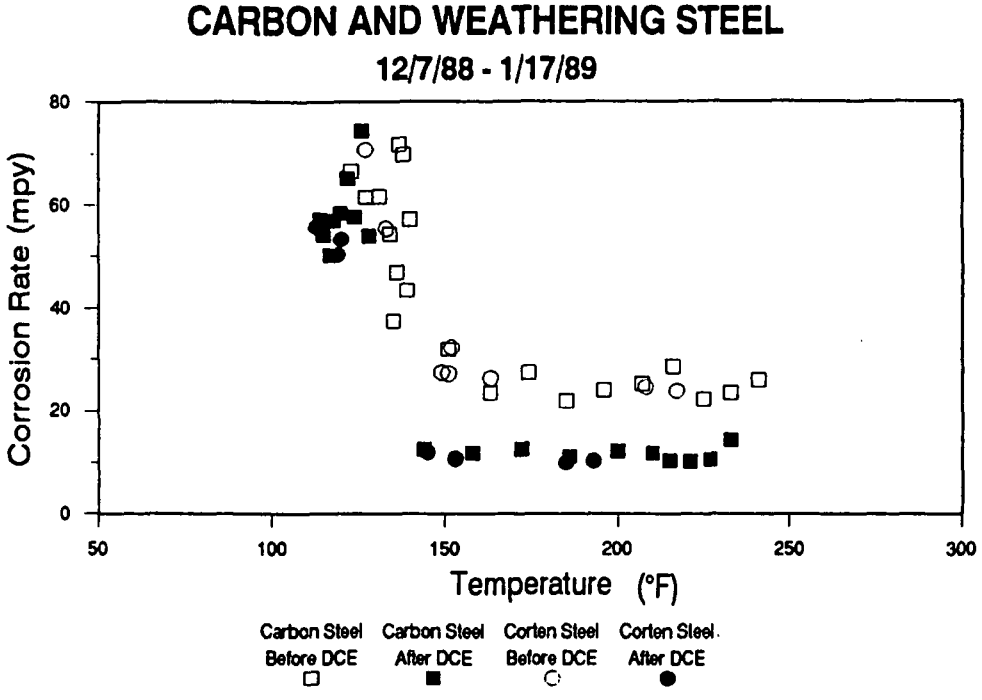

Figure 53. Corrosion data from the Cedar Springs mill without saltcake on the coupons.

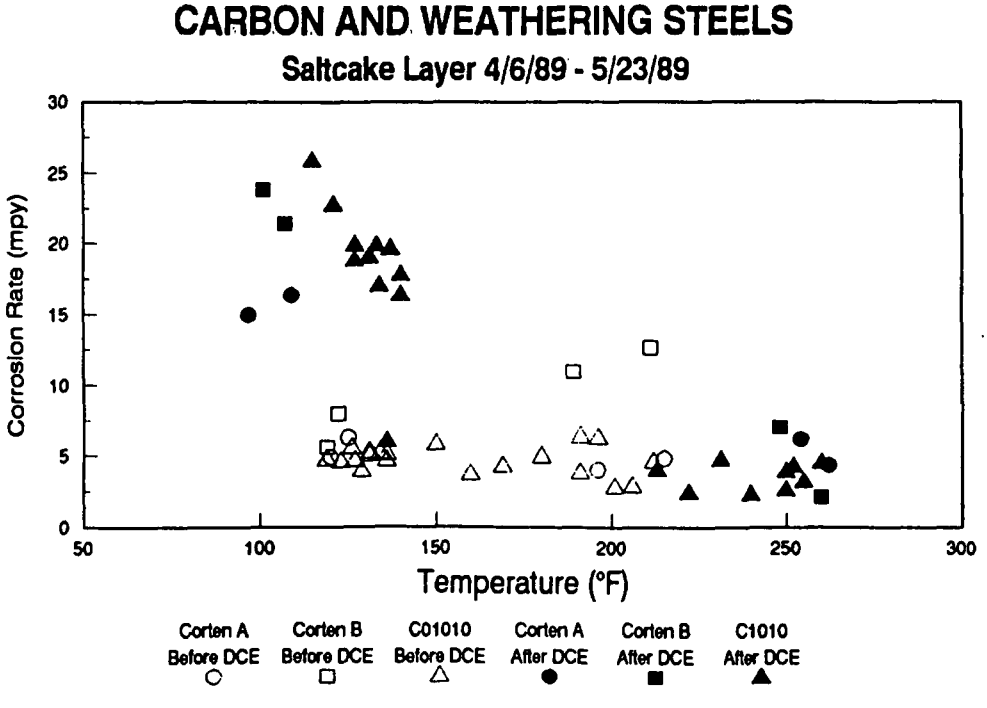

Figure 54. Corrosion data from the Cedar Springs mill with saltcake on the coupons.

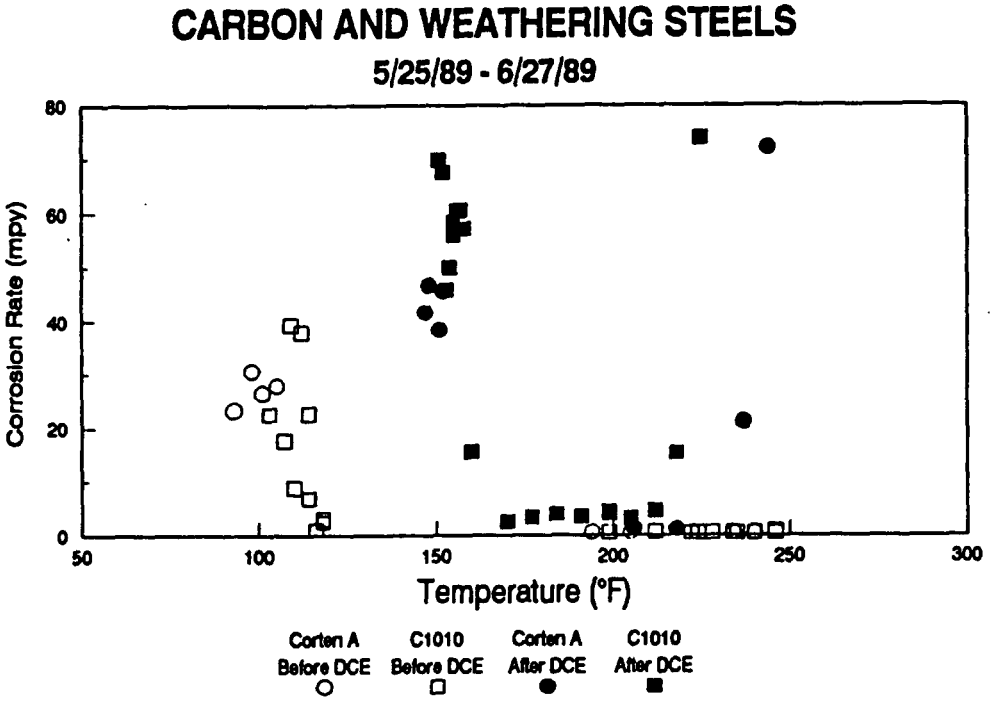

Figure 55. Corrosion data from a test run at the Cedar Springs mill without saltcake on the coupons.

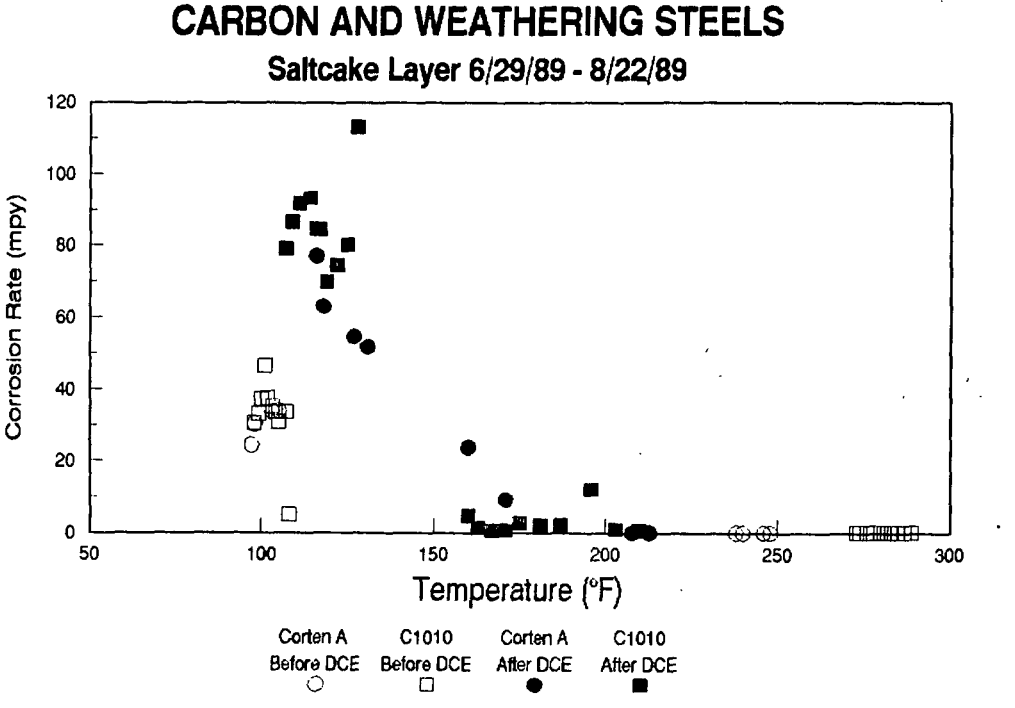

Figure 56. Corrosion data from the Cedar Springs mill with saltcake on the coupons.